INFORMATION TO USERS

The most advanced technology has been used to photograph and reproduce this manuscript from the microfilm master. UMI films the text directly from the original or copy submitted. Thus, some thesis and dissertation copies are in typewriter face, while others may be from any type of computer printer.

The quality of this reproduction is dependent upon the quality of the copy submitted. Broken or indistinct print, colored or poor quality illustrations and photographs, print bleedthrough, substandard margins, and improper alignment can adversely affect reproduction.

In the unlikely event that the author did not send UMI a complete manuscript and there are missing pages, these will be noted. Also, if unauthorized copyright material had to be removed, a note will indicate the deletion.

Oversize materials (e.g., maps, drawings, charts) are reproduced by sectioning the original, beginning at the upper left-hand corner and continuing from left to right in equal sections with small overlaps. Each original is also photographed in one exposure and is included in reduced form at the back of the book. These are also available as one exposure on a standard 35mm slide or as a 17" x 23" black and white photographic print for an additional charge.

Photographs included in the original manuscript have been reproduced xerographically in this copy. Higher quality 6" x 9" black and white photographic prints are available for any photographs or illustrations appearing in this copy for an additional charge. Contact UMI directly to order.

UMI

University Microfilms International
A Bell & Howell Information Company
300 North Zeeb Road, Ann Arbor, MI 48106-1346 USA
313/761-4700 800/521-0600

Order Number 1335983

Spatial fading characteristics of VHF broadcast signals in an urban environment

Banik, Tuhin, M.Eng.

McGill University(Canada), 1988

U·M·I
300 N. Zeeb Rd.
Ann Arbor, MI 48106

SPATIAL FADING CHARACTERISTICS OF VHF BROADCAST SIGNALS IN AN URBAN ENVIRONMENT

Tuhin Banik, B. Eng. (McGill)

A thesis submitted to the Faculty of Graduate Studies
and Research in partial fulfillment of the
requirements for the degree of
Master of Engineering

Department of Electrical Engineering
McGill University, Montreal
July 1988

ABSTRACT

This thesis is concerned with the measurement and characterization of radio signal spatial fading in urban micro-environments. Automated field strength measurements at ten FM broadcast frequencies were conducted in a small region of a built up urban center (the McGill University campus, Montreal, Canada).

The measurements show that the received signal comprises two independent fading components: *long term fading* (average power variations over large spatial intervals), and *short term fading* (rapid power fluctuations over small spatial intervals). A number of statistical and time series analysis methods (probability density, quantile-quantile plots, autocovariance, crosscovariance, spectral density) were exploited to characterize the fading behaviour (long term and short term) for different urban surroundings.

Since specific behavioural differences were observed, it is concluded that the methods used (experimental and statistical) provide a basis for characterizing spatial fading phenomena of mobile radio signals in urban areas.

SOMMAIRE

Ce mémoire se penche sur la mesure et la caractérisation de l'évanouissement spatial d'un signal radio dans les micro-régions urbaines. A cette fin, des mesures automatisées de champs électromagnétiques ont été relevées à l'intérieur d'une petite région d'un centre urbain (le campus de l'Université McGill, Montréal, Canada) pour dix fréquences FM de radiotélédiffusion (88-108 MHz).

Les mesures indiquent que le signal reçu est constitué de deux composantes indépendantes: les variations lentes (variations de la puissance moyenne sur de grandes distances) et les variations rapides (fluctuations de la puissance sur de courtes distances). Ces deux composantes ont été caractérisées à l'aide de diverses méthodes statistiques (i.e. tracé centile-centile, densité de probabilité), et d'analyse de signaux (autovariance, covariance, et spectre de puissances) pour identifier des différences d'un milieu à l'autre.

On a ainsi pu déduire des caractéristiques statistiques intéressantes, et consistantes dans le temps pour cette micro-région typique; l'ensemble des données recueillies constitue alors une base pour la caractérisation de l'évanouissement spatial d'un signal radio.

ACKNOWLEDGEMENTS

I wish to acknowledge the many discussions and valuable suggestions of Dr. J. LeBel of the Communications Research Centre, Ottawa. Sincere thanks are also extended to him and his colleagues at CRC, Mr. P. Bouliane, Mr. K. Bedal, and the late Mr. G. Craig, for peforming the measurements with the DOC/CRC mobile field instrumentation vehicle. This work would not have been possible without these measurements.

I would also like to express gratitude to my thesis supervisor, Dr. T.J.F. Pavlasek, for continued encouragement and support.

Special thanks are extended to Dr. L. Kaliouby for translating the abstract, and to Ms. K. Mosher for assisting with the proofreading of the manuscript.

Photography was done by Marc Banik, and the Instructional Communications Centre, McGill University, supplied the campus map.

The measurements were supported in part by DOC research contracts.

TABLE OF CONTENTS

LIST OF ILLUSTRATIONS

THESIS ILLUSTRATIONS

THESIS ILLUSTRATIONS

Chapter 1 :

INTRODUCTION

1.1 General Introduction

For many years, mobile radiocommunications have been of interest for those in need of communicating with others from within moving vehicles, be they in air, at sea, or on land [1.1]. Applications of land mobile radio systems (LMRS) include dispatch services, surveillance systems, citizen band radio, radio pagers, and more recently, cellular radiotelephone services.

The advantages obtained with the use of mobile radio systems are obvious. First, the systems are entirely wireless giving mobile receivers the ability to change position freely without losing communications in a given service area. Second, a mobile radio system is indispensable in situations demanding communication between two points which cannot be physically connected by wired systems, as in the case of all moving land vehicles, as well as ships and aircraft.

The service of a mobile radio system is limited by the magnitude of the received signal strength relative to the sensitivity of the receiver. In an urban environment, the transmitted signal suffers losses in power arising from reflections and obstructions from buildings. These losses will be displayed in the large scale variations (*long term fading*) [1.2] of the received signal.

Short term fading [1.2] describes the rapid fluctuations of the received signal power about the long term fading signal. The received signal is therefore a combination of the long term and short term fading components.

Because signal fading arises from the environment between the transmitter and receiver, the fading signal provides information as to how the environment actually degrades the transmitted signal. An understanding of the fading characteristics thus aids the design of LMRS where signal degradation resulting from spatial fading is common.

In recent years, there has been increasing interest in cellular radio networking as applied to mobile telephony [1.3]. Hence, the need arises to characterize the fading signal under a variety of environmental conditions, and particularly in urban areas, where shadowing, scattering, and reflection affects the performance of land mobile radio systems.

The present work addresses the problem of characterizing the spatial fading phenomena (long term and short term) at FM broadcast frequencies in an urban "micro-environment" (a small region of a large downtown area). Making measurements in this frequency range can provide exploratory data showing the nature of the long term and short term fading signals. Since the objective of the present work is to obtain exploratory data of the fading signal under urban conditions, the electromagnetic fields from commercial FM broadcast transmitters have been chosen for study. This is because a continuous test signal is always available and thus the signals can be readily measured at all times.

It is hoped that the results of this work will encourage similar studies in other frequency ranges and in other urban areas in order to enlarge the information base necessary for further understanding and prediction of signal fading in urban areas.

1.2 Statement of the Problem and Objectives

The problem which this thesis adresses is the development of a methodology for characterizing long term and short term spatial fading in urban areas. The three major aspects involved in such a problem are as follows:

(a). The *experiment design* considerations in characterizing the long term and short term spatial fading in an urban micro-environment,

(b). The consideration of meaningful *data analysis methods* to characterize the behaviour of long term and short term spatial fading,

(c). The *characterization of the statistical behaviour* of the long term and and short term fading using (a) and (b) above, as based on actual field measurements in a micro-environment.

Appendix E contains a list of abbreviations used in the thesis.

A bibliography of selected journal and conference papers on various aspects of mobile propagation is given at the end of the thesis for ready reference to background material.

All references are placed at the end of each chapter, under the designation of "End Notes".

1.5 End Notes

[1.1] A brief summary of the major developments in mobile radiocommunications can be found in, W.C.Y. Lee, *Mobile Communications Engineering*, New York, McGraw-Hill, 1982, pp.2-3.

[1.2] The concept of spatial long term and short term fading of mobile radio signals is described in, W.C.Y. Lee, *Mobile Communcations Engineering*, 1982, pp.169-171.

[1.3] The use of cellular radio networking as applied to mobile telephony was first introduced by Bell Telephone Laboratories, U.S.A., in 1978, under the trade name "Advanced Mobile Phone Service" (AMPS). A complete description of the AMPS features is given in, "Advanced Mobile Phone Service", special issue, *Bell System Technical Journal*, vol.58, January 1979.

Chapter 2 :

THE EXPERIMENT

2.1 General

This chapter describes the experiment design, the experimental method, the instrumentation used for measurements, and the amount of data collected from each field survey.

2.2 Experiment Design

The special features of the experiment are the following:

* The measurement sites are in close proximity to a number of high power FM transmitting sources [2.1], thereby providing continuously available, powerful test signals.

* The experiment involves making field strength measurements on a *microscopic scale* (referring to a small test region within a larger region) in an urban environment.

* The experiment of this study is in contrast to previous studies [2.2] where measurements were made on a *macroscopic scale* over a large region composed of smaller sub-regions. A microscopic scale study attempts to show differences in behaviour between individual street locations within a larger composite region (such as a city). In contrast, a macroscopic study would attempt to show differences in the behaviour of one large region as compared to another large region, such as two cities.

* The experiment is designed to identify the spatial long term fading and short term fading characteristics of broadcast signals in an *urban micro-environment.* The

long term and short term fading charactersitics of the micro-environment represent a new body of information which may be applied to the planning and design of radiocommunications services tailored to the urban micro-environment. Macroscopic measurements are of limited use in describing the features of the micro-environment.

Fig. (2.2.1) shows an example of an urban micro-environment (Sherbrooke St.) as investigated in the present work. The points of interest are the different sizes and shapes of urban buildings lining the street. More will be said of the specific micro-environment features in section (2.7).

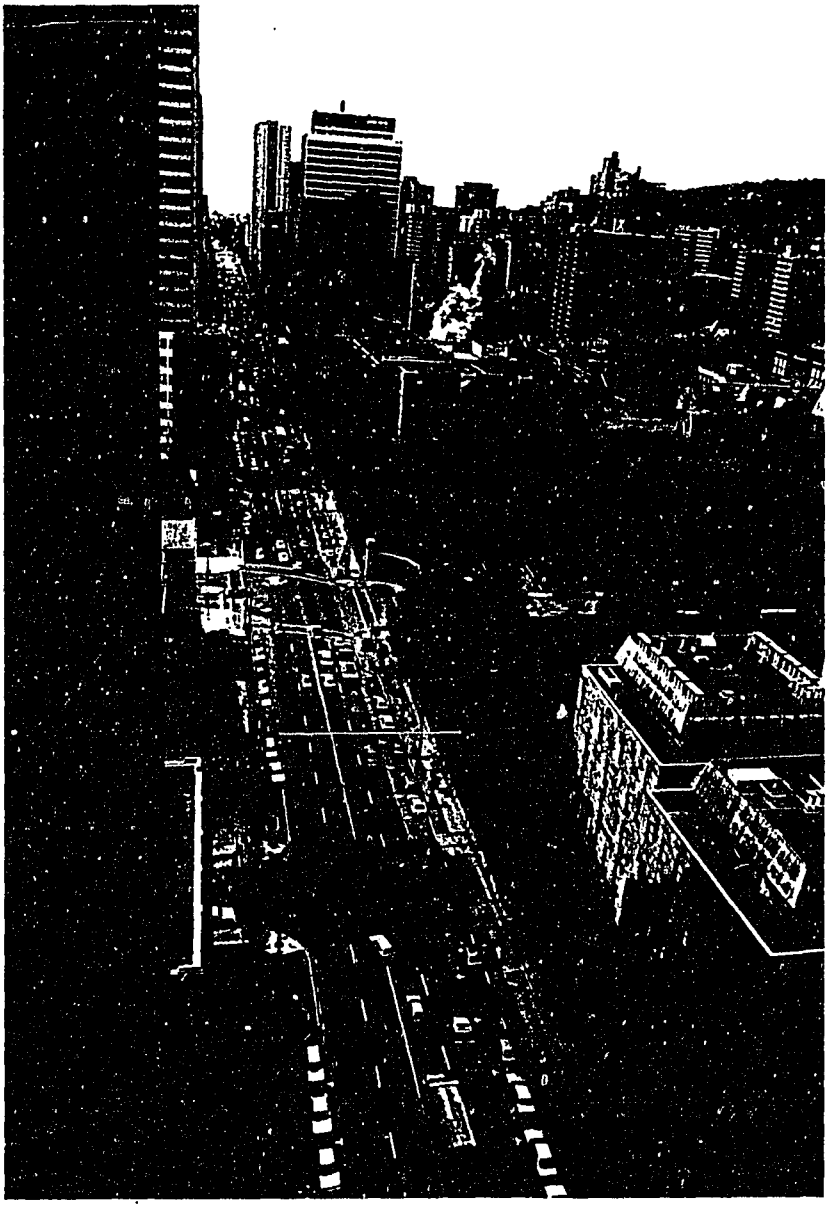

Fig. (2.2.1) An urban 'micro-environment': Sherbrooke Street, Montreal.

2.3 Experimental Method

To achieve the objective of gathering large amounts of field strength data on various streets in a busy downtown area, automated field strength measurements were performed with a mobile field instrumentation vehicle (MFIV) [2.3]. The MFIV, essentially a refurbished camping vehicle adapted for field measurements, houses a complete signal monitoring system : VHF/UHF scanning receivers, a data acquisition system, a line printer, and a 9-track tape drive, all of which operate under computer control. In order to run this equipment, a separate power supply (provided by diesel generators) is required to provide a stable mains voltage to the computer and rf equipment.

The MFIV is owned and operated by the Department of Communications (DOC), Communications Research Centre (CRC), Ottawa, Canada. A photograph of the MFIV is shown in Fig. (2.3.1). The MFIV has been used in the past for monitoring the electromagnetic environment in Canadian cities on a macroscopic scale (see LeBel in [2.2]).

Vertical and horizontal polarized receiving antennas were mounted on the rooftop of the MFIV at a height of roughly 3 meters above street level. The rooftop comprises a metallic mesh surface acting as an image plane.

During vehicle motion along the streets, the field strengths at several preprogrammed frequencies were sampled at rougly uniform spatial intervals. The field strength data, the vehicle postion along the street (relative to a specific starting point), and the time of each measurement, were all stored in memory and transferred onto magnetic tapes during measurements. Upon completion of the measurements, the tapes were transferred to a remote mainframe where the data were reduced and preprocessed. The data processing aspects are described in Chapter 3.

The MFIV was driven along city streets at a speed of about 10-20 km/hr so that observation by observation, the vehicle can be considered stationary (as compared to the velocity of propagation). In such case, Davis and Bogner [2.4] reported that the propagation between the base station and the mobile may be considered reciprocal, so that exchanging the base transmitter with a base receiver and the mobile receiver with

a mobile transmitter will give the same results. However, for convenience, measurements are made using a stationary base transmitter and a mobile receiver.

The transmitter characteristics are described in section (2.4), the receiver system in section (2.5), and the receiving antenna in section (2.6).

The measurement trajectories of each field survey (there were two surveys) are described in section (2.7).

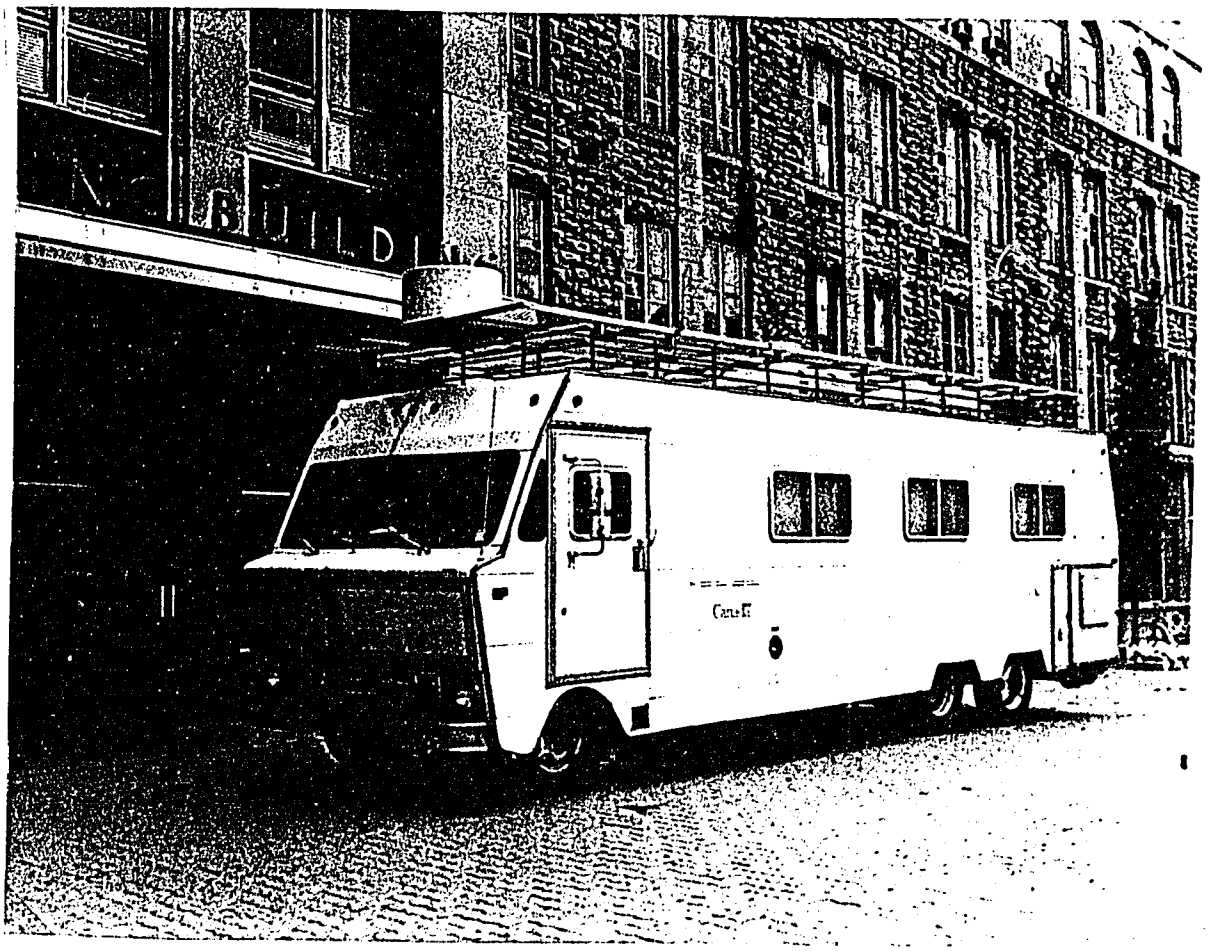

Fig. (2.3.1) The DOC/CRC mobile field instrumentation van (MFIV).

2.4 Transmitters

The transmitters for most of the ten FM broadcasting stations are colocated on an antenna tower on Mount Royal park in Montreal, Canada. The transmitters for other stations are located on nearby office buildings.

Table (2.4.1) lists the ten Montreal FM transmitters, their audio carrier effective radiated powers (ERPs) along the horizon, height above sea level in meters, transmitter location relative to the Mt. Royal antenna tower (e.g. (N),(S),(E),(W) indicates North, South, East, and West of Mt. Royal, respectively), and the transmitted polarization.

Fig. (2.4.1) shows a closeup view of the Mount Royal antenna tower as seen from a point on Mount Royal park.

Fig. (2.4.2) shows the CKOI antenna mast situated on top of the Bank of Commerce building on Peel street, as seen from the top of Peel Street.

Table (2.4.1). Charactersitics of Montreal FM Broadcast Transmitters (88-108 MHz).

STATION	F(MHz)	ERP (kW)	Height(m)	Location	Polarization
CFQR	92,5	41,4	298	Mt. Royal	Horizontal
CBM-FM	93,5	24,6	251	Mt. Royal	Horizontal
CKMF	94,3	41,4	298	Mt. Royal	Horizontal
CJFM	95,9	41,2	298	Mt. Royal	Horizontal
CKOI	96,9	307,0	217	Peel St.(SE)	Circular
CHOM	97,7	41,2	298	Mt. Royal	Horizontal
CBF-FM	100,7	100,0	251	Mt. Royal	Horizontal
CINQ	102,3	0,04	46,0	Downtown (NW)	Horizontal
CFGL	105,7	100,0	121	Mt. Royal	Circular
CITE	107,3	100,0	112	Downtown (E)	Circular

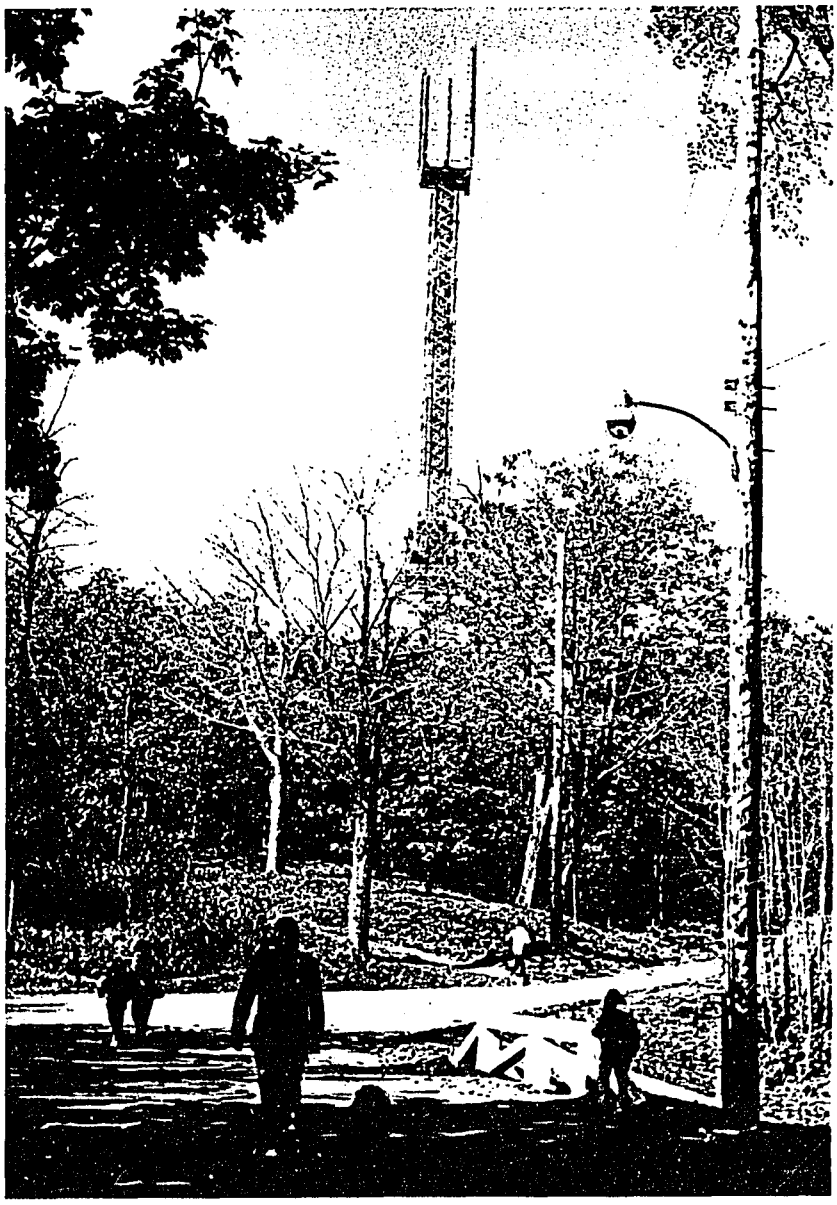

Fig. (2.4.1) Mount Royal FM-TV antenna tower.

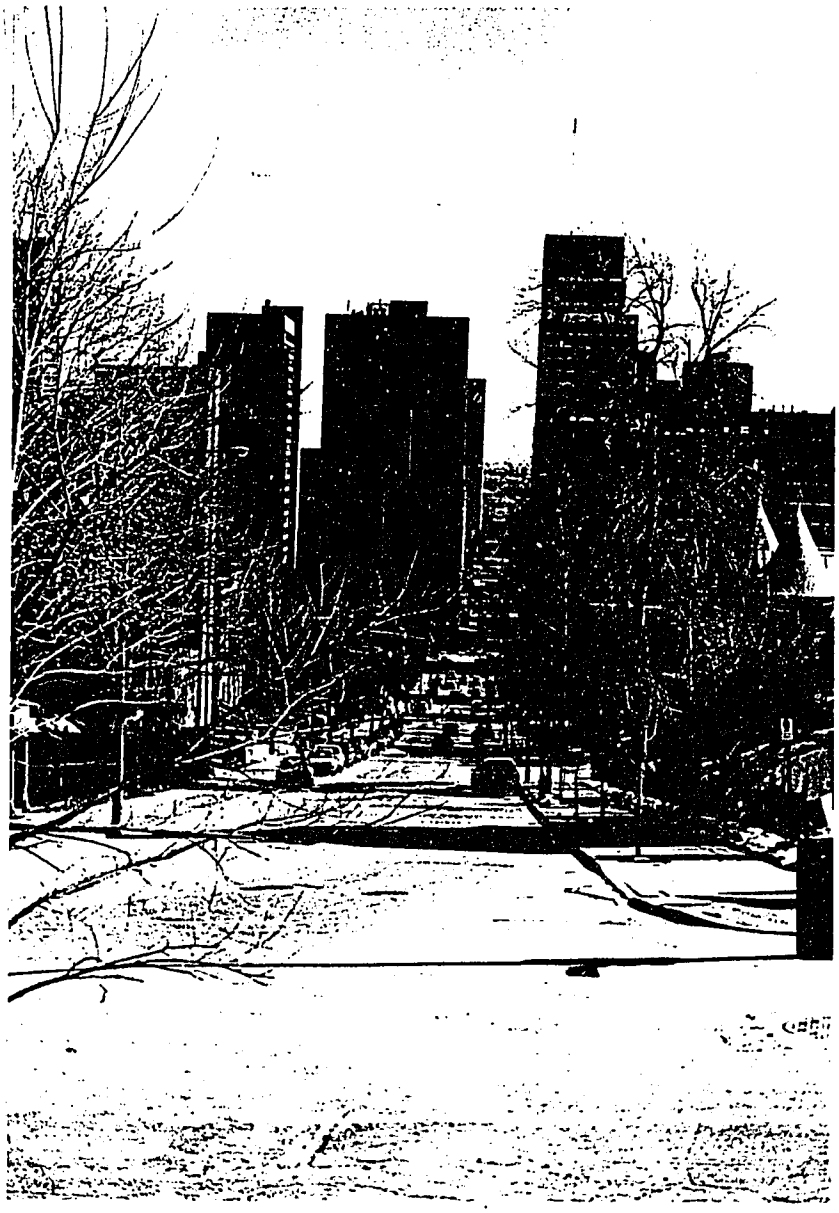

Fig. (2.4.2) Peel Street showing CKOI antenna tower.

2.5 Receiving Antennas

Rhode and Schwarz active dipole antennas were used to measure electric field strengths in the FM broadcast range (88-108 MHz). Separate elements for the vertical (type HE109) and horizontal (type HE114) polarizations provided the vertical and horizontal polarized signals. These are broadband active (high impedance) antennas with operation in the VHF range (20-200 MHz), extending up to TV channel 12.

The horizontal dipole consisted of two antennas coupled to a common output by means of a 90 degree hybrid. The two antennas were physically oriented at right angles to each other to provide omnidirectional coverage.

The vertical and horizontal antennas were mounted on a metallic mesh surface acting as an image plane (2,44 m by 7,35 m) on the rooftop of the instrumentation van [2.3]. The vertical and horizontal dipole elements were separated spatially by about 2,0 meters.

2.6 Data Gathering System

The data gathering system comprises a computer controlled (PDP-8) VHF scanning receiver with data acquisition and storage capabilities [2.3]. The measuring receiver is a calibrated triple conversion superheterodyne receiver followed by a precision detector [2.3]. The special features of the receiver system are as follows:

a). It can be preprogrammed from one frequency to another within microseconds via a programmable frequency synthesizer,

b). True RMS (root-mean-square) envelope detection is achieved by special circuitry with a dynamic range of about 60 dB,

c). TV channels (4,5 MHz bandwidth) are handled by measuring the audio portion of the channel, and later obtaining the video power by a known fraction of the total power in the channel,

d). A programmable synthesized generator is used for calibration purposes.

A complete description of the data gathering system (and the MFIV) is given in [2.3]. Fig. {2.6.1} shows a block diagram of the major components of the MFIV data gathering system.

The signal strengths are registered in units of decibels relative to 1 microvolt (dBμV) on magnetic tape together with the position of each measurement relative to the starting location. The start and end times of each measurement are also registered. Conversion to field strengths (dBμV/m) is carried out during the preprocessing step, and is described in Chapter 3.

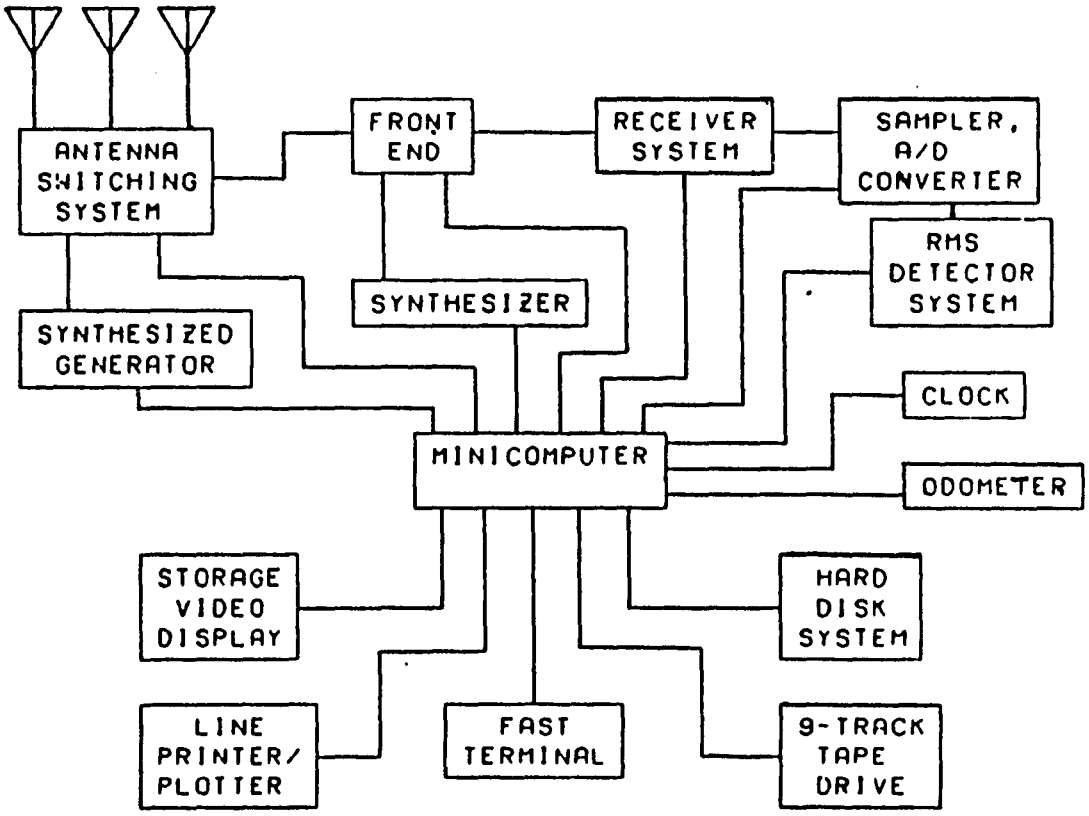

Fig. {2.6.1} Block diagram of the MFIV data gathering system [2.3].

2.7 Scope of Measurements

Two separate field surveys were carried out (March 1983, December 1984) in Montreal, Canada, both of which involved the MFIV.

The first survey comprised exploratory field strength measurements of 12 AM, 10 FM, and 4 VHF-TV broadcast frequencies on 19 streets on the McGill University campus precinct in downtown Montreal. The sampling interval was between 1,5 and 6,5 meters. This rate of sampling gave a very detailed representation (about 100 samples per wavelength) of the standing wave patterns at the AM broadcast frequencies with typical wavelengths of roughly 500 m. However, using the same rate of sampling at the FM & VHF-TV broadcast frequencies (55-205 MHz) was clearly inappropriate to describe the short term fading characteristics due to the shorter wavelengths (1,5 m to 3,5 m).

The purpose of the first survey was to investigate the ambient levels of EM radiation in an urban environment due to commercial FM broadcasting transmitters [2.1]. It should be noted that the measurements of this exploratory survey were not carried out with the specific intention of studying the long term or short term fading behaviour. However, a preliminary analysis of the data revealed interesting trends which prompted further investigation.

In order to further investigate such trends, a second survey was therefore conducted of only the ten FM stations over a reduced set of routes. This survey involved sampling the field at intervals of between 0,5 m and 0,9 m, giving more detail of the spatial intereference pattern than the previous survey. These detailed field measurements provide the basis of Chapter 5 on short term fading.

The measurement routes and other details of both field surveys are described in sections (2.7.1) and (2.7.2) respectively.

2.7.1 First Field Survey : March 1983

This section describes the micro-environment of the first field survey. Table {2.7.1.1} lists the measurement routes, the number of samples on each route (N), and the average sample spacing (T) in meters.

A map of the measurement trajectories is given in Fig. {2.7.1.1}.

From table {2.7.1.1}, the mean sample spacing of all 19 street locations is about 3,2 meters, or about one wavelength at f=93 MHz.

Figures {2.2.1} and {2.4.2} show photographs of two measurement trajectories, Sherbrooke Street (route #8) and Peel Street (route #7), as listed in Table {2.7.1.1}.

Table (2.7.1.1). Measurement Trajectories for March 1983 Survey.

Measuring Sequence	Starting Location	Ending Location	Route Length	Sample Size	Sample Spacing
1	University & Sherbrooke	Pine & University	630 m	N=318	1,98 m
2	Pine & University	Peel & Pine	434 m	N=163	2,66 m
3	Peel & Pine	McIntyre & Peel	75 m	N=16	4,69 m
4	McIntyre & Peel	Drummond & McIntyre	200 m	N=140	1,43 m
5	Drummond & McIntyre	Penfield & Drummond	112 m	N=53	2,11 m
6	Penfield & Drummond	Peel & Penfield	197 m	N=84	2,34 m
7	Peel & Penfield	Sherbrooke & Peel	273 m	N=91	3,00 m
8	Sherbrooke & Peel	Sherbrooke & University	422 m	N=160	2,64 m
9	McTavish & Penfield	Pine & McTavish	243 m	N=70	3,47 m
10	Pine & McTavish	Peel & Pine	102 m	N=21	4,86 m
11	Peel & Pine	Penfield & Peel	220 m	N=33	6,49 m
12	Penfield & Peel	Penfield & McTavish	97 m	N=16	6,06 m
13	Biology Road & Milton	Sherbrooke & Biology	370 m	N=287	1,29 m
14	Sherbrooke & Biology	McTavish & Sherbrooke	143 m	N=49	2,92 m
15	McTavish & Sherbrooke	Penfield & McTavish	293 m	N=97	3,02 m
16	Penfield & McTavish	Biology Road & Penfieldgate	265 m	N=60	4,42 m
17	Biology Road & Penfieldgate	Biology Road & Milton	389 m	N=225	1,73 m
18	University & Pine	University & Northend	251 m	N=103	2,44 m
19	Pine & Peel	Pine & Redpath	269 m	N=78	3,45 m

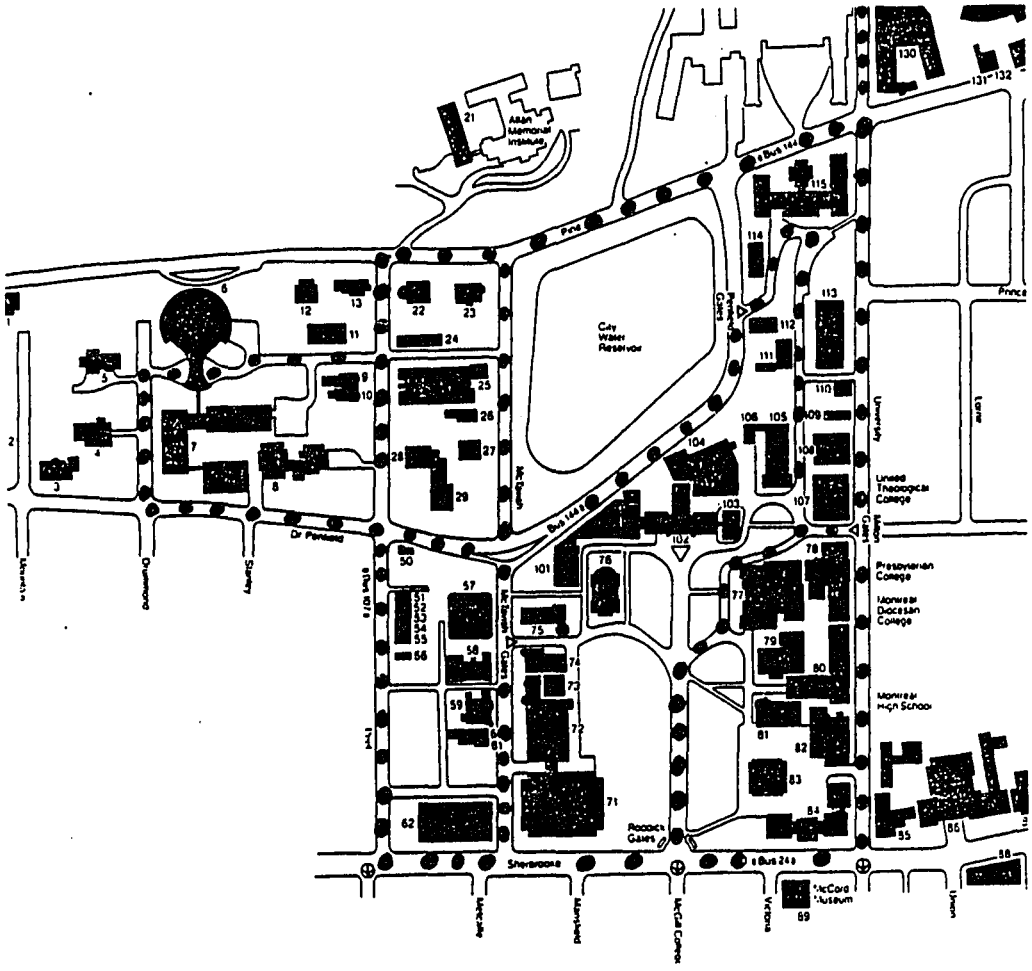

Fig. (2.7.1.1) Map of measurement trajectories on the McGill University campus. First field survey (of 12 AM, 10 FM, and 4 VHF-TV broadcast transmitters). Dots indicate survey routes.

2.7.2 Second Field Survey: December 1984

Table {2.7.2.1} lists the measurement routes for the second field survey. It should be noted that measurement routes are a subset of the routes of the previous survey, as shown in Fig. {2.7.2.1}.

Table {2.7.2.1}. Measurement Trajectories for December 1984 Survey.

Measuring Sequence	Starting Location	Ending Location	Route Length	Sample Size	Sample Spacing
1	University & Sherbrooke	University & Northend	825 m	N=1310	0,63 m
2	Roddick Gate & Sherbrooke	Milton Gate & University	375 m	N=721	0,52 m
3	Milton Gate & University	Biology Road/ Penfieldgate	255 m	N=283	0,90 m

Figure {2.7.2.2} shows route (#1), University Street from the intersection of Sherbrooke towards Northend.

Figure {2.7.2.3} shows route (#2), Roddick Gate towards the Arts Building on the McGill University campus.

Figure {2.7.2.4} shows route (#3), Milton Gate towards Penfieldgate, also on the McGill University campus.

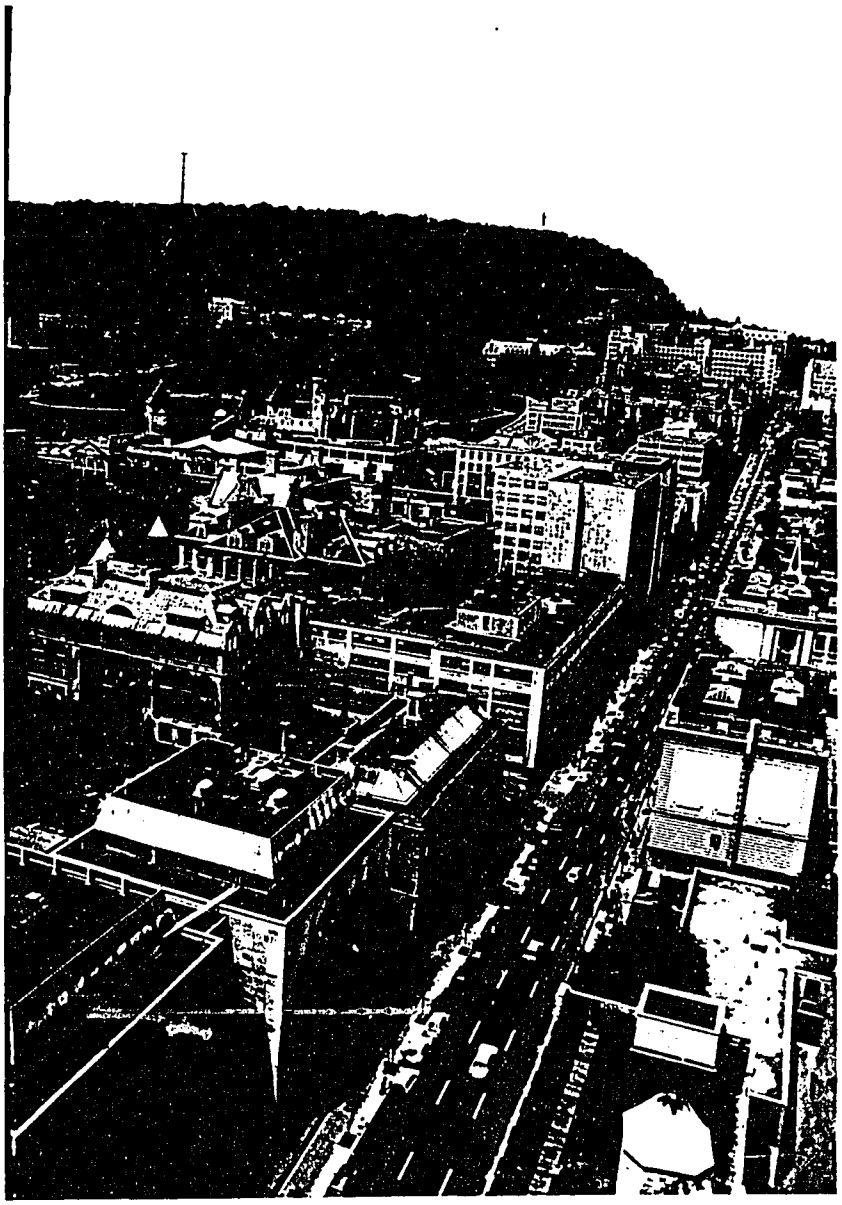

Fig. (2.7.2.2) View of University Street (route #1, second survey).

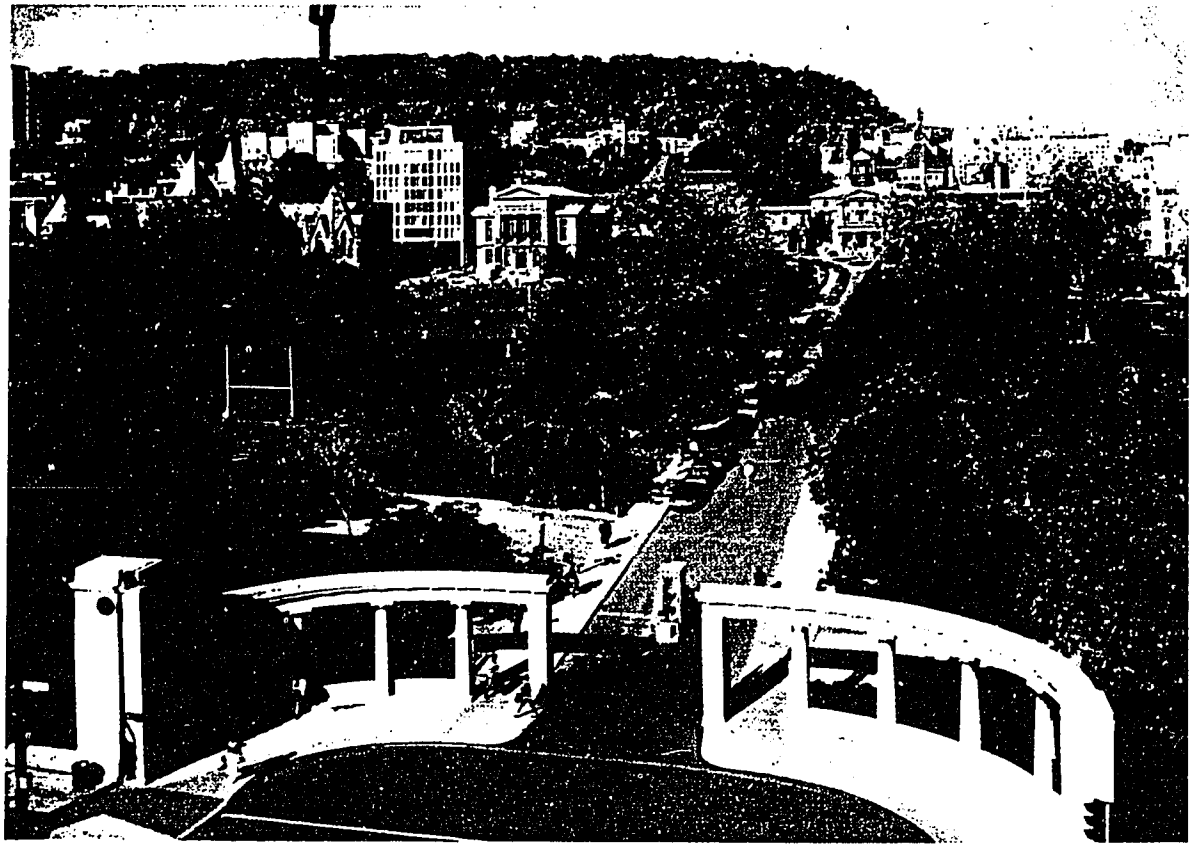

Fig. (2.7.2.3) View of lower McGill University campus showing Roddick Gate entrance (route #2, second survey).

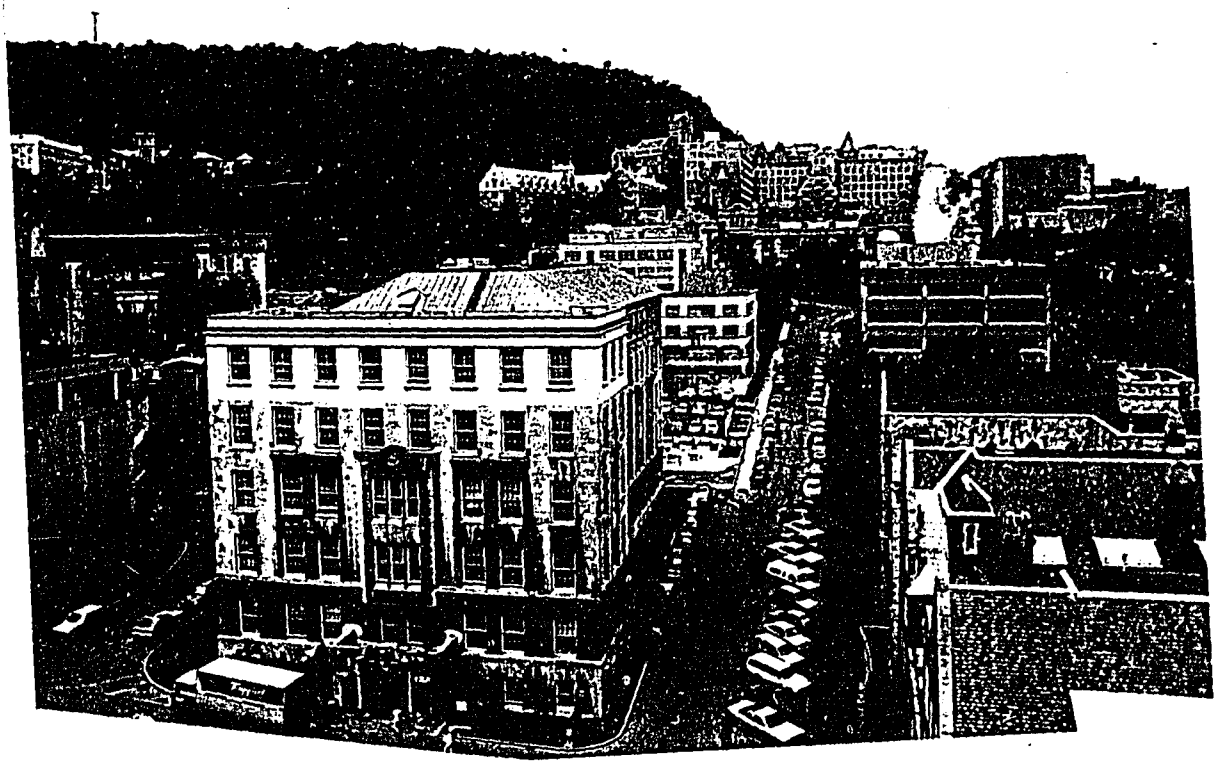

Fig. (2.7.2.4) View of route from Milton Gate to Penfield Gate (route #3, second survey).

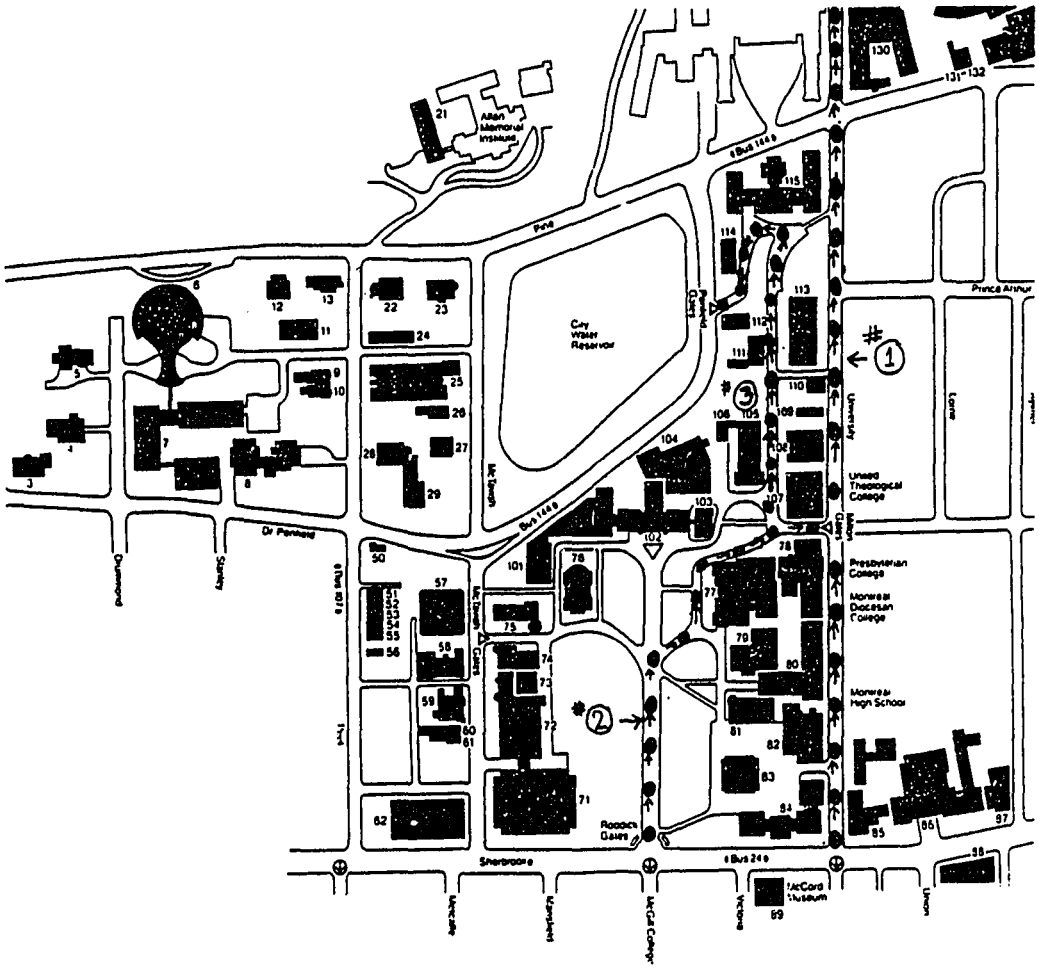

Fig. (2.7.2.1). Map of measurement trajectories on the McGill University campus. Second field survey (of 10 FM broadcast transmitters). Dots indicate survey routes.

2.8 Concluding Remarks

This chapter has described features of the experiment design, including the concept of micro-environment field measurements, the experimental method, and the scope of the field surveys carried out. It is evident that the study of spatial fading of the micro-environment requires gathering large amounts of data over a number of urban streets. To achieve this objective, an apparatus for performing automated measurements is required. In the present case, the apparatus involved a mobile van adapted to perform automated field measurements. The measuring vehicle is required to operate as a independent unit, and therefore requires a separate power supply to provide a stable mains voltage to on-board computer and rf equipment.

All the field strength data should be stored on tapes (or other storage media) such that data processing may be carried out separately from the data gathering. The following chapter describes various aspects of processing the field measurement data.

2.9 End Notes

[2.1] **T. Banik, T. Pavlasek, and J. LeBel,** "Electric Field Strength Surveys of Broadcast Signals in an Urban Environment", *Proc. International Conf. on Electromagnetic Interference and Compatibility (INCEMIC)*, Bangalore, India, Sept. 10-11, 1987, pp.341-344.

[2.2] See, for instance, the following studies describing macroscopic scale field strength measurements over large city regions:

Y. Okumura, E. Ohmori, T. Kawano, and K. Fukuda, "Field Strength and its Variability in Land-Mobile Radio Service", *Rev. Elect. Commun. Laboratories*, vol. 16, Sept.-Oct. 1968, pp.825-873.

R.J. Samuel, J.D. Parsons, and M.F. Ibrahim, "Mobile Radio Propagation in Inner London", *Second International Conference on Antennas and Propagation*, Heslington, York, England, Part 2, April 1981, pp.143-147.

J. LeBel, G.B. Craig, and P.R. Bouliane, "Measurement and Evaluation of Electromagnetic VHF and UHF Television Field Strengths in Urban Environments", *Proc. IEEE International EMC Symposium*, Arlington, Virginia, U.S.A., August 23-25, 1983, pp. 147-151.

[2.3] **J. LeBel,** "A Mobile Facility for Electromagnetic Environment Monitoring Applications", *Proc. International Electrical Electronics Conference and Exposition*, October 5-7, 1981, pp.10-11.

[2.4] **B.R. Davis and R.E. Bogner,** "Propagation at 500 MHz for Mobile Radio", *Proc. IEE Part F*, Vol.132, August 1985, p.307.

Chapter 3 :

DATA ANALYSIS METHODOLOGY

3.1 General

This chapter describes the data analysis procedures that were carried out on the raw data recorded by the instrumentation van. The methods of data reduction, preprocessing, and data transfer are described briefly. The objectives of the data analysis are stated, and the statistical analysis software packages developed are catalogued at the end.

3.2 Data Processing Procedures

1. *DATA REDUCTION AND PREPROCESSING*

Data reduction is the first step in the data processing procedures. It involves the conversion of the raw data from decibel microvolts (dBμV) to units of field strength, expressed in decibels relative to a microvolt per meter (dBμV/m) using the known antenna factor for each frequency. The conversion is carried out on the CRC mainframe computer system by a specially developed software package which employs the antenna factor versus frequency calibration curve. Other steps include incorporating correction for cable losses and attenuator pad settings for each frequency measured. The combination of all the above steps comprises the process of data reduction.

The next procedure which occurs before the start of any analysis is that of *preprocessing*. Preprocessing involves the conversion of the original records to a format for convenient processing and includes the addition of information such as the number of measurements on the trajectory. The preprocessing step is also performed at the CRC site using specially developed software. Once this step is performed, the data is ready for analysis.

Both the data reduction and preprocessing steps were carried out on the CRC mainframe computer system (Honeywell CP-6). All the reduced and preprocessed data was then copied onto a separate tape, which is then sent for analysis.

2. *DATA TRANSFER AND MANAGEMENT*

At the start of this study, data analysis of an exploratory nature was performed on the IBM mainframe system (IBM 4341) at McGill University. However, as the work progressed, it became apparent that the analysis did not require a mainframe system and it was thus decided to transfer the data and the analysis software to a microcomputer (PC) environment. The data analysis has since then been carried out on a PC. As experience has shown, the PC is the preferred system for data analysis because of greater convenience and lower computing costs.

The present form of data transfer is as follows. The preprocessed data, which is stored on a 9-track magnetic tape, is fed into an IBM mainframe computer. Once the data is transferred from tape onto mainframe disk storage, a data transfer between the mainframe system and a microcomputer is initiated via a file transfer program such as KERMIT or PCWS.

The transfer of data to a PC level is considered to be an important factor in obtaining results at a fraction of the cost of mainframe operation.

Table (3.2.1) shows the storage requirements of the conglomerate data sets of both field surveys. From this table, it is evident that the data acquired from future surveys can also be transferred to a PC, provided the PC is equipped to handle the storage requirements of the data.

Table (3.2.1). Memory Storage Requirements of Measurement Data.

Survey Date	Number of Streets	Number of Stations	Data Bank Size
March 1983	19	26 (V,H)	450 Kbytes (approx.)
December 1984	3	10 (V,H)	295 Kbytes (approx.)

3. *DATA ANALYSIS*

The data analysis was carried out on a PC's LIMITED 286 microcomputer equipped with the Intel 286 micropocessor and the Intel 287 math co-processor, 1 Megabyte RAM, an IBM enhanced graphics adapter (EGA) card, and an 80 Megabyte fixed disk. One high density (1.2 Mbyte) and one regular density (360 Kbyte) disk drive are also installed for floppy disk data transfers.

Data analysis software was developed using the F77L Fortran compiler [3.1]. In addition, for certain applications, the SSP/PC math library [3.2] was used in computing Bessel functions (see PDENS.EXE software).

Graphs were produced using the GOLDEN GRAPHICS graphics software [3.3].

3.3 Objectives of Data Analysis

The objectives of the data analysis are stated in terms of the long term and short term fading components. The techniques used to achieve the data analysis objectives are described in sections (3.3.1) and (3.3.2) respectively.

To perform the analysis of the measurements, software packages were developed for data retrieval as well as for statistical analysis. The software was

developed using the Lahey Fortran compiler [3.1], and were designed with as much flexibility as possible for future use. The software is further described in sections {3.5.1} and {3.5.2}.

3.3.1 Data Analysis Objectives: Long Term Fading

The objectives of the analysis of the long term fading signal may be categorized into two broad classes, (i), the spatial behaviour, and (ii), the statistical behaviour.

(i) *Spatial Behaviour:*

(a) To identify and quantify the shadow zones for a single transmitter along a typical built-up street,

(b) To compare the fading patterns of several transmitters on a given street.

(ii) *Statistical Behaviour:*

(a) To study the cumulative distribution function (CDF) behaviour of a particular transmitter on different streets,

(b) To estimate the shadow effect among parallel streets in a micro-environment,

(c) To compare the CDF of the vertical and horizontal fading components on a common street.

3.3.2 Data Analysis Objectives: Short Term Fading

The objective of the short term fading analysis is to characterize the stochastic nature for different urban surroundings. This involves the application of the following established methods of random data analysis and time series analysis: (i), the probability density function (PDF) of the short term variations, (ii), the spatial autocorrelation behaviour, (iii), the spatial crosscorrelation behaviour between the vertical and horizontal fading components, and (iv), the spectral domain behaviour using the notion of spatial frequency.

3.4 Analytical Techniques

The analytical techniques are divided into two categories: Long Term Fading, and Short Term Fading. These techniques are briefly stated in sections {3.4.1} and {3.4.2} and are discussed in Chapters 4 and 5. Appendices A, B, C, D, contain information on the computational aspects of the short term fading statistical analysis methods.

In order to obtain the slow and fast fading components of the received signal, a statistical lowpass filter was applied to the received signal consisting of rapid variations (short term fading) superimposed on a slowly varying signal (long term fading). The filter uses a running means approach such that the long term fading signal at a given position is obtained by averaging (in dB) a suitable number of equally weighted samples to the left and to the right of the local mean [3.4]. This gives an estimate of the local average power as a function of space.

In order to use such a filter based on signal averaging, it is first necessary to have equally spaced samples. This is accomplished by linear interpolation and is described in section {4.2}. The statistics of the received signal are essentially unchanged by the interpolation, as verified by comparing the CDFs of the interpolated versus original data.

Figures {3.5.1} to {3.5.3} are a series of block diagrams showing the sequence of statistical analysis procedures used in the data analysis and their interelationships. Reference to these diagrams will be useful in following the various steps described in Chapters 4 and 5.

3.4.1 Analytical Methods - Long Term Fading

To achieve the objectives of section {3.3.1}, the following analytical methods were implemented to describe the long term fading characteristics:

A. *Statistical Filtering* of the (regularly spaced) received signal was carried out to show the average power variations as a function of position along measurement trajectory,

B. *Theoretical Quantile-Quantile* (Q-Q) plots were used to compare the statistical behaviour for various street locations for a given station,

C. *Empirical Quantile-Quantile* (Q-Q) plots were used to compare the statistical behaviour of the vertical and horizontal polarization components.

3.4.2 Analytical Methods - Short Term Fading

In accordance with the objectives of section {3.3.2}, the following random data analysis methods were exploited to study the short term fading data. Computational aspects of these methods are discussed in Appendices A, B, C, D as follows:

- *Probability density function (PDF)* (Appendx A)
- *(Spatial) autocovariance function (ACVF)* (Appendix B)
- *(Spatial) crosscovariance function (CCVF)* (Appendix C)
- *(Spatial) power spectral density function (PSD)* (Appendix D).

3.5 Software Developed for Data Analysis

The software devised for the purpose of data analysis may divided into two two broad types, Basic Data Retrieval Software (BDRS) and Specialized Data Analysis Software (SDAS). These are described in the following subsections. The software operations are described in the form of three block diagrams: the overall structure, Fig. {3.5.1}, the BDRS, Fig. {3.5.2}, and the SDAS, Fig. {3.5.3}.

OVERVIEW OF DATA PROCESSING SOFTWARE

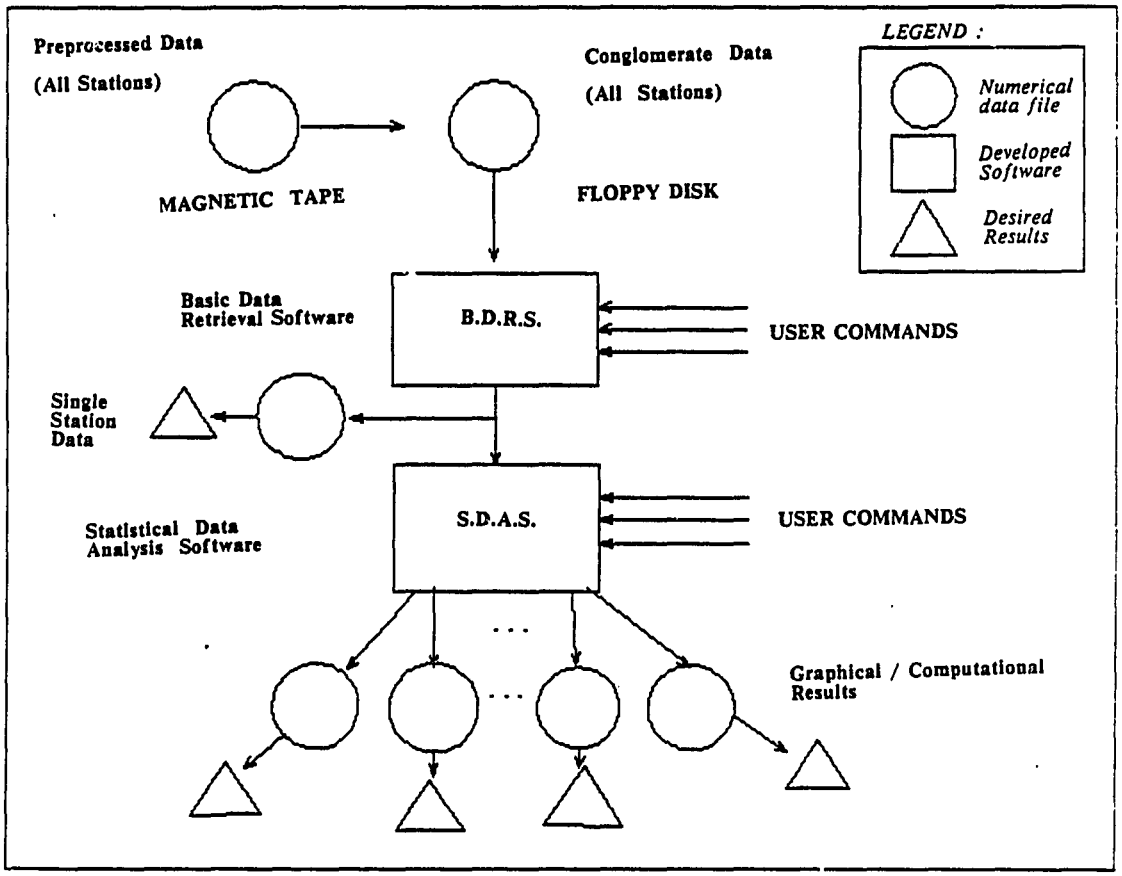

Fig. (3.5.1) Block diagram of data processing software developed.

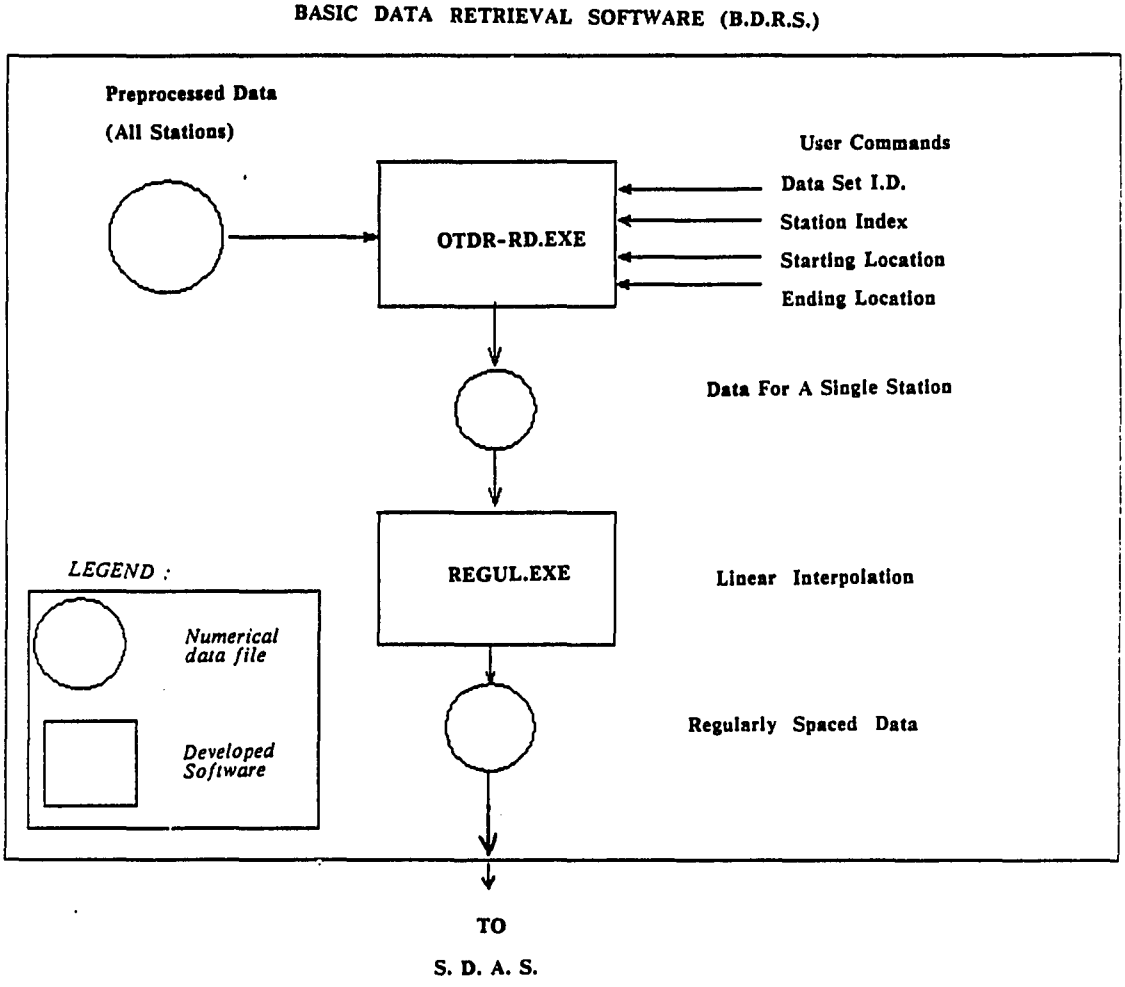

Fig. (3.5.2) Block diagram of data retrieval software (BDRS).

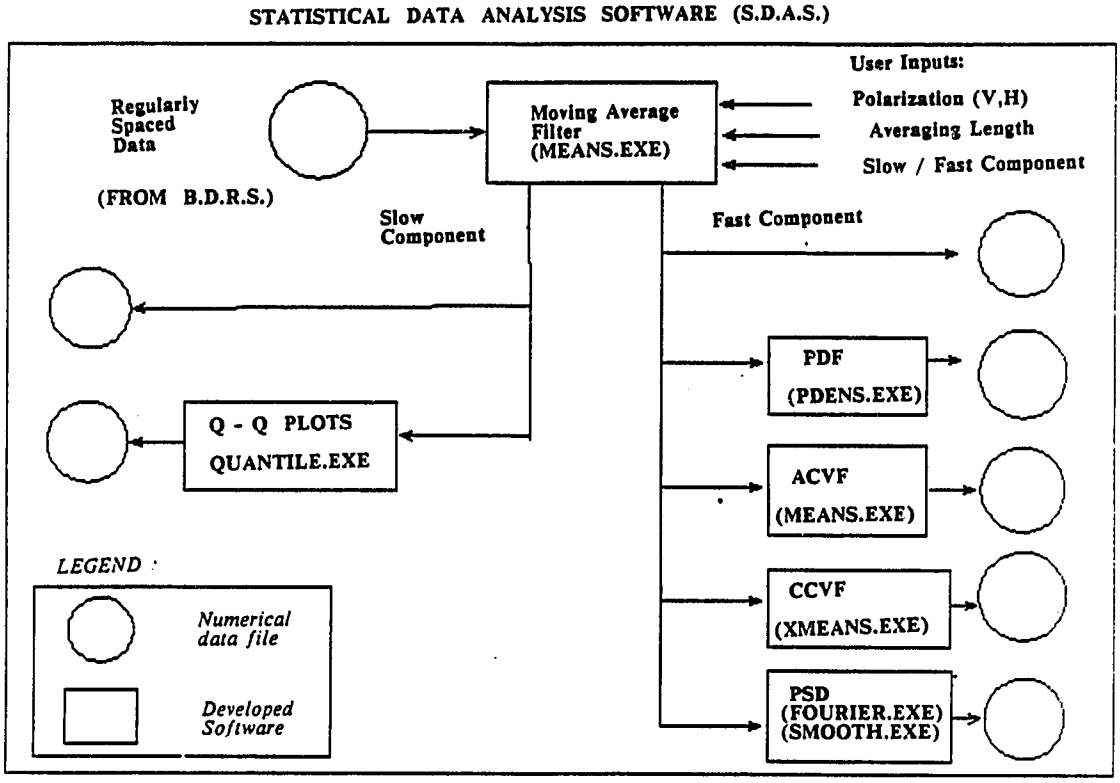

Fig. (3.5.3) Block diagram of statistical analysis software (SDAS).

3.5.1 Basic Data Retrieval Software (BDRS)

A program was needed to retrieve the data for a single station and measurement trajectory from the conglomerate data bank of all the stations, hence the development of the Basic Data Retrieval Software (BDRS). The output file created by the BDRS contains the data for a given station along a selected measurement trajectory. This file will serve as the input to further statistical processing by use of the SDAS (Specialized Data Analysis Software). A block diagram showing the form of the BDRS software is given in Fig. (3.5.2)

BDRS Software (Data Extraction from Conglomerate Data Bank):

OTDR-RD.EXE: Reads the preprocesed data set and writes the data for a desired station along a chosen trajectory to an output file. During program execution, the user enters the measurement data set (date of survey), the station index, the starting location (street and cross street), and the ending location (street and cross street). The program then writes the desired data for all the polarization components to a file.

Storage size: 450 Kbytes

Linear Interpolation on Irregular Data:

REGUL.EXE : Generates equally spaced data points using linear interpolation on the irregularly spaced data.

Storage Size : 95 Kbytes

3.5.2 Specialized Data Analysis Software (SDAS)

In order to perform a statistical analysis of the data, the specialized data analysis software (SDAS) was employed. This section contains a brief catalog of the SDAS software, which includes six programs.

Fig. (3.5.3) shows an overview of the main components of the SDAS software.

Statistical Lowpas Filter for a Single Variable plus Autocovariance Function (ACVF):

MEANS.EXE : This is a statistical lowpass filter for a single variable. The user specifies the filter size in wavelengths and the choice of polarization, i.e., vertical or horizontal polarization. The user also selects either the long term or short term fading component. For the long term fading, the local mean field values (averaging in dB) for the desired polarization are computed and written to a file. If the user selects short term fading, the program writes the short term fading data to a file. The user may also request the computation of the normalized autocovariance function *(NACVF)* for both positive and negative spatial shifts. If such is the case, the theoretical Rayleigh fading correlation curve is computed for comparison with the experimental correlation curve.

Storage Size : 95 Kbytes

Statistical Lowpass Filter for Two Variables plus Crosscovariance Function (CCVF):

XMEANS.EXE : This is a statistical lowpass filter for two variables. The program simultaneously filters both the vertical and horizontal polarizations. The user selects the desired filter size in wavelengths, and the two long term or short term fading signals are written to a file. In the case of short term fading the normalized crosscovariance function (*NCCVF*) for positive and negative spatial shifts may be calculated, and the output written to a file.

Storage Size : 125 Kbytes

Probability Density Function (PDF) plus Best Fit Theoretical Distribution:

PDENS.EXE : Computes the probability density function (PDF) for the short term fading signal. The PDF is computed for the experimental data, the ordinate representing probability betwen 0.00 and 1.00, while the abcissa represents the magnitude of the short term fading in decibels (or volts). The user enters the resolution of the PDF by setting an appropriate bin size. The user may choose to compute of the central of moments of the experimental PDF. If this is the case, the coefficients of skeweness and kurtosis are computed from the higher order moments of the experimental PDF. If desired, the user may choose a best fit statistical distribution to model the experimental distribution. (A choice of six possible theoretical distributions are given: Gaussian, Rayleigh, Lognormal, Rician, Log-Rician, and a combination of the Lognormal and the best fit Log-Rician ("CLNLR" as described in Chapter 5). The last three distributions involve optimizing the linear correlation coefficient between the experimental and theoretical PDFs.

Storage Size : 108 Kbytes

Theoretical (or Empirical) Quantile-Quantile (Q-Q) Plots:

QUANTILE.EXE : Prepares the (slow or fast fading) data for an empirical [3.5] or theoretical Q-Q plot [3.6]. These are useful probability plots for comparing the behaviour of two cumulative distributions.

Storage Size : 95 Kbytes

Discrete Fourier Transform and Power Spectral Density:

FOURIER.EXE: Computes the (unsmoothed) power spectrum of the short term fading by direct evaluation of the DFT (and not by the correlation function). Normalization to spectral density is carried out by dividing the square magnitude at each frequency by the total spectral power. Both magnitude and phase are computed. The software processes two signal records (vertical and horizontal polarization) simultaneously.

Storage Size : 65 Kbytes

Smoothed Spectral Estimate of Power Spectral Density (PSD):

SMOOTH.EXE : Smooths the power spectral density (PSD) magnitude (or phase) using a smoothing window. The user enters the window size which is a percentage of the total number of samples. The user chooses from four possible smoothing windows: Rectangular, Hanning, Hamming, Blackman [3.7].

Storage Size : 55 Kbytes

3.6 Concluding Remarks

This chapter has shown that despite the large number of measurements, analysis may be carried out on a microcomputer (PC). Operating in a PC environment has the advantages of easier data management and lower operating costs.

To operate effectively on a PC, however, it is recommended that the *minimum* microcomputer hardware requirements be : (1) a fixed internal disk (greater than 10 Mbyte), (2) a 16/32 bit microprocessor (e.g. Intel 8286), (3), a 16/32 bit math co-processor (e.g. Intel 8287), (4) a 640 Kbyte RAM, (5) an Enhanced Graphics Adapter (EGA) card, (6) at least one double density (360 K) disk drive.

3.7 End Notes

[3.1] F77L Fortran is a trademark of Lahey Computer Systems, Inc.

[3.2] SSP/PC is a scientific subroutine software library adapted for microcomputers.

[3.3] Special built-in features include polynomial, cublic spline interpolation, and best fit linear regression. These features were found to be particularly helpful for carrying out the data analysis.

[3.4] The technique of signal averaging in decibels is discussed in, **B.R. Davis and R.E. Bogner**, "Propagation at 500 MHz for Mobile Radio", *Proc.IEE Pt. F*, August 1985, p. 316.

[3.5] Theoretical and empirical Q-Q plot construction techniques are discussed in, **J.M. Chambers, W.S. Cleveland, B. Kleiner, and P.A. Tukey**, *Graphical Methods for Data Analysis*, Boston, Duxbury Press, 1983.

[3.6] The method of constructing a *Gaussian* Q-Q plot is described in, **J.M. Chambers et al.**, *Graphical Methods for Data Analysis*, 1983, p.227, Table 6.5.

[3.7] The four smoothing windows are discussed in, **A.V. Oppenheim and R.W. Schafer**, *Digital Signal Processing*, New York, McGraw-Hill, 1975, pp.239-250.

Chapter 4:

LONG TERM FADING CHARACTERISTICS

4.1 Introduction

This chapter presents the spatial long term fading (SLTF) characteristics of the FM transmitter signals in an urban micro-environment [4.1].

As described in Chapter 1, the received signal consists of a rapidly varying signal superimposed on a slowly varying signal. Spatial long term fading (SLTF) refers to the slow variations of the received signal at the mobile receiving antenna.

As the receiving antenna moves along an urban street, spatial long term fading effects are encountered at the mobile. The SLTF effects arise mainly from signal obstructions produced by intervening hills, buildings, trees, and other natural or man-made obstacles. The intervening obstacles produce shadowed regions in which the average power at the mobile drops relative to unobstructed regions.

Since the SLTF signal is an indicator of local average power variations, the study of long term fading helps to probe the influences of the surrounding environment. Such probing can increase the understanding of the nature of propagation in the presence of man-made structures.

Fig. {4.1.1(a)} shows a sample signal (field strength) profile as recorded by a mobile receiver travelling along a typical city street, University Street from Sherbrooke to Northend (see Fig.{2.7.2.2}), for the vertical polarization of an elevated broadcast transmitter, station CKOI [4.2]. The dashed line represents the long term fading signal, obtained using a moving average statistical filter, and is reproduced in Fig. {4.1.1.(b)} for the sake of clarity. More will be said of the filtering technique in section {4.1}.

From Fig. {4.1.1.(b)}, it is evident that the long term fading component represents the *trend information* of the received signal. The trend shows where the average power is higher (less obstructed region), where it is lower (more obstructed region), and the regions in transition from more to less obstruction. It also shows the amount of power

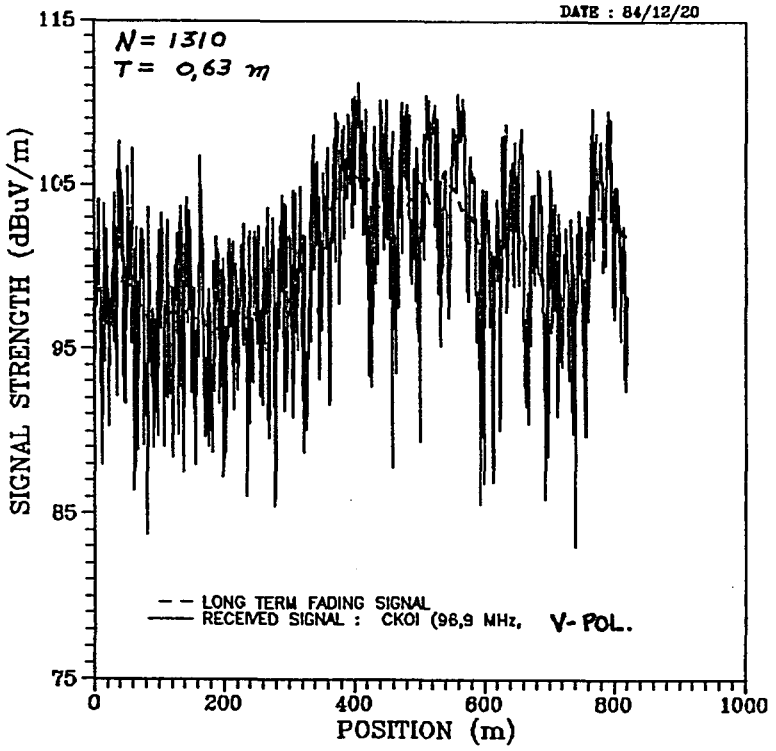

(a) *Received signal strength profile* measured on University Street (route #1, second survey). Station CKOI (96,9 MHz), Vertical polarization. Dashed line shows long term fading component.

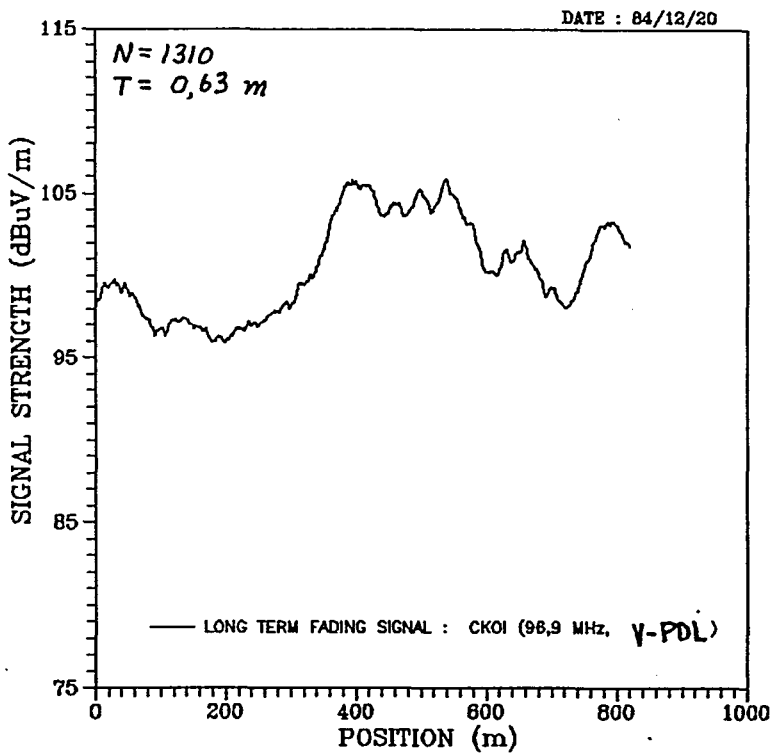

(b) *Spatial long term fading (SLTF) profile of received signal, obtained by moving averages.* (Averaging computed over twenty wavelengths, k=103 consecutive samples, spaced at 0,63 m intervals).

Fig. (4.1.1)

loss as compared to a less obstructed region. This helps to identify the amount of shadow loss in an obstructed region. Such considerations of the fading pattern are of interest in this chapter, and further examples will be given to illustrate certain effects.

It is evident that many factors contribute to the propagation between a base transmitter and a mobile receiver in urban environments. Davis and Bogner [4.3] concluded the following:

> *"because of the number and complexity of factors influencing the propagation to a vehicle, and because weather and time of day were not found to be significant influences, it was concluded that experimental assessment is a cost effective method for determining accurately a service area".*

The present chapter is motivated by precisely such an experimental assessment to investigate the long term fading conditions of FM broadcast signals in an urban micro-environment. The FM transmitter signals are used as test signals because they can provide ready insight into local building shadow effects, the effects of transmitter location, and the effects of street orientation [4.1]. Extension of similar measurements to other frequency ranges (especially the 800/900 MHz cellular band), and to other urban areas is indicated in order to provide a broader base of data for comparison and understanding.

The present chapter considers the following aspects of spatial long term fading as encountered in an urban micro-environment:

(a). Identification and Quantification of Shadow Zones,

(b). Effect of Different Transmitter Locations,

(c). Effect of Street Shadowing,

(d). Effect of Street Orientation,

(e). Comparison of Polarization Behaviour.

The data analysis methods are discussed in section (4.2), and the results are presented in section (4.3). A short chapter summary is given at the end.

4.2 Methods of Data Analysis

4.2.1 Method of Generating Regularly Spaced Samples

Since the long term fading signal is estimated by averaging an equal number of samples to the left and to the right of the local mean field strength, it is preferable to use evenly spaced samples. This ensures that the estimate of the mean value is based on an equal weighting of samples to the left and to the right of the local mean. In actual practice, field strength data is not recorded at exactly evenly spaced intervals on any given street. This gives rise to the need for generating an evenly spaced set of data from the actual data.

In order to generate regularly spaced data from the actual irregularly spaced data, a linear interpolation procedure was carried out on the received signal. The value of the field strength at evenly spaced intervals was (linearly) interpolated by a point to the left and to the right of it. The effect of linear interpolation on the received signal is that only the relative position of the peaks and valleys may be offset, however the cumulative distribution (CDF) is essentially unchanged from that of the orginal data.

Having carried out the interpolation procedure described, the field strength data was filtered statistically to separate the long term and short term fading components. The filtering procedure is described below.

4.2.2 Method of Estimating the Local Mean Field Strength

The long term fading behaviour can be estimated by averaging a suitable number of statistically independent samples over an appropriate averaging length. The choice of the averaging length is a compromise between loss of trend information on the one hand, and of reducing statistical uncertainty in the estimate of the local mean, on the other.

Assuming the short term fading has a Rayleigh distribution [4.4], Lee [4.5] reported that the local average power of a mobile radio signal can be estimated with a standard deviation of 1,56 dB using an averaging length (2L) of 20λ. Lee's method states that the sufficient number of statistically uncorrelated samples, for estimating the local average power, is 36 based on a 90 percent confidence interval [4.5].

In view of Lee's method [4.5] and that of Davis and Bogner [4.6], it was decided to adopt a consistent strategy of averaging the decibel field values over an interval of 20 wavelengths at the measured frequency. In principle, if the short term fading is Rayleigh distributed, averaging the decibel field strengths gives a value of about 2,5 dB lower than averaging the power (in watts) and then converting to decibels [4.6].

If the (short term fading) distribution is not exactly Rayleigh, the difference between the two averages might differ by 2,5 dB. In analyzing propagation measurements at 500 MHz, Davis and Bogner [4.6] reported a difference of about 2 dB with a standard deviation of the order of 0,5 dB for the residual difference of the two averaging methods. Davis and Bogner thus conluded that either method of averaging may be used to represent local field strengths [4.6].

We shall use a minimum of 36 uncorrelated samples, to estimate the local mean. The following discussion relates to estimating the local mean field strength, $m(i)$, from the discrete samples of the received signal, $r(i)$.

It is well known [4.7] that the mobile radio signal, $R(x)$, can be modeled as a multiplicative (in voltage) random process of a long term fading random process, $M(x)$, and a short term fading randm process, $S(x)$, Eq. (4.2.1):

$$R(x) = M(x) \cdot S(x) \quad V/m \qquad (4.2.1)$$

In practice, the received signal is recorded in logarithmic (decibel) units (dBμ V/m) rather than voltages. Denoting the decibel field strengths by $r(x)$, $m(x)$, and $s(x)$, Equation (4.2.1) becomes,

$$r(x) = \{m(x) + s(x)\} \qquad dB\mu V/m \tag{4.2.2}$$

In Eq. (4.2.2), it is desired to represent the true local mean field strength, $m(x)$, by some value, $\hat{m}(x)$, given knowledge of $r(x)$, *a priori*.

Realizing that $m(x)$ is described by the slow variations in the received signal, $r(x)$, the concept of *statistical lowpass filtering* can be used to advantage. Denoting the spatial impulse response of the filter by $h(x)$, the local mean $\hat{m}(x)$ can be estimated from $r(x)$ as follows, where $2L$ is the spatial averaging length. Thus,

$$\hat{m}(x) = \frac{1}{2L}\int_{z=x-L}^{z=x+L} h(x-z)\cdot r(z)dz \tag{4.2.3}$$

In practice, the impulse response, $h(x)$, is a unit multiplier, leaving the integration over the received envelope, $r(x)$ (expressed in decibels). An averaging length of twenty wavelengths will be used throughout:

$$2L = 20\lambda \tag{4.2.4}$$

The discrete variable expression for the local mean estimate is obtained by replacing the continous spatial index (x) by the discrete spatial index (i), and by replacing the integration by summation in Eq. (4.2.3). This gives,

$$\hat{m}(i) = \frac{1}{2L+1}\sum_{j=-L}^{j=L} r(i+j) \tag{4.2.5}$$

where the summation is performed over L samples to the left and L samples to the right of the local mean.

4.2.3 Quantile-Quantile Plots

Quantile-Quantile (or Q-Q) plots [4.8] are a useful way of comparing the statistical behaviour of two sets of data, a common need in exploratory data analysis [4.9]. A Q-Q plot gives a visual comparison of the CDF behaviour of one random variable (Y) versus the CDF behaviour of a second random variable (X).

On a Q-Q plot, the similarity of the statistical behaviour between the X and Y distributions is indicated by the straightness of the data points on a line. If all the data points are found to lie on a straight line of unity slope, $y = x + B$, the distributions have identical behaviour except for a possible difference in the median value (indicated by the value of B). Similarly, if the slope is less than one, the variability in X is greater than that of Y, and vice versa if the slope is greater than one.

The Q-Q plot technique allows various parameters (e.g., minimum, median, maximum) to be determined rather easily by way of visual inspection. It also facilitates a comparison between an experimental distribution and a theoretical distribution (such as Gaussian, for example), by realizing that any departure from linearity indicates the extent to which the distributions differ. Such a Q-Q plot is often referred to as a *theoretical Q-Q plot* [4.10]. In contrast, an *empirical Q-Q plot* [4.11] allows a similar comparison, except that in this case, the second distribution is another experimental distribution. A recent theoretical development [4.12] indicates the value of such techniques in exploratory data analysis.

In the course of the present work, both the *theoretical* and *empirical* Q-Q plots are used to study the long term fading data. The theoretical and empirical Q-Q plots allow, for example, (i), the comparison of the shadow effects between different street locations, and (ii), a comparison of the statistical behaviour of the vertical and horizontal polarization components. These comparisons are described in sections {4.3.3} and {4.3.5} respectively.

4.3 Results

The long term fading results are categorized into five sections as follows:

Section {4.3.1} : Identification of Shadow Zones,
Section {4.3.2} : Effect of Different Transmitter Locations,
Section {4.3.3} : Shadowing Effect Comparison between Street Locations,
Section {4.3.4} : Effect of Street Orientation,
Section {4.3.5} : Comparison of Polarization Behaviour.

The results are mainly presented as graphs displaying the SLTF patterns for different street locations of the micro-environment.

4.3.1 Identification of Shadow Zones

Figure {4.3.1.1} shows a graph of the spatial long term fading (SLTF) patterns of station CKOI, vertical and horizontal polarization, on the campus route from Roddick Gate to Milton Gate, a photograph of which is shown in Fig. {2.7.2.2}.

As indicated on the graph, the sample spacing is T=0,52 m (or 0,17λ) and the total number of samples is N=721. The number of consecutive samples in estimating the local mean field strength is k=119, as obtained for an interval of twenty wavelengths.

According to Davis and Bogner [4.13] and Lee [4.5], the number of *uncorrelated* samples in the interval *2L* determines the uncertainty to which the local mean is estimated. In this case, the samples are taken at T=0,52 m intervals and are correlated until about 0.8λ [4.14], which in this case is about 2,5 m (or about 5T). Thus in this set of k *consecutive* samples, there are roughly 0,2k *independent* samples.

Assuming for the moment that $s(x)$ has a Rayleigh distribution with a standard deviation of about 5,6 dB [4.13], the standard deviation of $\hat{m}(i)$ due to $s(i)$ should be about $5{,}6/\sqrt{0{,}2k}$. Hence, for k=119, the standard deviation of $\hat{m}$ due to s should be of the order of 1,1 dB.

This shows that the statistical uncertainty in the local mean field strength decreases as the number of uncorrelated samples in estimating the mean increases

[4.15]. Generally speaking, if 36 or more uncorrelated samples are averaged, the local mean will be estimated with a standard deviation of about 1 dB [4.5].

As seen in Fig. (4.3.1.1), the SLTF patterns on the trajectory of the station shows that the signal strength decreases slowly upto about 200 meters (in a radially outward line-of-sight (LOS) region) beyond which the pattern shows a rapid decrease of almost 17 dB from 200 m to 375 m. This rapid decrease in average signal strength can be attributed to the shadowing of the MacDonald Engineering Bldg. (bldg. 77) as indicated on the map, Fig. (2.7.1.2).

As seen by the graph, the patterns for both polarizations are almost identical except for a shift in magnitude because of higher signal power in the horizontal plane.

The local mean variations thus can be used to estimate the location of shadow regions and the amount of the shadow from surrounding buildings.

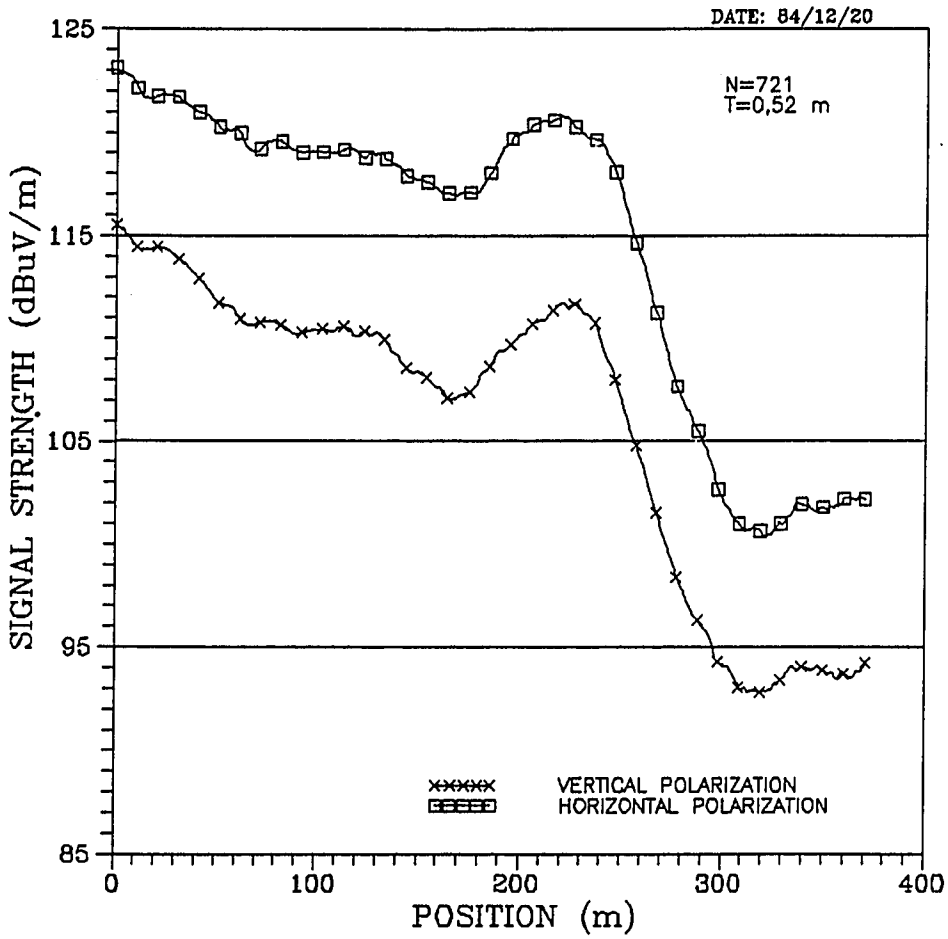

Fig. (4.3.1.1) *Spatial long term fading (SLTF) patterns showing shadow zone* (on route #2, second survey). Station CFQR (92,5 MHz), vertical and horizontal polarization. The received signal profiles (not shown) were averaged over twenty wavelengths (k=119 *consecutive samples*) using regularly spaced data.

4.3.2 Effect of Transmitter Locations

Fig. {4.3.2.1} shows the SLTF patterns for three FM transmitters (CFQR,CK-OI,CITE) on the route from Roddick Gate to Milton Gate, vertical polarization [4.1]. The three transmitters are located at different points in the city, as indicated in Table {2.2.1}.

Figure {4.3.2.1} shows that the pattern corresponding to the CKOI transmitter, located approximately 2 km southwest of the CFQR transmitter on the corner of Peel Street and Dorchester Blvd., is quite different from that of CFQR, or even that of station CITE, whose transmitter is located to the east. The differences in the observed SLTF patterns can be attributed to the obstructions produced by different buildings for each transmitter.

For example, in the case of station CKOI, the amount of shadowing can be seen by the 18 dB drop between 200 m and 375 m. This value is greater than that of the shadow of the CFQR signal (about 8 dB), whose transmitter is located diametrically opposite. The difference can be attributed as follows. In the case of CKOI (h=217 m), the shadowing can be attributed to the MacDonald Engineering Building, with an average height of about 70 m above sea level. In the case of CFQR (h=298 m), the shadowing is attributed to the Cyril James and Physical Plant Buildings, at about the same average height above sea level. Thus, the relative height of the CFQR transmitter is roughly (298 m - 70 m) = 228 m with respect to the shadowing obstacle, whereas the relative height of the CKOI transmitter with respect to its shadowing obstacle is roughly (217 m - 70 m) = 157 m. This shows that the greater the transmitter height relative to the shadowing obstacles, the lower the amount of shadowing produced by the obstacle for a receiver stationed behind it.

For comparison, the pattern corresponding to the CITE transmitter is shown. The pattern for the CITE transmitter, which is east of the CFQR trasnmitter, is opposite in shape to the other two transmitters - that is, its shadow zone corresponds to the region before 275 m while the unshadowed zone is in the region after 275 m. The shadow zone in this case is produced by the buildings bordering on the west side of University Street on the lower campus, which in fact, do not produce shadows for either the

CFQR or the CKOI transmitters on the corresponding route. Hence the difference in behaviour of the CITE transmitter.

In the region beyond 250 m, the shadowed region of the CFQR and CKOI transmitters correspond to an unshadowed region for the CITE transmitter, as this region is apparently unobstructed from the source.

Fig. {4.3.2.2} illustrates the corresponding behaviour for the horizontal polarization. The results indicate that the SLTF behaviour of the horizontal and vertical polarization is quite similar [4.1]. This suggests the possibility of using the horizontal polarization for mobile propagation [4.16].

All the fading patterns shown in Figs. {4.3.2.1} and {4.3.2.2} were obtained by averaging the number of samples contained in an interval of twenty wavelengths at the frequency measured. For example, the number of consecutive samples used in the averaging for stations CFQR (92,5 MHz), CKOI (96,9 MHz), and CITE (107,3 MHz) were 125, 119, and 108, respectively.

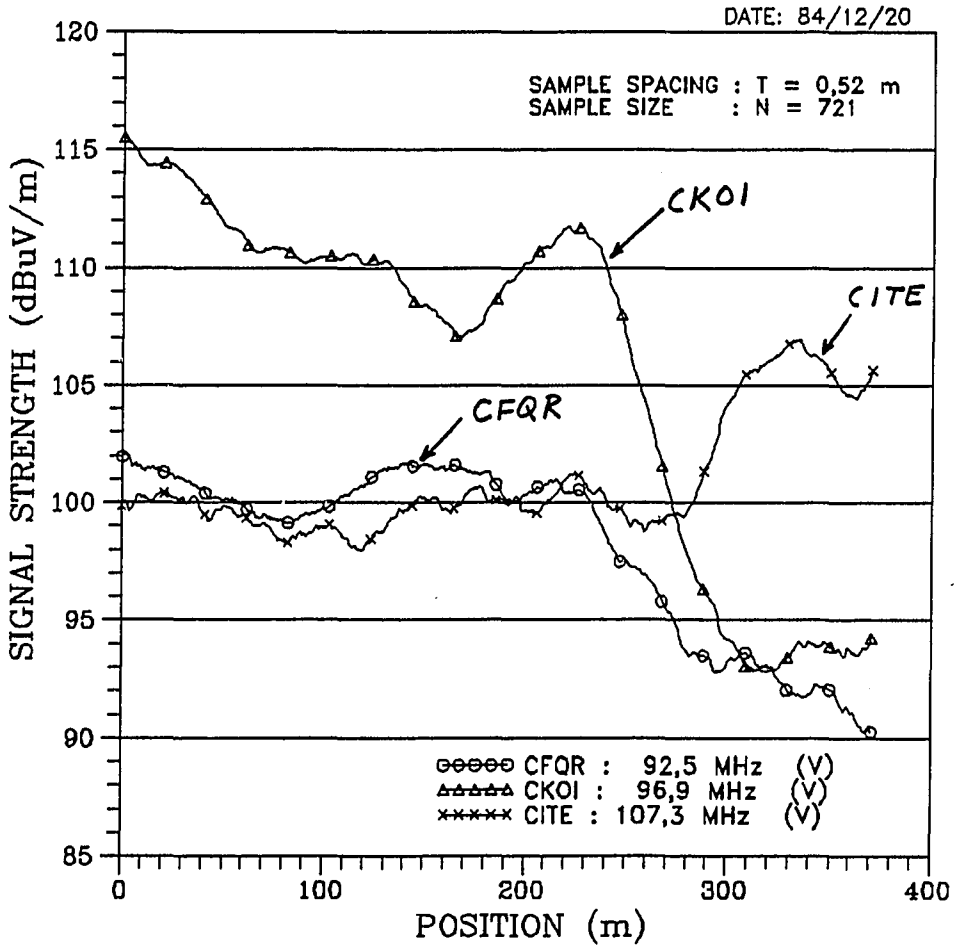

Fig. (4.3.2.1) *Effect of transmitter location illustrated by SLTF patterns of three FM transmitters* (CFQR,CKOI,CITE). Route #2, second survey. Vertical polarization.

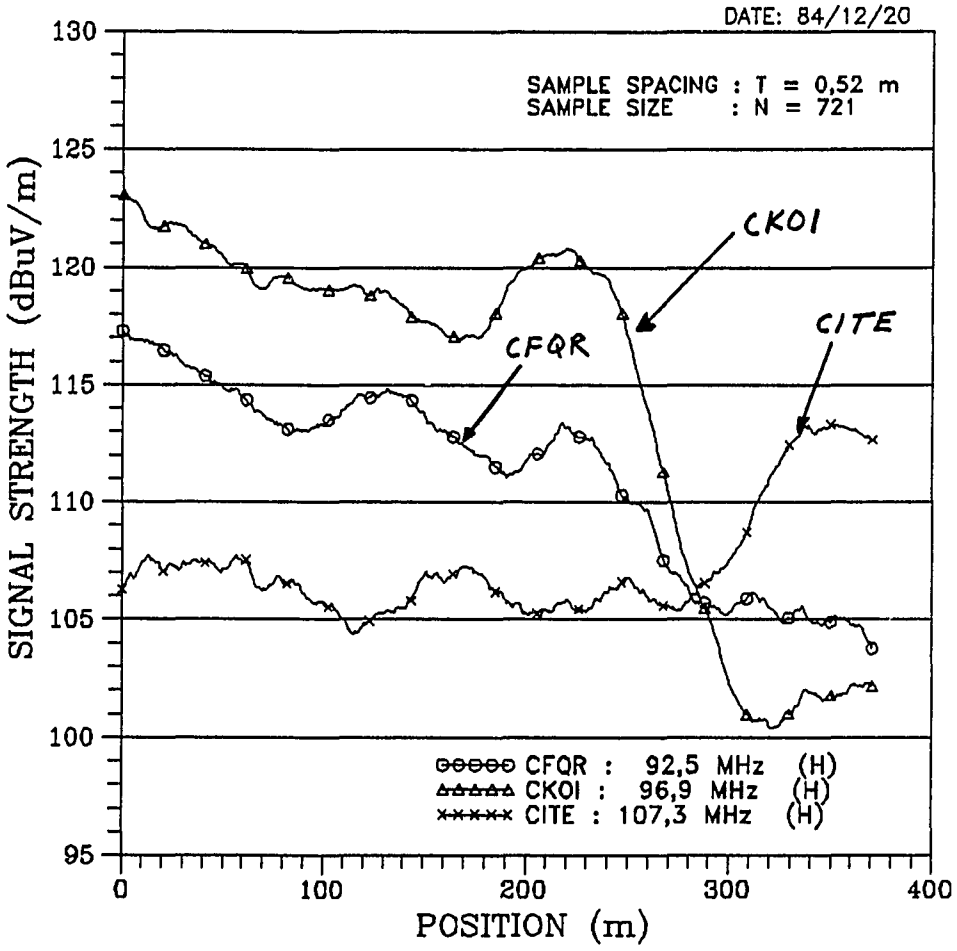

Fig. (4.3.2.2) *Effect of transmitter location illustrated by SLTF patterns of three FM transmitters* (CFQR, CKOI, CITE). Route #2, second survey. Horizontal polarization.

4.3.3 Shadowing Effect Comparison between Street Locations

This section presents experimental results of the shadow effects compared between individual streets [4.1]. Both the vertical and horizontal polarizations are considered.

The method of estimating the shadow effect is the comparison of median long term fading (LTF) field strengths. The theoretical Q-Q plot technique [4.10] described eariler facilitates a comparison of both the median levels as well as the variability.

Shown in Figure {4.3.3.1} is a sample Q-Q plot for the SLTF statistics of station CFQR (92,5 MHz). The graph shows 6 cumulative distributions corresponding to three streets (#1,#2,#3 of second field survey) and two polarizations (vertical and horizontal). The *median value* can be extracted from this type of plot by taking the ordinate corresponding to the zero abcissca value, i.e., the 50th percentile.

Similar graphs (not shown) were plotted for other stations, and their median values were likewise obtained.

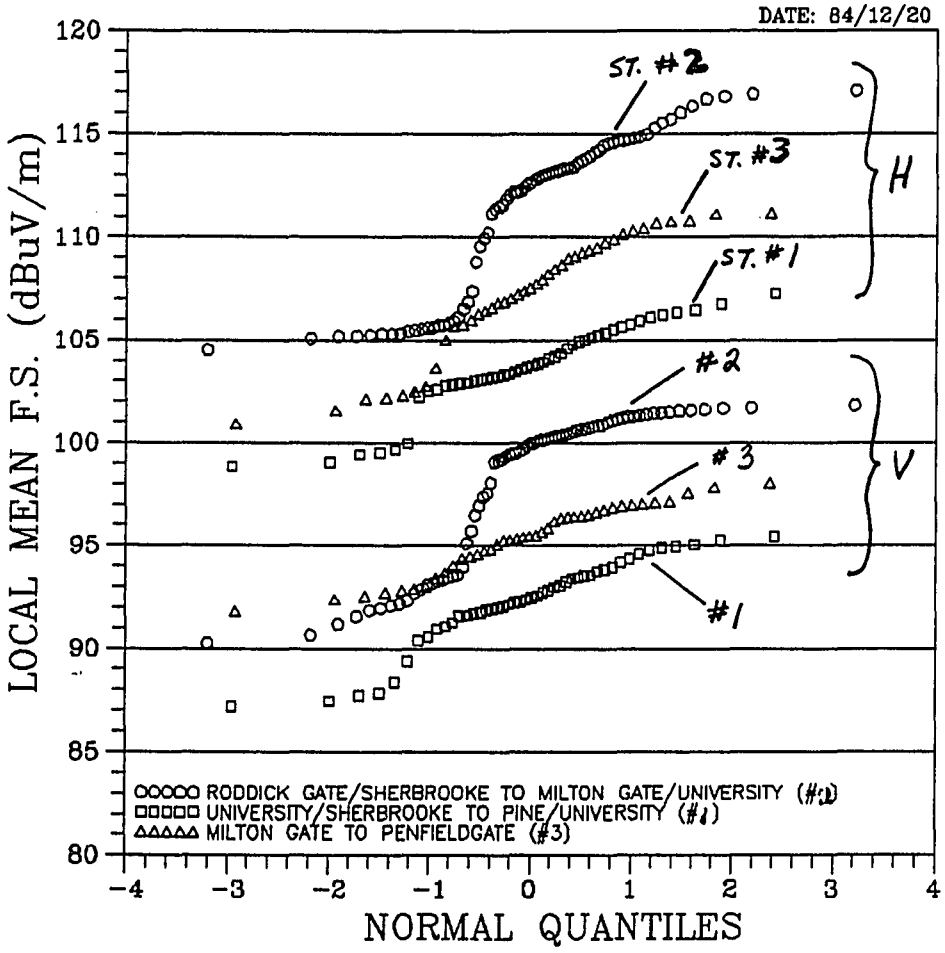

Fig. (4.3.3.1) *Shadowing in a micro-environment illustrated by a Gaussian (normal) theoretical Q-Q plot.* The plot shows vertical and horizontally polarized LTF data measured on 3 parallel streets (routes #1,#2,#3, second survey), station CFQR (92,5 MHz). Median field strengths correspond to the Z=0 quantile (i.e. 50th percentile).

Since the three streets are roughly parallel and of roughly equal mean distance from the transmitter, the median field strength indicates the extent to which a built-up street is shadowed relative to an open area.

For example, street #2 is relatively unobstructed from the Mt. Royal transmitter (see Fig. (2.7.2.3)) whereas street #1 is more obstructed by buildings (see Fig. (2.7.2.2)). Thus, in comparing the median field strengths for station CFQR (located on Mt. Royal) of street #2 (100,0 dBuV/m) versus that of street #1 (92,5 dBuV/m), the median indicates that street #2 is less obstructed than street #1. It is therefore evident that the *median LTF field strengths can be used as an indicator of shadowing among parallel streets*, provided that the streets are at roughly equal mean distance from the source.

Tables (4.3.3.1) and (4.3.3.2) summarize the median LTF field strengths for the vertical and horizontal polarization for four FM transmitters (CFQR,CKMF,CK-OI,CITE) as measured on three trajectories (#1,#2,#3) on the McGill University campus.

Table (4.3.3.1).Median LTF field strengths in dBμV/m on three campus streets, vertical polarization. Second survey.

Station I.D.	Street (#1) N=1310, 850 m	Street (#2) N=721, 380 m	Street (#3) N=283, 260 m
CFQR	92,5	100,0	95,5
CKMF	92,5	99,0	96,0
CKOI	98,0	109,0	97,5
CITE	100,0	100,0	102,0

Table (4.3.3.2).Median LTF Field Strengths in dBμV/m on three campus streets, Horizontal Polarization. Second survey.

Station I.D.	Street (#1) N=1310, 850 m	Street (#2) N=721, 380 m	Street (#3) N=283, 260 m
CFQR	104,0	113,0	107,5
CKMF	103,0	112,5	107,0
CKOI	105,0	118,0	105,5
CITE	107,0	106,0	108,5

To evaluate the data in Tables (4.3.3.1) and (4.3.3.2), a 'scatter plot' [4.17], is helpful in showing the median values for all four stations and for both polarizations, given in Fig. (4.3.3.2).

The scatter plot affords a convenient manner of studying the median field strengths of the three streets. On this type of plot, similarity in behaviour between the ordinate and the abcissa is indicated by the closeness of the data points to the line $y=x$.

In Fig. (4.3.3.2), the line $y=x+10$ is superimposed, as the horizontal polarization median field strengths are about 10 dB higher than those of the vertical polarization. In such case, the distance of points away from the line indicates dissimilar behaviour when comparing the data of the three streets. On the other hand, if the data points lie close to the line $y=x+10$ for all three streets, the meaning is that the median difference between the horizontal and vertical components is always about 10 dB.

From the graph, it can be seen that for the case of CFQR, the behaviour for street 2 shows the largest distance from the line, whereas street 1 is closest to the line. This suggests that on street 2, the horizontal polarization to vertical polarization power ratio (given by the difference in dB) is larger than it is on street 1. The same behaviour is observed for station CKMF, also located on the Mt. Royal antenna tower.

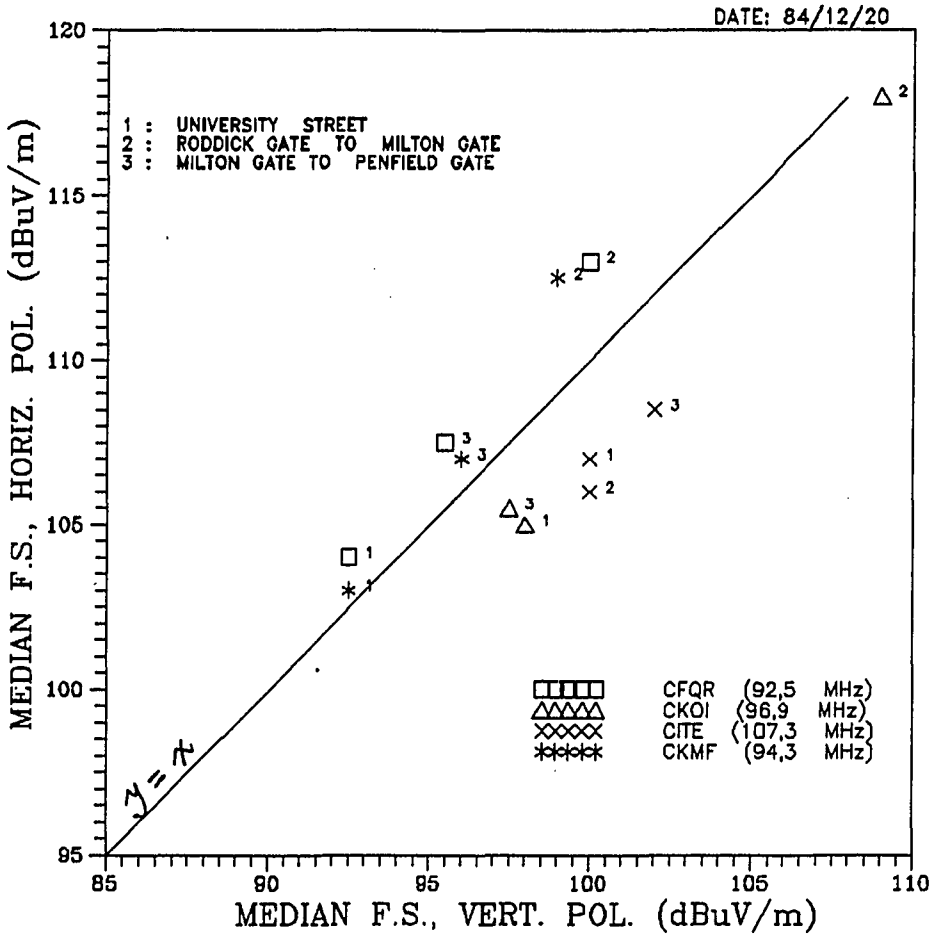

Fig. (4.3.3.2) *Shadowing in a micro-environment illustrated by a scatter plot.* The plot shows the median LTF field strengths of the vertical and horizontal polarizations on 3 parallel streets (routes #1,#2,#3, second survey) for 4 FM stations: CFQR (92,5 MHz), CKMF (94,3 MHz), CKOI (96,9 MHz), CITE (107,3 MHz).

The shadow effect between different streets can also be evaluated graphically on this type of plot. For example, for station CFQR, a median difference of 7,5 dB between streets 2 and 1 is obtained for the vertical polariazation, whereas a median difference of 4,5 dB is obtained between streets 2 and 3. Relating these numbers to the street building density, one finds that the median values are reasonable in suggesting that street 2 is the least shadowed, and that street 1 is the most shadowed. Hence, the scatter plot provides a convenient evaluation of the shadow effect among parallel streets.

It is interesting to note that the behaviour for CKMF is almost identical to that of CFQR. This is because the CKMF and CFQR transmitters are colocated at equal heights, are of equal radiated power, and have similar antenna patterns. The data for stations CKOI and CITE reveal that the shadow effects are different for transmitters located at different points in a city.

Tables {4.3.3.3} and {4.3.3.4} compare the median LTF field strengths for station CFQR, vertical and horizontal polarizations respectively, as measured in two independent field surveys on similar paths (see maps, Figs. {2.7.1.1} and {2.7.1.2}).

Fig. {4.3.3.3} shows a scatter plot of the data in Tables {4.3.3.3} and {4.3.3.4}. As with Fig. {4.3.3.1}, behavioural similarity betwen the ordinate and the abcissa is indicated by the closeness of the data points to the line $y=x$. Therefore, from Fig.{4.3.3.3}, it is evident that the median field strengths of the LTF data are practically the same for both surveys. In other words, it is evident from the data that the *median LTF values are essentially independent of time for a given street location.* Other stations also indicate that the median LTF field strengths are nearly reproducible (to within +/- 2,0 dB).

In an experimental study of propagation measurements at 500 MHz, Davis and Bogner [4.18] reported that the propagation was not significantly influenced by weather and time of day, showing similar behaviour with the present findings:

> *"the measurements of field strength show good repeatability, independently of time of day and weather conditions, provided that local fast fading effects are averaged out"*

Table (4.3.3.3). Comparison of median LTF field strengths (dBμV/m) for two independent field surveys, Vertical Polarization. Station CFQR (92,5 MHz).

Street I.D.	March 1983 (V) Median F.S.	December 1984 (V) Median F.S.	Difference (dB) (1983-1984)
1	93,0	92,5	+ 0,5 dB
2	102,0	100,0	+ 2,0 dB
3	95,5	93,5	+ 2,0 dB

Table (4.3.3.4). Comparison of median LTF field strengths (dBμV/m) for two independent field surveys, Horizontal Polarization. Station CFQR (92,5 MHz).

Street I.D.	March 1983 (V) Median F.S.	December 1984 (V) Median F.S.	Difference (dB) (1983-1984)
1	104,0	104,5	0,0 dB
2	112,5	113,0	- 0,5 dB
3	106,5	107,5	- 1,0 dB

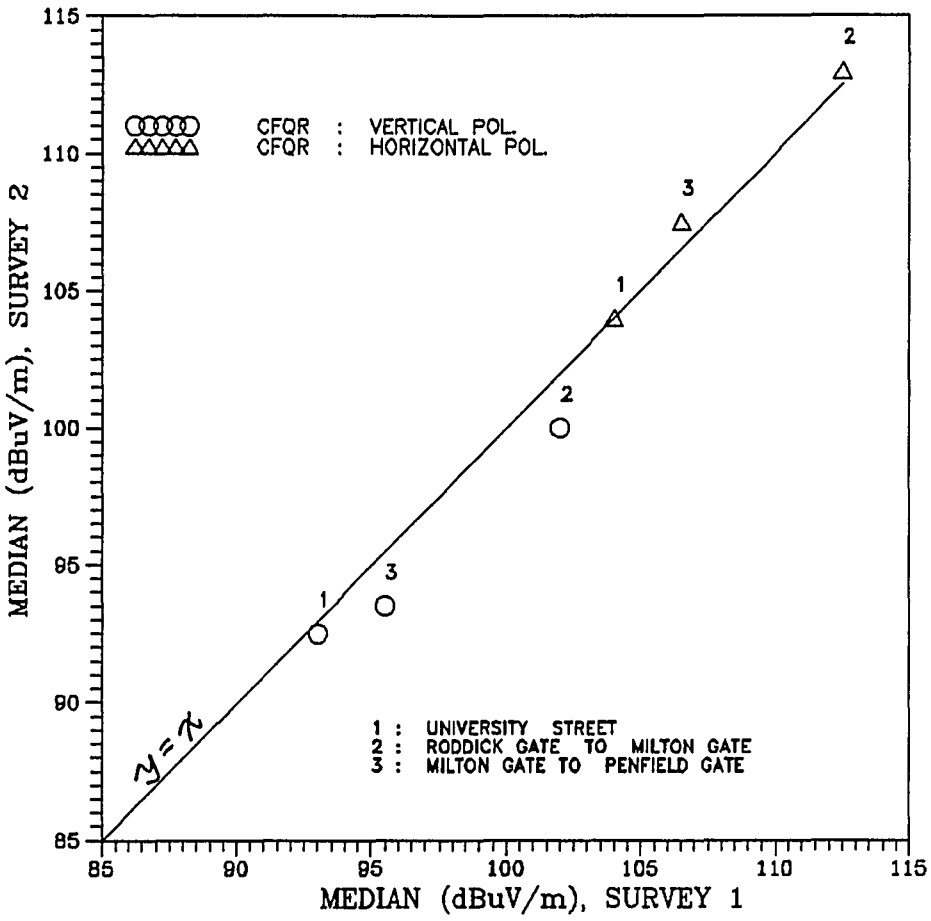

Fig. (4.3.3.3) Comparison of median LTF field strengths from two independent surveys (March 1983, December 1984) illustrated by a scatter plot. The plot shows the data for three parallel streets (routes #1,#2,#3), vertical and horizontal polarization. Station CFQR (92,5 MHz).

4.3.4 Effect of Street Orientation

Fig. (4.3.4.1) shows the SLTF patterns for stations CFQR and CKOI on Peel Street going towards Sherbrooke Street, a radially directed street for each transmitter.

A photograph of Peel Street showing the CKOI transmitter is given in Fig. (2.4.2). In the case of CFQR, the receiver moved away from the transmitter, while in the case of CKOI, the receiver moved towards the transmitter. The fading patterns are consistent with the monotonic increase (or decrease) in average power as expected on a radial path.

Fig. (4.3.4.2) shows the SLTF patterns for the same two stations on arc-directed scan. In one case, the transmitter (CFQR) is located to the right of the receiving antenna, while in the other case (CKOI) the transmitter is located to the left of the receiving antena. In both cases, the receiving antenna moved along an arc of nearly constant radius from the transmitters.

As seen by Fig. (4.3.4.2), the behaviour for both stations is practically constant as expected from an arc-oriented street. The behaviour deviates slightly for station CKOI near the start and end of the street which corresponds to shadowed regions. At these locations the CKOI transmitter is shadowed by buildings whereas the CFQR transmitter is not, because its location is in the opposite direction, there are no shadowing obstacles, and therefore the field behaviour for the two is different [4.1].

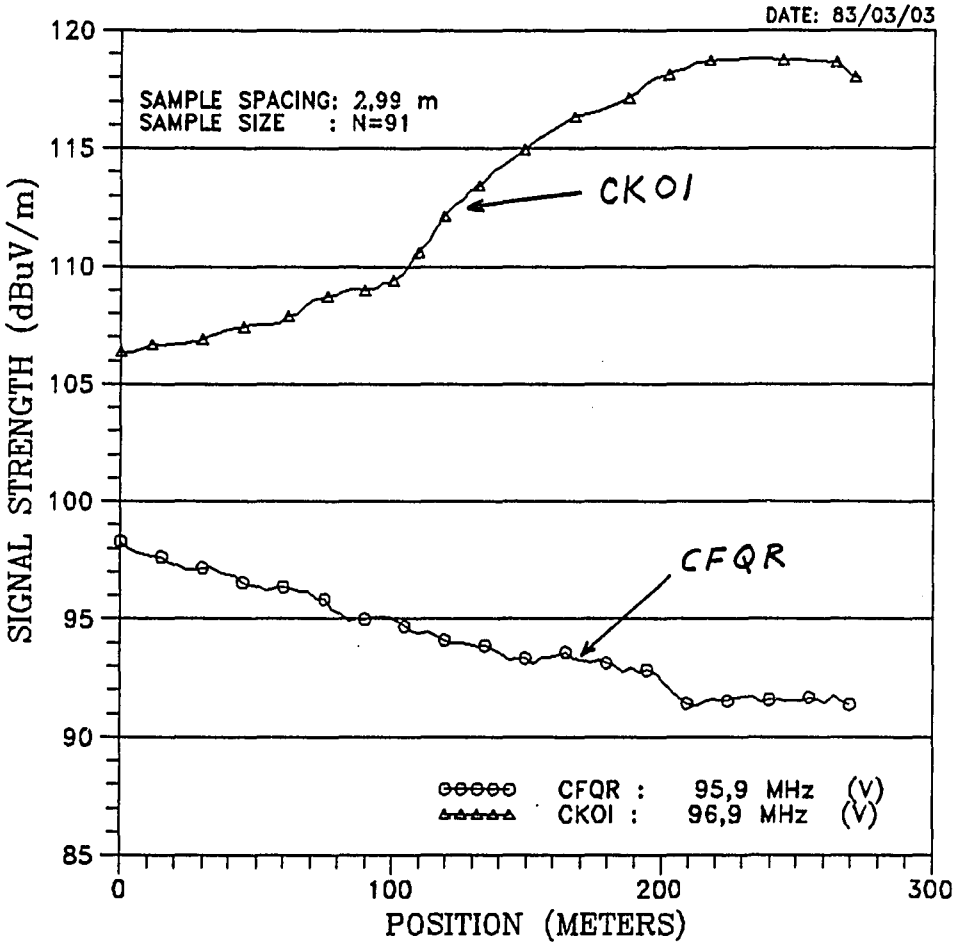

Fig. (4.3.4.1) Effect of street orientation: *Radial street.* SLTF patterns for stations CFQR (92,5 MHz) and CKOI (96,9 MHz) as measured on Peel Street (route #7, first survey). Vertical polarization.

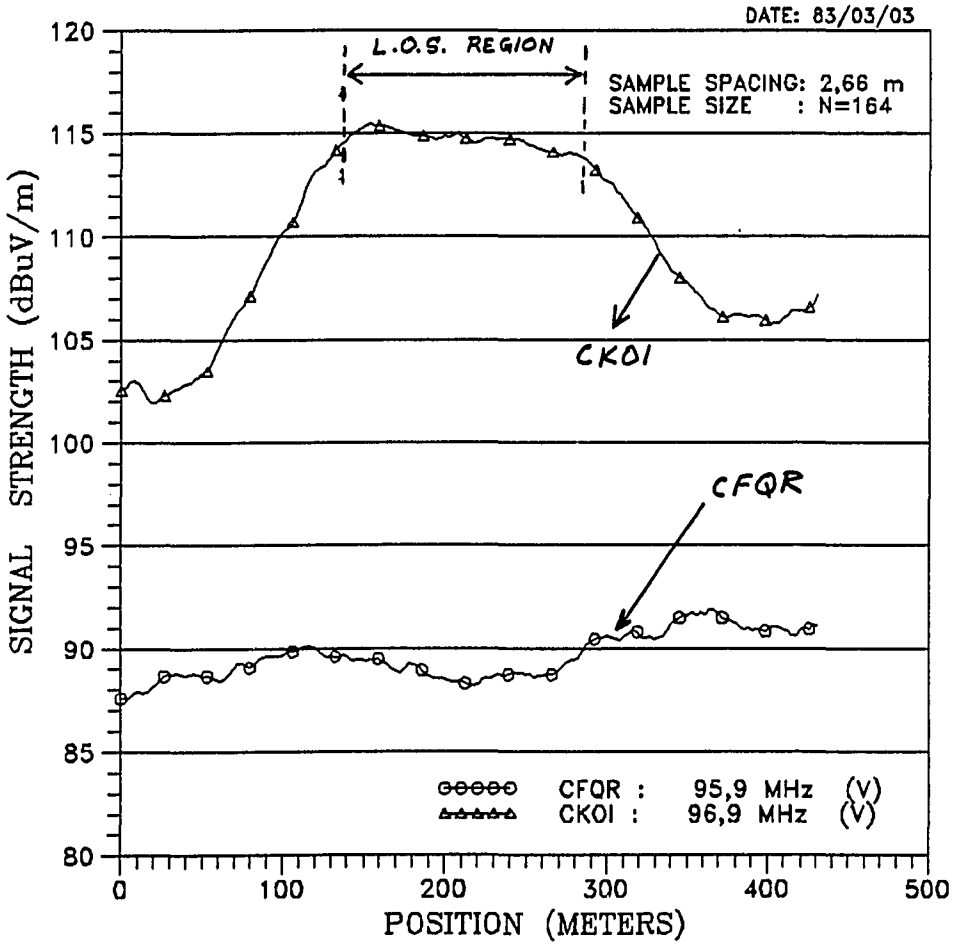

Fig. (4.3.4.2) Effect of street orientation: *Circumferential street*. SLTF patterns for stations CFQR (92,5 MHz) and CKOI (96,9 MHz) as measured on Pine Avenue (route #2, first survey). Vertical polarization.

4.3.5 Comparison of Polarization Behaviour

Fig. {4.3.5.1} shows an empirical Q-Q plot [4.11] comparing the cumulative statistical behaviour of the vertical and horizontal LTF signals on Sherbrooke Street (Fig. {2.2.1}) and Peel Street (Fig. {2.2.2}) for station CFQR. As described in the previous section, the CQFR data measured on Peel Street indicates a roughly outward radial path, while the corresponding data for station CKOI indicates an inward radial path. Sherbrooke Street being roughly perpendicular to Peel Street therefore corresponds to an arc-directed street for the same two transmitters.

Figure {4.3.5.2} shows the corresponding Q-Q plot for station CKOI on the same two street locations.

From Figs. {4.3.5.1} and {4.3.5.2}, it can be seen that the statistical behaviour of the vertical and horizontal polarizations for the two street locations is clearly different. On this type of plot, if all the data points lie on a straight line of unity slope, the two cumulative distributions (vertical and horizontal) have similar behaviour. Thus the slope (and the range) are indicative of the signal variability.

For example, in Fig. {4.3.5.1}, the data plotted for the two streets shows two evident features of the vertical and horizontal polarization behaviour.

First, the data points of Peel Street are closer to the line $y=x-10$ than those of Sherbrooke Street.

Second, the slope of the Peel Street data is evidently steeper than that of the Sherbrooke Street data. This shows greater variability in the horizontal (as opposed to vertical) polarization on Sherbooke Street as compared to Peel Street. Similar, though not identical, behaviour is apparent for station CKOI, Fig. {4.3.5.2}, except that, in this case, most of the data points for both streets lie above the line $y=x-10$, indicating a slightly higher vertical to horizontal power ratio for CKOI as compared to CFQR.

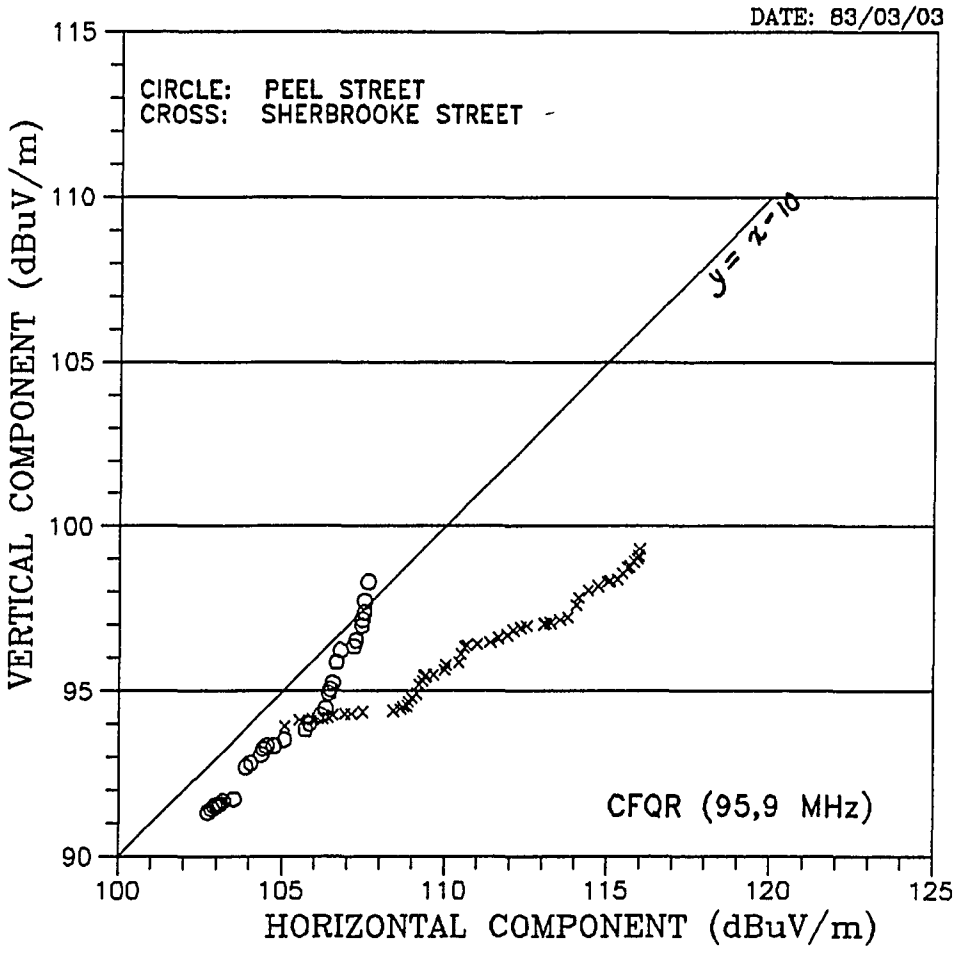

Fig. (4.3.5.1) Empirical Q-Q plot showing CDF behaviour of vertical and horizontal polarization LTF components. Measured on Peel Street and Sherbrooke Street. Station CFQR (92,5 MHz).

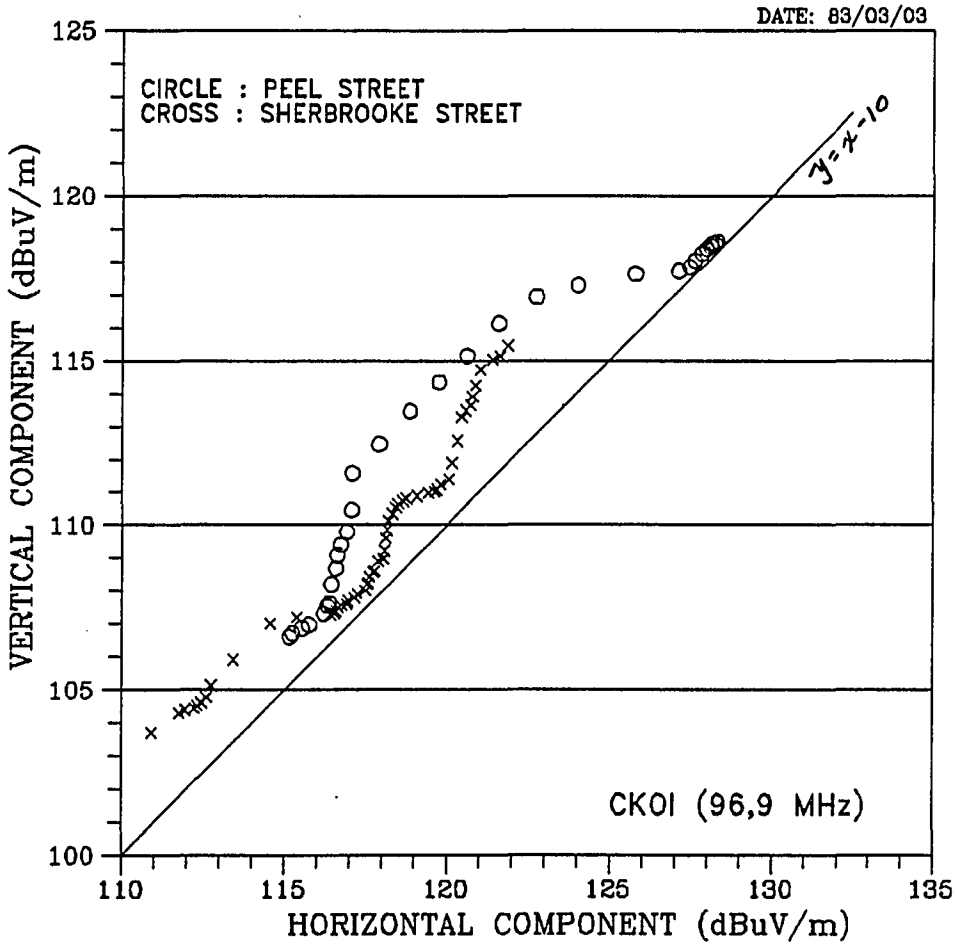

Fig. (4.3.5.2) Empirical Q-Q plot showing CDF behaviour of vertical and horizontal polarization LTF components. Measured on Peel Street and Sherbrooke Street. Station CKOI (96,9 MHz).

4.4 Summary

The present chapter has considered several aspects of the spatial long term fading (SLTF) signal characteristics in an urban micro-environment.

In studying the behaviour of the SLTF signal, it is important to keep in mind the following considerations: (a), for estimating the local mean, the use of regularly spaced data is preferred, (b), the averaging can be performed in decibel field values or in watts (the former gives values about 2,5 dB lower than the latter in the case of Rayleigh fading), (c), the choice of a proper averaging length is a tradeoff between reducing statistical uncertainty (due to short term fading) and of preserving enough information of the trend features, (d) the requirement of averaging over at least 36 *uncorrelated* samples (the use of correlated samples does not reduce the standard deviation of the local mean estimate), and finally, (e), the use of a meaningful experiment design (this relates to the measurement trajectories in order to allow meaningful comparisons to be made between different streets, e.g. radial-arc type streets).

In addition, it was found that the statistical behaviour of the long term fading did not change appreciably for two independent surveys separated by about 18 months. This shows that the SLTF behaviour is relatively insensitive to time. The study of the temporal behaviour of the long term fading is in itself a subject of further study and research; no attempt was made to study temporal behaviour in the course of the present work. Recent work of the seasonal variations of mobile radio signals has been reported by LeBel [4.19].

It has been shown that significant shadowing effects from buildings can be expected as a mobile receiver travels in an urban environment. Building shadows of the order of 18 dB can be expected relative to line of sight (LOS) regions. Furthermore, it was established that (i), the fading patterns for the vertical and horizontal polarizations are similar in behaviour, and (ii), the obstructed regions of a particular transmitter can correspond to a LOS region of another transmitter (located at a different position). These observations illustrate the possible benefit of a macroscopic spatial diversity scheme to combat the observed shadow fading [4.20].

Furthermore, it has been shown that differences in behaviour exist when comparing the statistical behaviour of the vertical and horizontal CDFs on various streets. Specifically, it was observed that on a radial street the *median* vertical to horizontal polarization power ratio (difference in dB) is slightly higher than it is on a circumferential street. This suggests a possible *polarization enhancement effect of the vertical component on a radial street.* Further investigation of this effect in other urban micro-environments using the methods described [4.11] is therefore suggested to provide a broader base of data for comparison and modeling.

4.5 Concluding Remarks

This chapter has shown that spatial long term fading effects in urban areas can be identified from micro-environment field measurements. The local mean field strength, estimated by signal averaging over twenty wavelengths at the measured frequency, was shown to provide the trend information of the received signal. The choice of twenty wavelengths was based on a compromise of reducing statistical uncertainty in the local mean and of loss of trend information.

The rate of sampling is another consideration in performing fade measurements. The present study used sampling rates of about one wavelength and about one-fifth wavelength, with both rates giving reasonably repeatable results. Thus, if only the slow variations (long term fading) of the signal are of interest, it is not necessary to use a sampling interval below one wavelength, based on the assumption that estimation of the local mean requires averaging over uncorrelated (statistically independent) samples.

Finally, it is noted that the use of Q-Q plots are helpful tools for assessing the statistical behaviour of long term fading data. In the present study, the statistical behaviour was compared for different streets and between polarization components. Based on the understanding obtained from the Q-Q plots, a more general usage of such techniques is suggested for analysis of propagation measurements.

4.6 End Notes

[4.1] **T. Banik, T. Pavlasek, and J. LeBel,** "Long Term Fading Characteristics of VHF Broadcast Signals in an Urban Environment", *Proc. 38th IEEE Vehicular Technology Conference, Phialdelphia, Pennsylvania*, June 15-17, 1988, p.205-212.

[4.2] The receiving antenna was situated at a height of about 3,0 m above street level.

[4.3] **B.R. Davis and R.E. Bogner,** "Propagation at 500 MHz for Mobile Radio", *Proc. IEE*, Part F, no.5, August 1985, p.307-320.

[4.4] **R.H. Clarke,** "A Statistical Theory of Mobile Radio Reception", Bell System Technical Journal, vol. 47, July-August 1968, pp.957-1000.

[4.5] **W.C.Y. Lee,** "Estimate of Local Average Power of a Mobile Radio Signal", *IEEE Trans. on Vehicular Technol.*, vol.VT-34, no.1, February 1985, p.22-27.

[4.6] **B.R. Davis and R.E. Bogner,** "Propagation at 500 MHz for Mobile Radio", August 1985, pp 315-316.

[4.7] **W.C.Y. Lee,** "Estimate of Local Average Power of a Mobile Radio Signal", Feb. 1985, p.23.

[4.8] **M.B. Wilk and R. Gnanadesikan,** "Probability Plotting Methods for the Analysis of Data", *Biometrika*, vol.55, 1968, pp.1-17.

[4.9] Discussions of Q-Q plot techniques are found in the following texts:

J.W. Tukey, *Exploratory Data Analysis*, Reading, Massachusetts, Addison-Wesley, 1977.

J.M. Chambers, W.S. Cleveland, B. Kleiner, and P.A. Tukey, *Graphical Methods for Data Analysis*, Boston, Duxbury Press, 1983.

[4.10] See **Chambers et al.,** *Graphical Methods for Data Analysis*, 1983, pp.197-227.

[4.11] See **Chambers et al.,** *Graphical Methods for Data Analysis*, 1983, pp.48-57.

[4.12] **K. Kafadar and C.H. Spiegelman,** "An Alternative to Ordinary Q-Q Plots: Conditional Q-Q Plots", *Computational Statistics & Data Analysis*, North Holland, Elsevier Science Publishers B.V., vol.4, 1986, pp.167-184.

[4.13] **B.R. Davis and R.E. Bogner,** "Propagation at 500 MHz for Mobile Radio", August 1985, p.310.

[4.14] **W.C.Y. Lee,** "Antenna Spacing Requirement for a Mobile Radio Base-Station Diversity", *Bell Syst. Tech. J.*, vol. 50, July-August 1971, pp. 1859-1874.

[4.15] Based on the central limit theorem, which states that the standard deviation of the distribution of the set sample means (each set of sample size k) is given by,

$$\sigma_{\bar{x}} = \frac{\sigma}{\sqrt{k}}$$

[4.16] **R.E. Bogner,** private communication, June 1, 1988.

[4.17] For a detailed description of scatter plots, see, **Chambers et al.,** *Graphical Methods for Data Analysis*, 1983, pp.75-127.

[4.18] **B.R. Davis and R.E. Bogner**, "Propagation at 500 MHz for Mobile Radio", p.317.

[4.19] **J. LeBel**, "Seasonal Mobile Radio Signal Variations in Non-Urban Environments", *Proc. IEEE Montech Conference*, Montreal, Canada, December 1987, pp. 177-180.

[4.20] **W.C. Jakes, Jr. (Ed.)**, *Microwave Mobile Communications*, New York, Wiley, 1974, pp.377-386.

Chapter 5 :

SHORT TERM FADING CHARACTERISTICS

5.1 Introduction

This chapter presents the short term fading (STF) characteristics of the data of the second survey.

Lee [5.1] reported that, in a mobile radio environment, the rapid power fluctuations (short term fading) are independent of the slow power variations (long term fading) of the received signal. This is because the short term fading arises from multipath propagation whereas the long term fading arises from path-loss propagation [5.1].

Fig. (5.1.1) shows a typical FM broadcast (short term fading) signal strength profile, normalized to the local mean. The data is for station CFQR (92,5 MHz), vertical polarization, on University Street. From the graph, it can be seen that fades as deep as 20 dB below the mean can occur. Lee [5.2] reported that succesive nulls can be expected over distances of about one-half wavelength (about 1,6 m at 92,5 MHz).

Attempts to reduce the severity of short term fading have resulted in several mobile diversity schemes [5.3]. One such scheme (*spatial selection diversity*) is discussed in the context of the autocovariance function (ACVF) later in the chapter.

Several investigators have studied short term fading in urban areas at various mobile frequencies [5.4]. These studies were carried out with the objective of studying propagation over large regions (as opposed to studying the behaviour of sub-regions, as is done here). Such studies may be referred to as *macroscopic scale* studies.

In contrast to the macroscopic scale studies, the present study is an investigation of short term fading on a *microscopic scale*. In such case, the objective is to characterize the behaviour of individual streets of different physical makeup. Such an approach may form the basis for comparison with theoretical models.

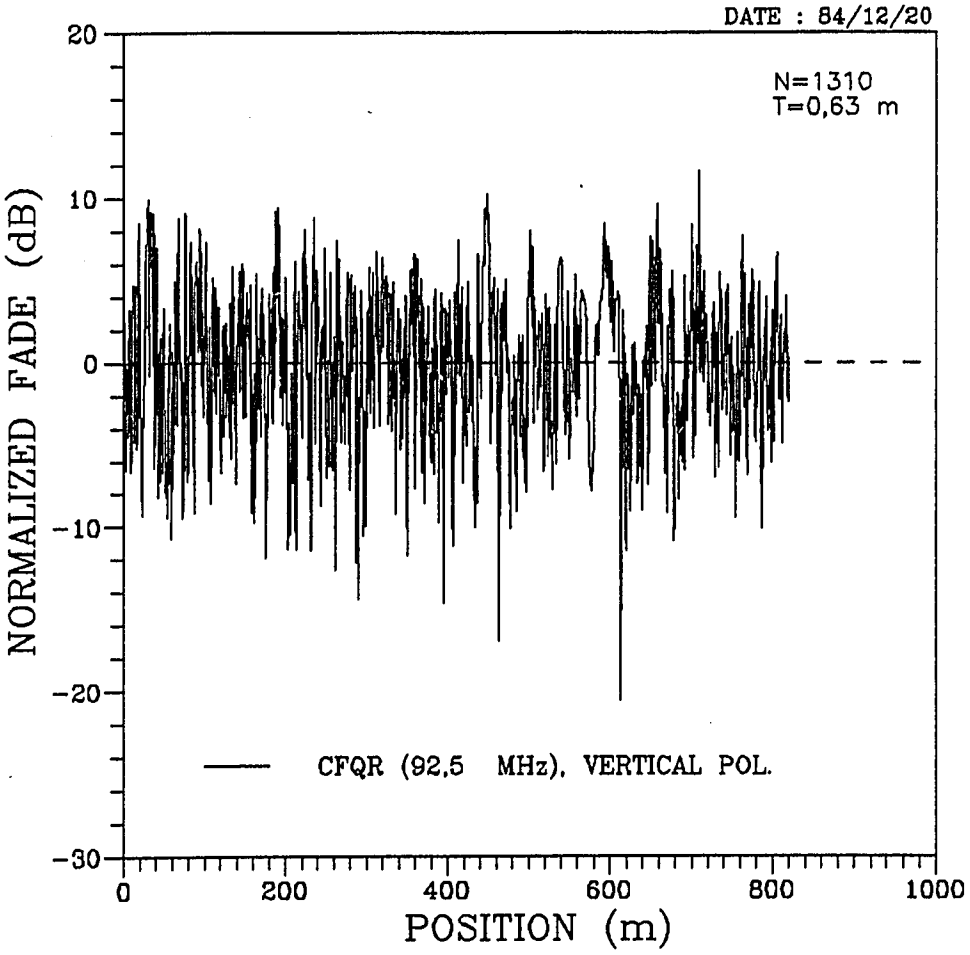

Fig. (5.1.1) Short term fading (STF) profile measured on University Street (route #1, second survey). Station CFQR (92,5 MHz), vertical polarization.

The scope of the present work, however, is restricted to the characterization of short term fading in a particular urban micro-environment (micro signifies *microscopic scale).*

The following is a brief review of two commonly used models of short term fading.

Clarke [5.5] proposed that the vertically polarized electric field, $|E_z|$, received at the mobile antenna is the superposition of a large number of plane waves ($N > 10$) travelling in a horizontal direction and arriving from all possible azimuthal angles. The waves are assumed to be uniformly distributed in phase, and are of equal Gaussian amplitude distribution [5.6]. In view of Clarke's model, it can be shown that the field amplitude has a Rayleigh distribution [5.7].

Aulin [5.8] later proposed a model which incorporated plane waves propagating both in the horizontal and vertical directions (as would occur in an urban environment) where the mode of propagation is due to scattering. However, Aulin showed that the PDF to be unaffected as compared to the case of just horizontally travelling waves (that is, the amplitude PDF is still Rayleigh) [5.8].

If there is a significant direct wave component (in addition to the scattered components), it can be shown that the PDF of the field amplitude is Rician [5.9]. In the case of urban mobile propagation, therefore, one might expect the field amplitude to be Rician on account of the short range between base and mobile (usually under 10 km), and because of the large height difference between the base transmitter and the mobile receiving antenna (thus providing a line-of-sight in many locations in a city).

In the present chapter, the results report measurements of two orthogonal electric field components (vertical and horizontal) on three street locations. The fields were sampled at approximately five to six samples per wavelength for most streets at the highest FM frequency measured (107,3 MHz). Since the short term fading has an effective wavelength of roughly one half the spatial wavelength [5.2], the Nyquist

sampling theorem [5.10] requires a sample spacing (T) of 1/2 the effective wavelength, that is, $T \leq \lambda/4$. This is the minimum sampling requirement for *non-aliased* spectral domain representation [5.10], as discussed in section {5.3.4}.

5.2 Data Analysis Methods

The short term fading (STF), $s(x)$, represents the rapid fluctuations about the local mean value. As shown in chapter 4, the received signal, $r(x)$, is comprised of short term fading superimposed on a long term fading signal, $m(x)$.

Since $r(x)$ is recorded in logarithmic (rather than linear) units, the short term fading is the difference in dB between $r(x)$ and $m(x)$.

Thus,

$$[\hat{s}(x)]_{dB} = [r(x)]_{,dB\mu V/m} - [\hat{m}(x)]_{,dB\mu V/m} \qquad (5.2.1)$$

In Eq. (5.2.1) it is assumed that $\hat{m}(x)$ has been determined *a priori* by Eq. (4.2.5).

Four methods were exploited from the techniques of random signal analysis to analyze the short term fading component, $s(x)$. The methods are listed below and are described in Appendices A, B, C, and D, respectively.

* *probability density function (PDF),*
* *autocovariance function (ACVF),*
* *crosscovariance function (CCVF),*
* *power spectral density (PSD).*

The above methods were chosen to facilitate a comparative study of the fast fading on different streets and of the orthogonal polarization components.

A large number of graphs were produced in order to gain understanding of the short term fading behaviour for different streets, and for both polarizations. However, only a sample of each kind is presented in the thesis for the sake of brevity.

5.3 Results

This section presents the experimental results pertaining to the four methods described.

The results of the short term fading charactersitics are presented in sections {5.3.1} to {5.3.4} and are divided as follows:

* Section {5.3.1}: *probability density function (PDF),*
* Section {5.3.2}: *autocovariance function (ACVF),*
* Section {5.3.3}: *crosscovariance function (CCVF),*
* Section {5.3.4}: *power spectral density (PSD).*

In each section the results presented are in three forms:

(a). Examples of the graphical results to show the nature of the behaviour.

(b). Examples of tabulations of numerical descriptors of the graphical results which allow a ready comparison among data for different cases (streets, polarization).

(c). Scatter plots which provide a visual comparison of the tabulated results.

These three forms of presentation allow a systematic study of the results and provide the basis for their evaluation.

Each section ends by a set of comments and observations about the results.

5.3.1 Probability Density Function

This section presents the *probability density function (PDF)* from the measurements of the second survey. Of the ten FM stations studied, the characteristics of two FM stations will be presented for the sake of brevity. The frequencies chosen are those of stations CFQR (92,5 MHz) and CKOI (96,9 MHz), located at different points in the city.

The following descriptive statistics of the PDF are tabulated for each street: the sample size (N), *minimum, maximum, mean, standard deviation, coefficient of skewness, and coefficient of kurtosis.* The meaning of such parameters can be appreciated by a graph of the PDF, for example, Figures (5.1.3.1) and (5.1.3.2).

The meaning of each of the descriptive parameters is discussed briefly in the Table (5.3.1.1), in the context of short term fading.

Table (5.3.1.1). Descriptive parameters of experimental PDF.

* *Minimum:*	*Lowest* recorded signal fluctuation in dB about the local mean.
* *Maximum:*	*Highest* recorded signal fluctuation in dB about the local mean.
* *Mean:*	*Expected value* of the PDF: gives a measure of the most likely value of data.
* *Standard Deviation:*	*Root of the second central moment* of the PDF - gives a measure of the spread in the data.
* *Skewness:*	*Coefficient of Skewness* of the PDF - gives a measure of the *symmetry* of the distribution about the mean. A skewness of zero indicates a symmetrical distribution, less than zero a distribution with a longer left tail (negatively skewed), greater than zero a distribution with a longer right tail (positively skewed).
* *Kurtosis:*	*Coefficient of Kurtosis* of the PDF - gives a measure of the *peakedness* of the PDF relative to a Gaussian distribution (zero kurtosis). A value greater than zero indicates a distribution with shorter tails than a Gaussian (leptokurtic); a value less than zero indicates a distribution with longer tails than a Gaussian (platykurtic).

The coefficients of skewness (γ) and kurtosis (β) are computed from the second and third (M_2, M_3) and second and fourth (M_2,M_4) central moments of the experimental PDF, respectively.

When computed in the following manner, the coefficients of skewness and kurtosis for a Gaussian distribution are both zero [5.11]:

$$\gamma = \frac{M_3}{\sqrt{M_2^3}} \qquad (5.3.1.1)$$

$$\beta = \frac{M_4}{M_2^2} - 3.0 \qquad (5.3.1.2)$$

where the jth central moment, M_j is computed from the experimental PDF (see Appendix A, Eq.(A.10)).

Thus non-zero values of γ and β indicate differences in behaviour relative to a Gaussian distribution.

In all of the short term fading results, a statistical lowpass filter of twenty wavelengths was used on regularly spaced data, as described in chapter 4.

Experimental PDF Characteristics

This section presents the characteristics of the experimental PDF of the second field survey on three street locations. The three streets are as described in section {2.7.2}.

Figures {5.3.1.1} and {5.3.1.2} show graphs of the experimental PDF corresponding to street #1 (University Street), for station CFQR, vertical and horizontal polarization, respectively. Superimposed on each plot is a best fit *logarithmic Rician* [5.12] distribution of the same mean and variance. It should be noted, for example, that in comparing the two polarizations, the vertical component has greater spread than the horizontal component, indicated by the *greater width* of the vertical PDF, and by its standard deviation of 4,05 dB versus 3,84 dB for the horizontal. In addition, it can be seen that the horizontal PDF is slightly more skewed to the left than the vertical. This is indicated by its coefficient of skewness (-0,55) as compared to the vertical (-0,43). Finally, it can also be seen that the horizontal PDF is more peaked than the vertical component when compared against the log-Rician. This is again supported by the higher coefficient of kurtosis (0,93) for the horizontal as compared to the vertical (0,54). Similar comparisons can be made by comparing the PDF for the two polarizations on other streets, and likewise for the same polarization between different

streets, for example, between street 1 and 3.

Tables {5.3.1.2} to {5.3.1.5} present the PDF statistics for stations CFQR (92,5 MHz) and CKOI (96,9 MHz) respectively on the three street locations.

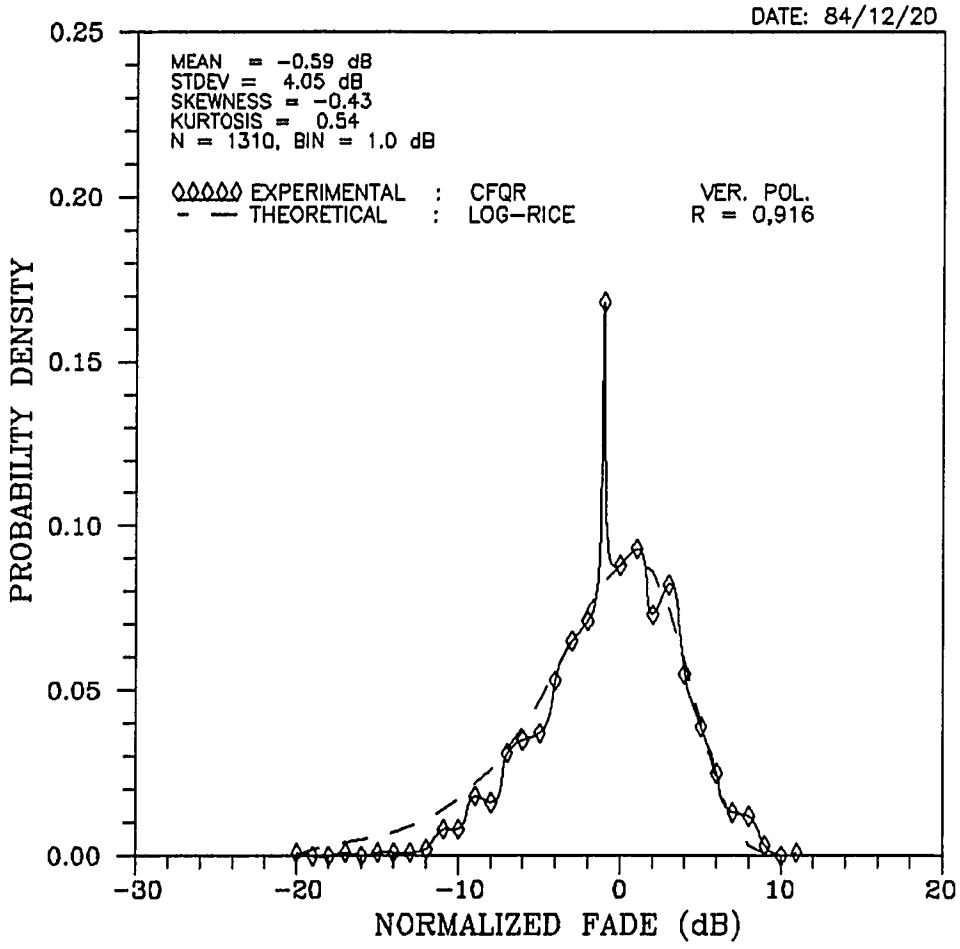

Fig. (5.3.1.1). PDF of short term fading. Dashed line shows best fit logarithmic Rician distribution. Station CFQR (92,5 MHz). Vertical polarization.

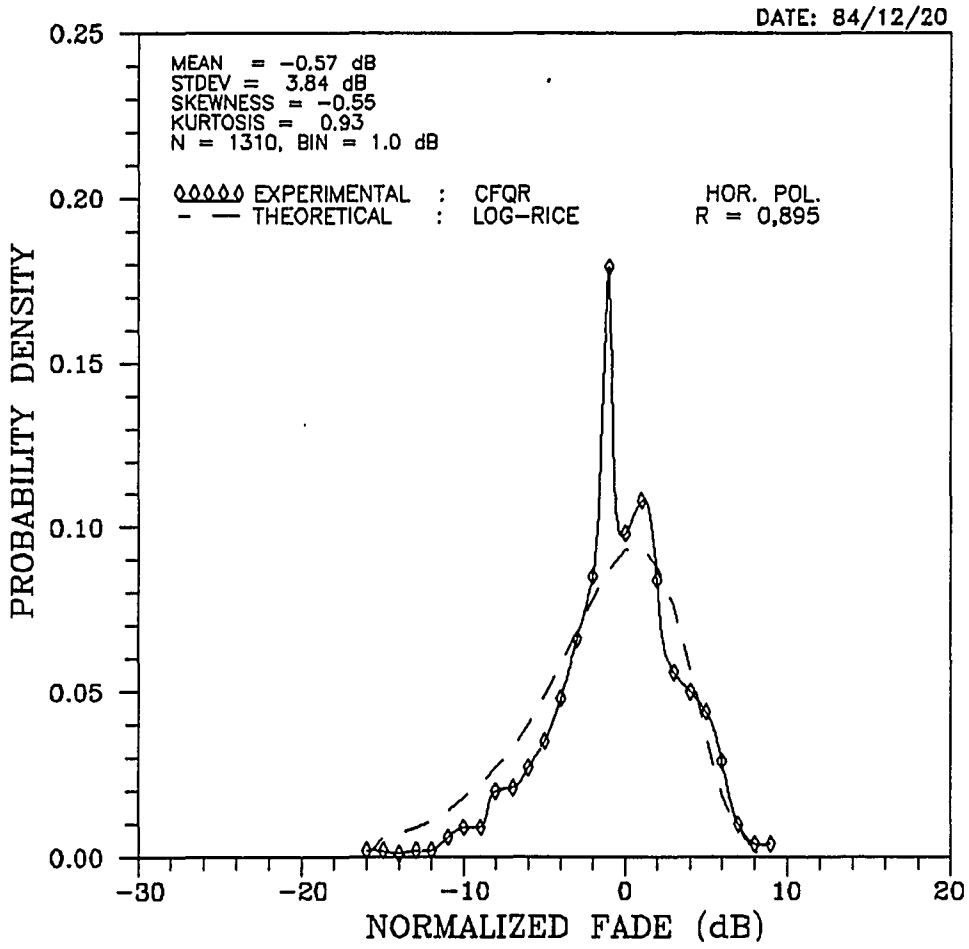

Fig. (5.3.1.2). PDF of short term fading. Dashed line shows best fit log-Rician distribution. Station CFQR (92,5 MHz). Horizontal polarization.

Experimental PDF characteristics of short term fading (84/12/20).
Filter size is 20 wavelengths, regular data.

STATION CFQR (92,5 MHz)

Table (5.3.1.2). (A) *Vertical Polarization.*

Street	N	Min (dB)	Max (dB)	Mean (dB)	Stdev(dB)	Skewness	Kurtosis
St. 1	1310	-20,6	11,6	-0,59	4,05	-0,43	0,54
St. 2	721	-17,4	10,6	-0,62	4,10	-0,83	0,91
St. 3	283	-14,3	10,6	-0,55	3,47	-0,65	1,43

Table (5.3.1.3). (B) *Horizontal Polarization.*

Street	N	Min (dB)	Max (dB)	Mean (dB)	Stdev(dB)	Skewness	Kurtosis
St. 1	1310	-16,9	9,8	-0,57	3,84	-0,55	0,93
St. 2	721	-16,3	9,5	-0,61	4,17	-0,48	-0,02
St. 3	283	-15,5	9,3	-0,65	3,94	-0,67	0,81

Experimental PDF characteristics of short term fading (84/12/20).
Filter size is twenty wavelengths, regular data.

STATION CKOI (96.9 MHz)

Table {5.3.1.4}. (A) *Vertical Polarization.*

Street	N	Min (dB)	Max (dB)	Mean (dB)	Stdev(dB)	Skewness	Kurtosis
St. 1	1310	-16,6	10,0	-0,61	3,71	-0,80	1,12
St. 2	721	-14,3	10,6	-0,55	3,47	-0,65	-1,43
St. 3	283	-13,1	9,9	-0,55	3,70	-0,61	0,59

Table {5.3.1.5}. (B) *Horizontal Polarization.*

Street	N	Min (dB)	Max (dB)	Mean (dB)	Stdev(dB)	Skewness	Kurtosis
St. 1	1310	-18,1	9,4	-0,63	3,85	-0,75	0,92
St. 2	721	-14,9	9,5	-0,57	3,38	-0,98	2,50
St. 3	283	-11,2	8,7	-0,71	3,49	-0,66	0,26

A useful means of interpreting the tabulated results is to use a 'Scatter Plot' [5.13]. Examples are given for the four parameters (mean, standard deviation, skewness, kurtosis) in the tables in Figures (5.3.1.3) to (5.3.1.6). Such plots enable a graphical comparison of each parameter for the various conditions of measurement. In these plots there is a unity slope line which indicates similarity of the behaviour of the ordinate (horizontal pol.) and abcissa (vertical pol.). The separation of the points from the line indicates the degree of dissimilarity.

Thus in Fig. (5.3.1.3) (MEAN) the vertical and horizontal polarization results for street 1 are closer to the line and to each other. These are therefore similar. The points for street 2 are also similar to each other but clearly differ from street 1. The points for street 3 simultaneously differ from each other as well as from the other two streets.

The scatter plots therefore provide a ready evaluation of the tabulated results and thus in turn of the basic results in the original PDF graph.

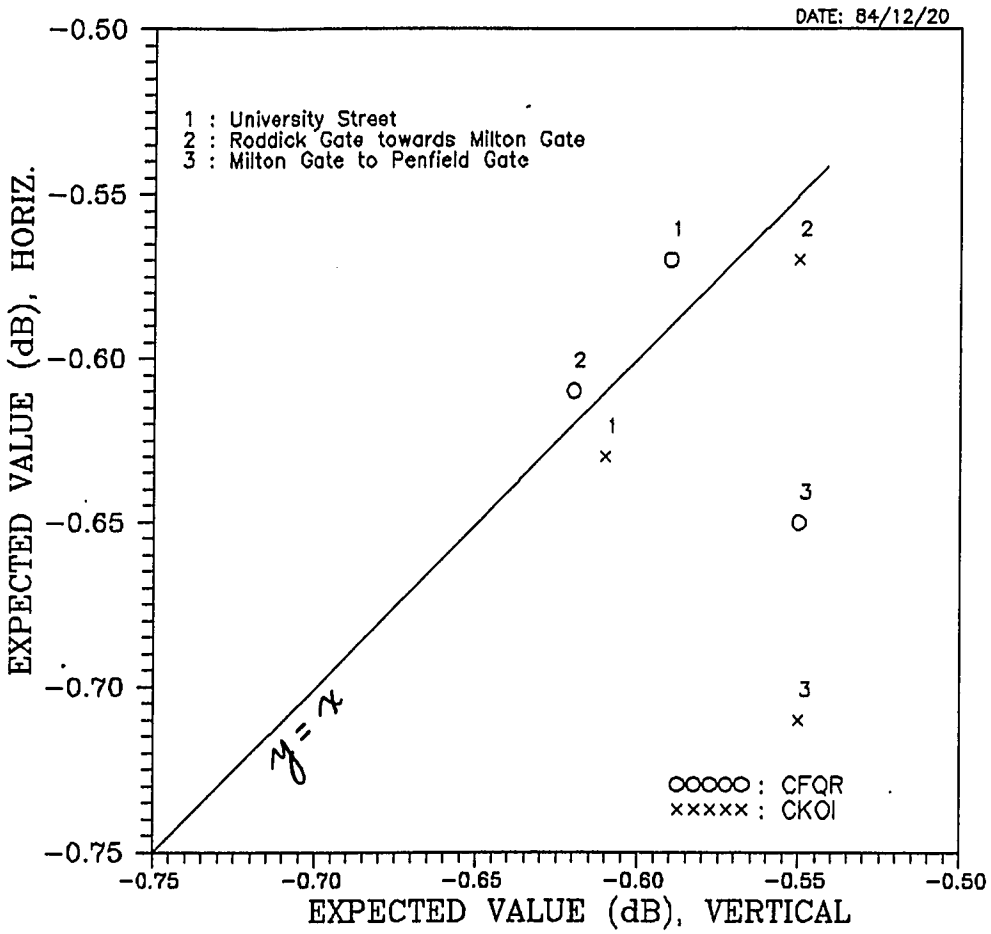

Fig. (5.3.1.3) Scatter plot showing *expected values* of the PDF (routes #1, #2, #3, second survey). Stations CFQR (92,5 MHz), CKOI (96,9 MHz). Vertical and horizontal polarization.

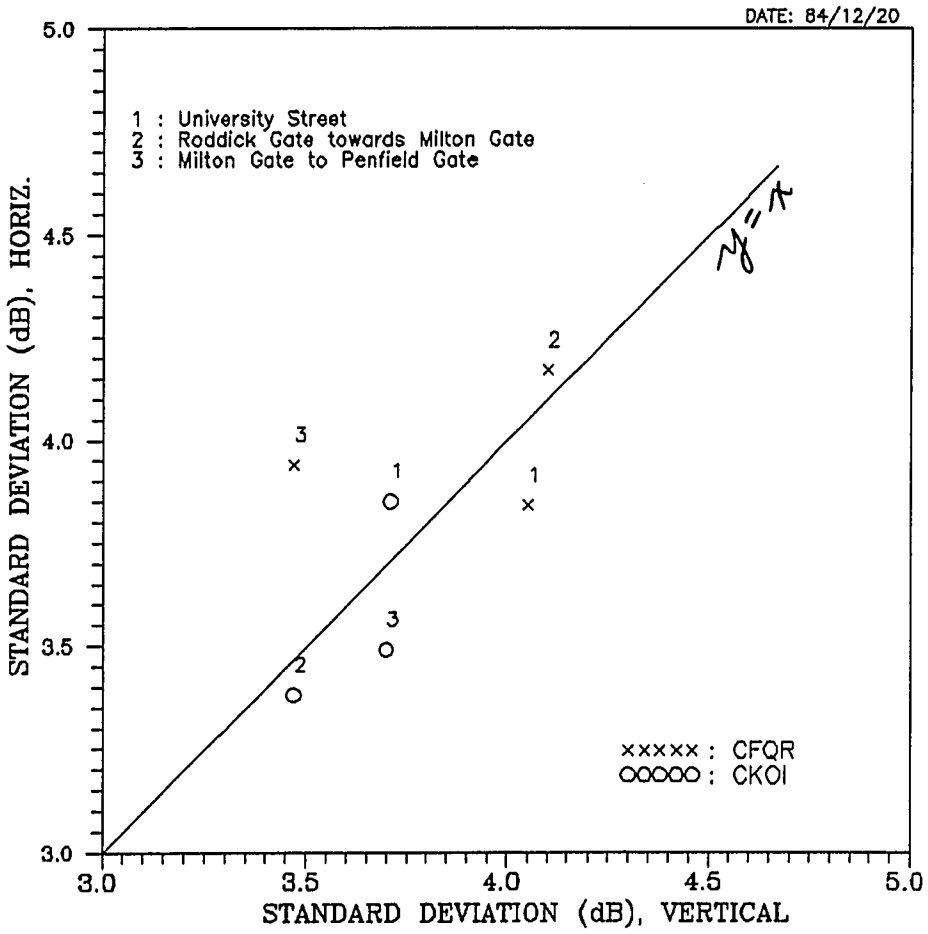

Fig. (5.3.1.4) Scatter plot showing *standard deviations* of the PDF (routes #1, #2, #3, second survey). Stations CFQR (92,5 MHz), CKOI (96,9 MHz). Vertical and horizontal polarization.

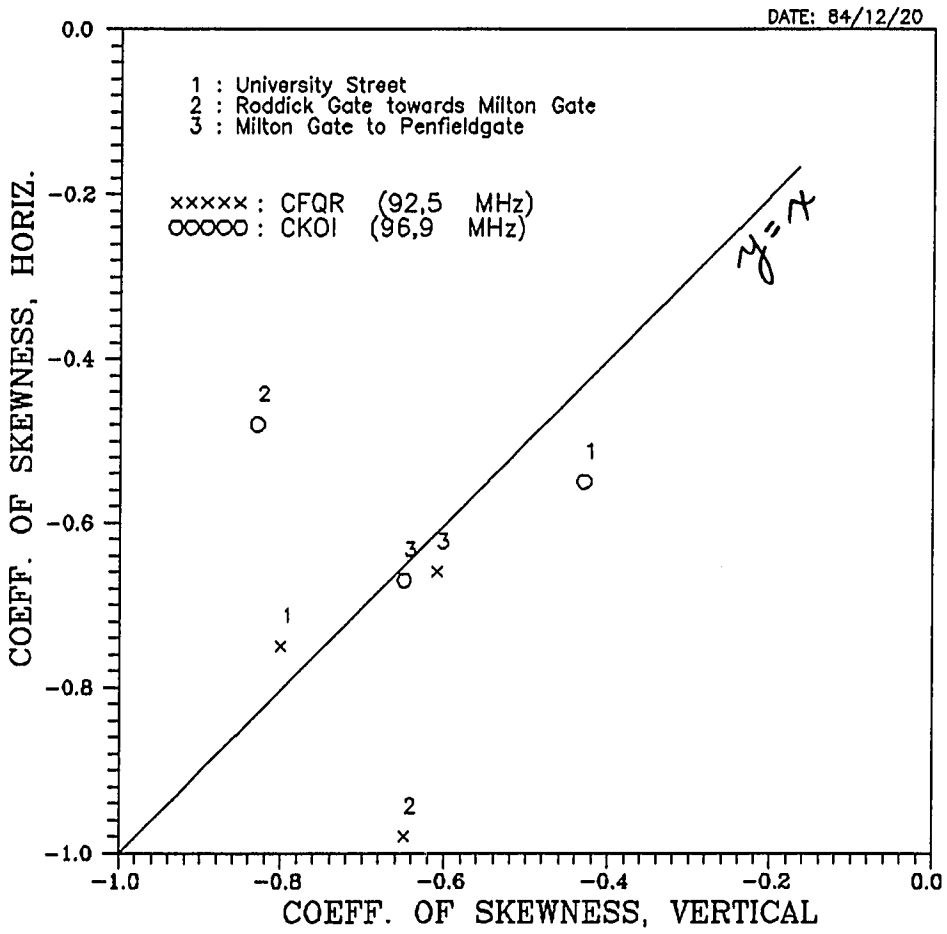

Fig. (5.3.1.5) Scatter plot showing *coefficients of skewness* of the PDF (routes #1,#2,#3, second survey). Stations CFQR (92,5 MHz), CKOI (96,9 MHz). Vertical and horizontal polarization.

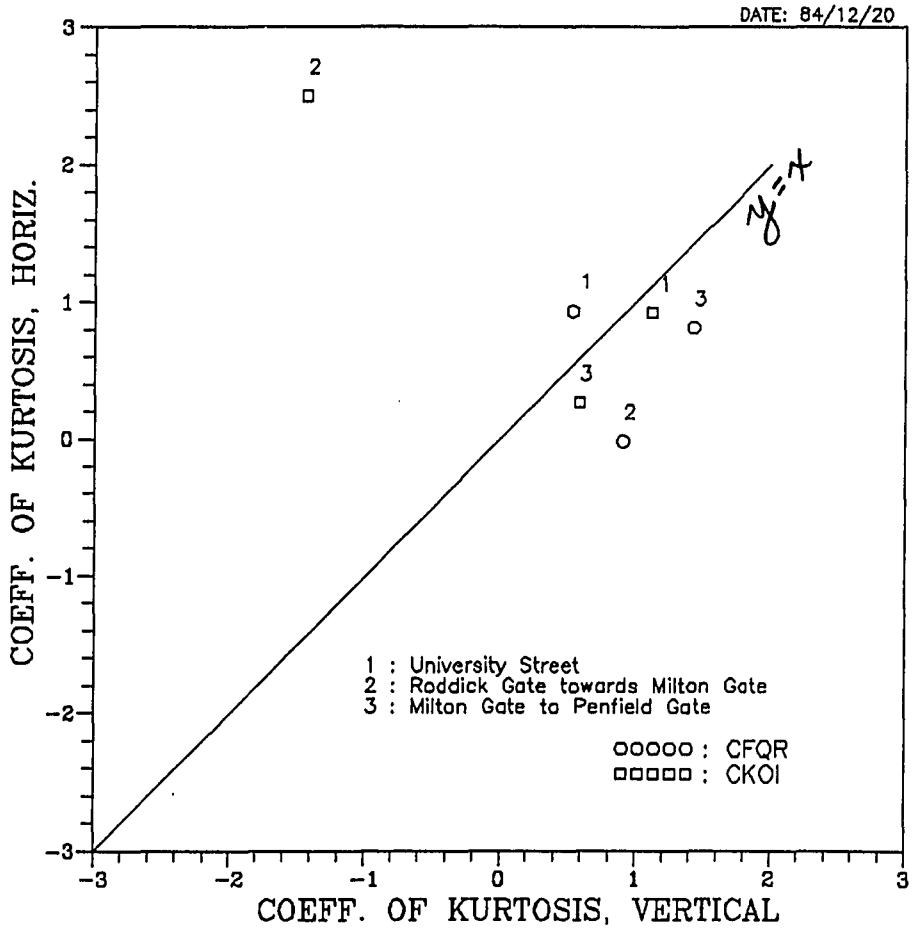

Fig. (5.3.1.6) Scatter plot showing *coefficients of kurtosis* of the PDF (routes #1,#2,#3, second survey). Stations CFQR (92,5 MHz), CKOI (96,9 MHz). Vertical and horizontal polarization.

Modeling the Experimental PDF

In order to describe the experimental PDF analytically, an attempt was made to model the PDF by a number of well known theoretical distributions with the objective of determining the one with the best fit. In total, six theoretical distributions were considered: *Gaussian, Rayleigh, Lognormal, Rician, Logarithmic Rician* [5.12], and in addition a combination of the lognormal and the log-Rician (called the *'CLNLR'* distribution) is proposed here. More will be said about the CLNLR distribution.

The closeness of the fit was determined by computing the linear correlation coefficient [5.14] between the experimental PDF and the theoretical PDF. In order to obtain the best possible fit to the experimental PDF, the steady component of the Rician distribution was incremented in a loop until a maximum correlation coefficient was reached.

A software package was developed to model the experimental data by one of the following theoretical distributions:

(a). Gaussian,
(b). Lognormal,
(c). Rayleigh,
(d). Rice,
(e). Logarithmic Rice,
(f). Combination of Lognormal and Logarithmic Rice (CLNLR).

Of the six distributions listed above, the last one, (f), is proposed as a new approach based on the author's experimentation with various distributions in order to determine the one which yields the best correlation coefficient.

The CLNLR is essentially a *piecewise construction* of the lognormal and the log-Rician distributions. The CLNLR matches the (best fit) lognormal for values below 0 dB, and matches the (best fit) log-Rician for values above 0 dB. At the 0 dB

value, the CLNLR assumes the average of the lognormal and log-Rician PDF's.

Denoting the lognormal, log-Rician, and CLNLR PDF's by $p_a(y)$, $p_b(y)$, and $p_c(y)$, respectively, we have,

$$p_c(y) = p_a(y) \qquad (y < 0dB)$$

$$= p_b(y) \qquad (y > 0dB)$$

$$= \frac{p_a(y) + p_b(y)}{2} \qquad (y = 0dB)$$

The theoretical implications of such a piecewise construction have not been considered and may well not be justified by rigorous mathematical arguments. Nevertheless, the procedure outlined here is observed to give a better fit to the data in almost all cases, and is therefore presented as the result of experimentation with the curve fitting.

The correlation coefficient (R) [5.14] is a measure of the goodness of fit between the theoretical and experimental distributions. A high value of R (i.e. $R > 0,85$) indicates a good fit, a low value indicates a poor fit.

Where applicable, the theoretical distribution used the first and second central moments of the experimental PDF as its mean and variance.

In the cases involving the Rice or log-Rice distributions, the computation of the best fit theoretical distribution involved optimizing the correlation coefficient by varying the value of the steady component until a maximum correlation is reached.

Figure {5.3.1.7} shows an example of an experimental PDF modeled by a lognormal and log-Rician distribution. (The data are normalized about the long term fading component in all PDF graphs). The experimental PDF shows a narrow peak at about -0,5 dB. This peak cannot be predicted by either the lognormal nor the log-Rician models. Below the 0 dB value, the graph shows that the lognormal fits the experimental data better than the log-Rice, however the reverse is true for positive dB

values. The correlation coefficient for the lognormal (R=0,916) and the log-Rician (R=0,918) PDFs are about equal.

Figure {5.3.1.8} shows the corresponding CLNLR distribution plotted versus the same experimental PDF. Clearly, the fit of the CLNLR is better than either the lognormal or the log-Rician (indicated by the higher R value: R=0,934). Other data (not shown) for other stations and street locations indicate similar behaviour. Hence, it is evident that the *piecewise construction technique of combining the lognormal and log-Rician distributions gives a better fit to the experimental PDF than either the lognormal or the log-Rician PDFs.*

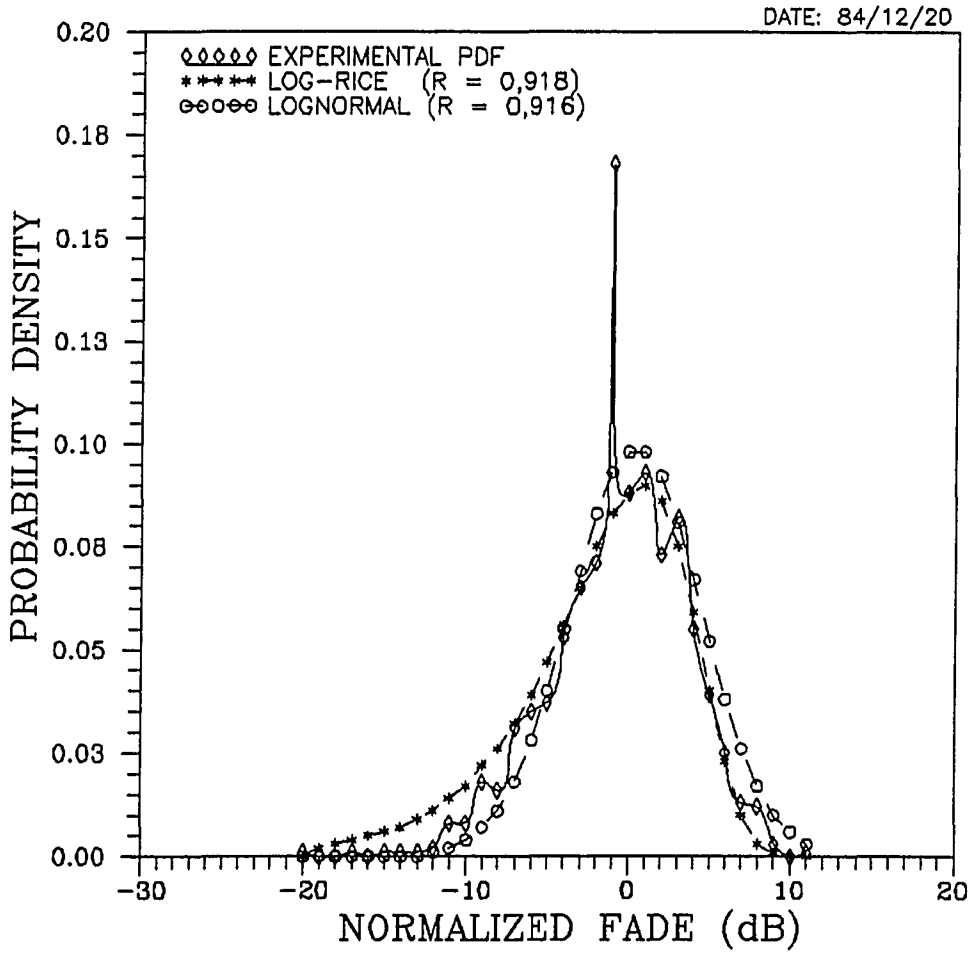

Fig. (5.3.1.7) Model of experimental PDF by the *lognormal* and *log-Rician* PDFs. Experimental PDF corresponds to CFQR (92,5 MHz) on University Street. Vertical polarization.

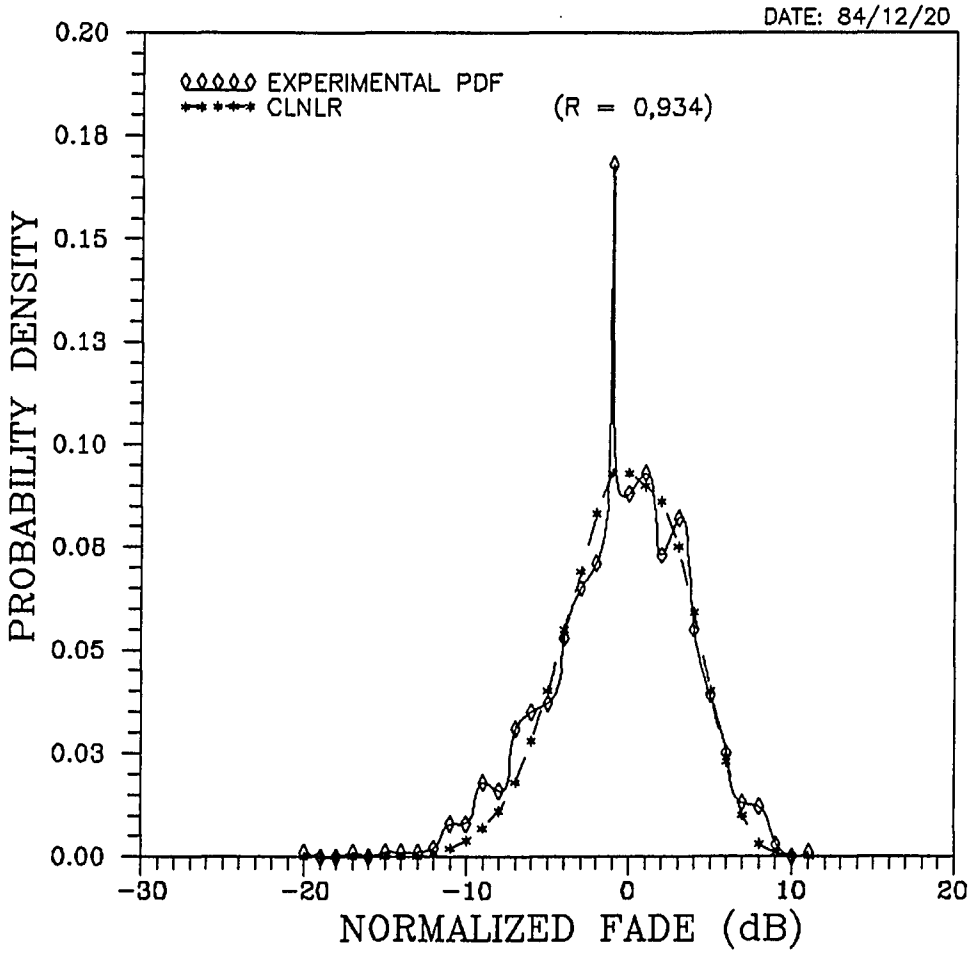

Fig. (5.3.1.8) Model of experimental PDF by the '*combination of the lognormal and best fit log-Rician' (CLNLR)* PDFs. Experimental PDF corresponds to CFQR (92,5 MHz) on University Street. Vertical polarization.

The best fit results between the experimental and theoretical PDF for all three streets are summarized in Table (5.3.1.6) for station CFQR (92,5 MHz) and Table (5.3.1.7) for station CKOI (96,9 MHz).

Table (5.3.1.6). Correlation coefficient comparison of six theoretical PDFs. Station CFQR (92,5 MHz).

Street	Pol.	Gaussian	Rayleigh	Rice	Lognormal	Log-Rice	CLNLR
1	V	0,73	0,66	0,88	0,92	0,92	0,93
	H	0,69	0,47	0,86	0,91	0,90	0,92
2	V	0,74	0,51	0,87	0,90	0,920	0,922
	H	0,64	0,62	0,89	0,91	0,91	0,923
3	V	0,59	0,77	0,86	0,86	0,92	0,93
	H	0,62	0,42	0,79	0,79	0,84	0,86

Table (5.3.1.7). Correlation coefficient comparison of six theoretical PDFs. Station CKOI (96,9 MHz).

Street	Pol.	Gaussian	Rayleigh	Rice	Lognormal	Log-Rice	CLNLR
1	V	0,71	0,30	0,86	0,89	0,89	0,90
	H	0,69	0,35	0,85	0,88	0,89	0,90
	V	0,67	0,29	0,86	0,81	0,85	0,88
2	H	0,65	0,07	0,83	0,79	0,83	0,85
	V	0,70	0,41	0,91	0,86	0,91	0,93
3	H	0,60	0,24	0,76	0,73	0,77	0,78

From Tables (5.3.1.6) and (5.3.1.7) it can be seen that the last column generally gives the highest correlation coefficient in all cases. The log-Rice distribution [5.12] generally provides the second best fit in most cases.

Fig. (5.3.1.9) shows a scatter plot of the correlation coeffcients in Table (5.3.1.1). The scatter plot shows the horizontal and vertical polarization correlation coefficients of three theoretical distributions (lognormal, log-Rician, CLNLR). As shown, the CLNLR gives the highest correlation of the three PDFs.

Fig. (5.3.1.10) shows the scatter plot corresponding to the data in Table (5.3.1.2), agian for the lognormal, log-Rician, and CLNLR distributions.

Interestingly, it is evident from the scatter plots that the vertical polarization has a better fit (to any of the models considered) than the horizontal polarization. The reason for such behaviour is not immediately evident from the limited data available (3 streets). This suggests the need for further data in other micro-environments for comparison and understanding of the phenomenon.

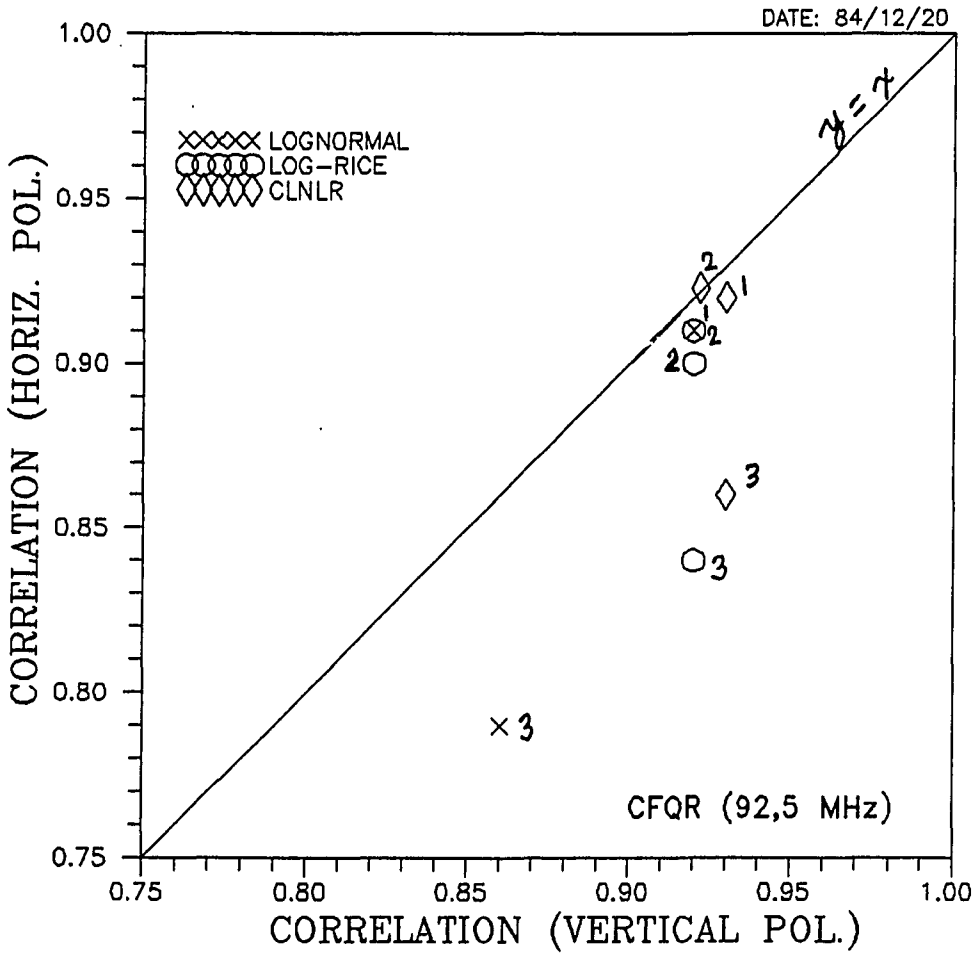

Fig. (5.3.1.9) Scatter plot showing best fit correlation coefficients of three PDFs: lognormal, log-Rician, and CLNLR. Data are for three campus routes of the second survey. Station CFQR, vertical and horizontal polarization.

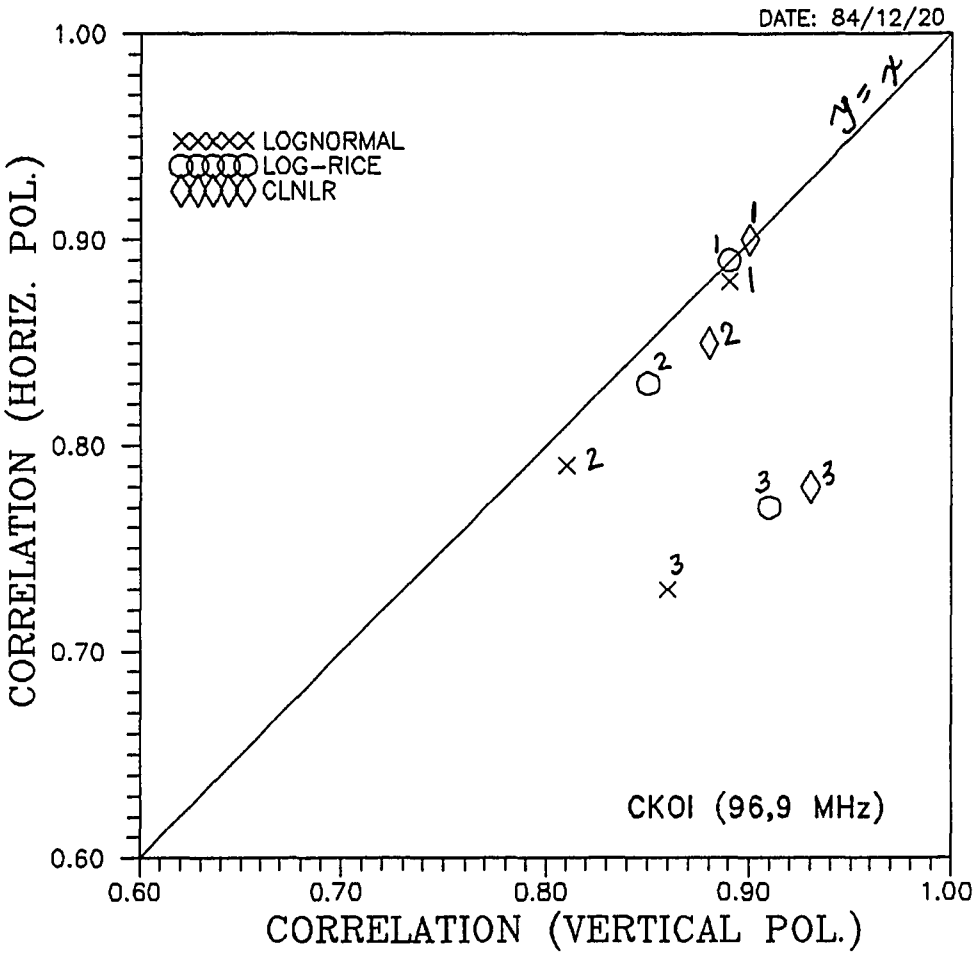

Fig. (5.3.1.10) Scatter plot showing best fit correlation coefficients of three PDFs: lognormal, log-Rician, and CLNLR. Data are for three campus routes of the second survey. Station CKOI, vertical and horizontal polarization.

5.3.2 *Autocovariance Function*

Introduction

This second type of analysis of the short term fading was the (spatial) *autocovariance function* (ACVF). Computational aspects of the ACVF are described in Appendix B. The ACVF curve identifies the spatial separation at which the short term fading signals become uncorrelated.

In order to reduce the probability of a deep signal fade at the receiver (due to short term fading), the concept of *space diversity* [5.15] can be used. In this procedure, uncorrelated fading signals received by two (or more) spatially separated branches at the mobile are combined so as to reduce the probability of a deep fade relative to the case of a single branch. In addition to space diversity, other diversity schemes exist (time, frequency, polarization, angle) [5.15]. However, space diversity appears to be favored over the other types for mobile radio use [5.15].

Lee [5.16] reported that mobile radio signals in a suburban environment are decorrelated in a spatial interval of about 0.8λ. However, a separation of $0,5\lambda$ gives practically uncorrelated signals at the mobile, the reason being that the signals are considered independent as long as the autocorrelation coefficient is below 0,2 [5.17]

Perhaps the simplest combining scheme is that of *spatial selection diversity*, a switching scheme which selects the maximum signal [5.18] from a number of spatially separated antennas (called branches), each of which provides a separate uncorrelated fading signal. In such a scheme, Jakes [5.18] reported that using two branches offers an improvement of 10 dB (at the 99% reliability level), while using four branches offers an improvement of 16 dB (at the 99% reliability level) over a single branch. In principle, the use of a greater number of branches offers even better results [5.18], but the extra cost and complexity is a limiting factor.

Davis and Bogner [5.19] stated that an assumption in a selection diversity operation is that the field strength measured after the vehicle moves $\lambda/2$ is the same as would be measured on an antenna mounted further forward on the vehicle. According to Davis and Bogner [5.19], "this will be true only if the vehicle itself does not

substantially modify the field, and that this is independent of the presence or absence of a second antenna. This assumption would only be approximately true in practice."

In the present work it is assumed the vehicle does not substantially modify the field, so that the observed behaviour represents the actual field behaviour.

In the results that follow, an important parameter in the ACVF curve is the spatial shift of the first zero crossing, that is, the spatial decorrelation interval. The results are presented as tables of the spatial decorrelation intervals as obtained on various street locations and for both polarizations. To evaluate and compare the spatial decorrelation intervals for different cases, scatter plots [5.13] will be used (as for the case of the PDF).

Figures {5.3.2.1} and {5.3.2.2} are sample ACVF plots of the vertical and horizontal short term fading components. The graphs are for station CKOI (96,9 MHz) on St.#2 (Roddick Gate to Milton Gate). Each graph shows two curves: one of the experimental correlation curve, and another of the theoretical curve for the case of Rayleigh fading [5.20].

The theoretical curve is computed from the following equation :

Rayleigh Fading Correlation Coefficient (Vertical Polarization):

$$R_{theo}(\tau) = J_0^2(\beta\tau) \qquad (5.3.2.1)$$

As seen from the graphs, the spatial decorrelation interval (theoretical and experimental) can be read by noting position of the first zero crossing. For example, it is seen from Figs. {5.3.2.1} and {5.3.2.2} that the first zero crossings are about 4,5 m for the vertical polarization and about 8,2 m for the horizontal polarization. Such results are summarized in Tables {5.3.2.1} to {5.3.2.3} corresponding to the ACVF data for stations CFQR (92,5 MHz), CKOI (96,9 MHz), and CITE (107,3 MHz).

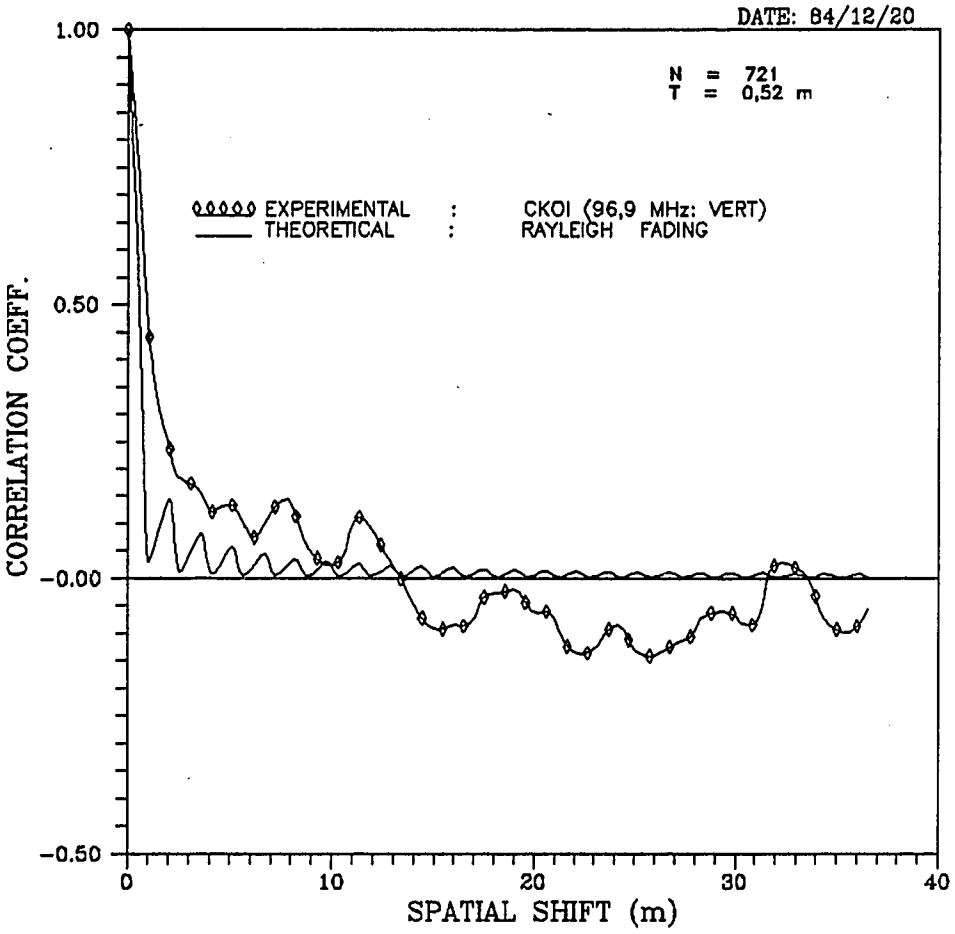

Fig. (5.3.2.1) Autocovariance Function (ACVF) curves. *Theoretical (Rayleigh fading) and experimental data.* Curves computed for a maximum lag of 0,1N samples. Station CFQR (92,5 MHz). *Vertical polarization.*

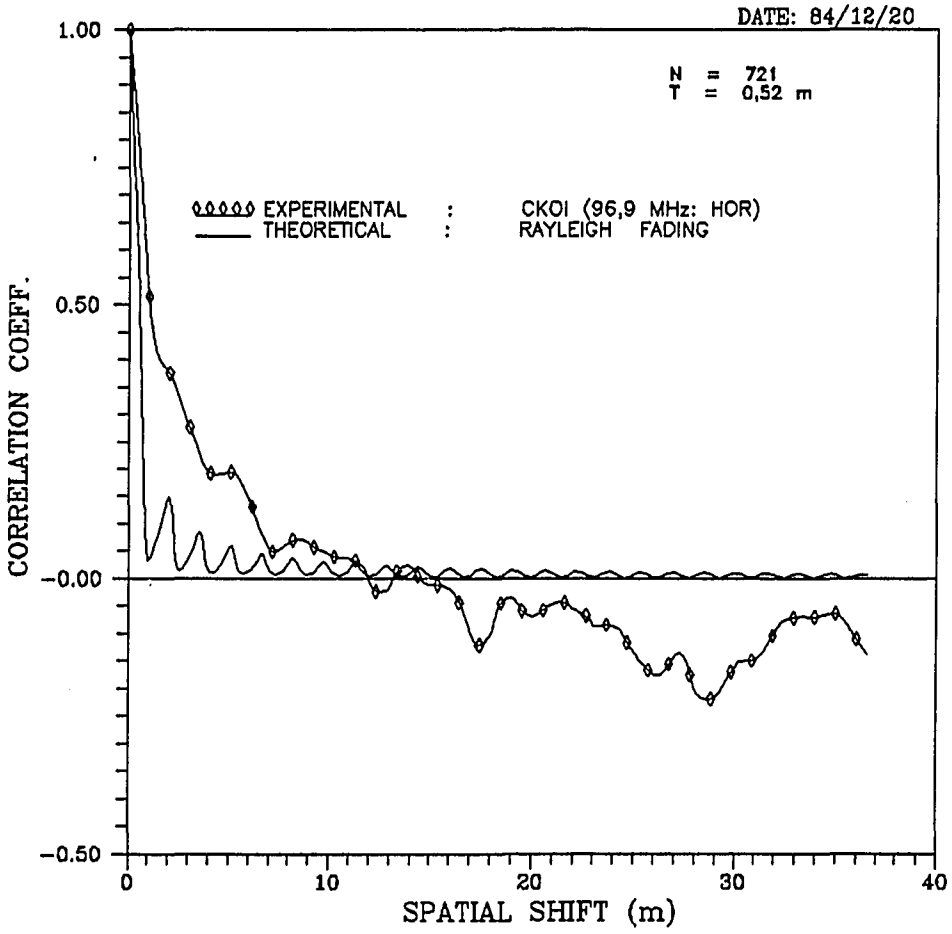

Fig. (5.3.2.2) Autocovariance Function (ACVF) curves. *Theoretical (Rayleigh fading) and experimental data.* Curves computed for a maximum lag of 0,1N samples. Station CFQR (92,5 MHz). *Horizontal polarization.*

Autocovariance Characteristics (Survey 2)

This section presents the results of the *spatial autocovariance* (ACVF) characteristics of the short term fading signals. The spatial decorrelation interval for each street location is obtained by plotting the *normalized autocovariance function (NACVF)* versus the (discrete) spatial shift parameter, x, and noting the position of the first zero crossing. A solid line joining the discrete points of the NACVF is drawn in each case using cubic spline interpolation.

Tables {5.3.2.1} through {5.3.2.3} present the spatial decorrelation intervals for three FM broadcast stations (CFQR,CKOI,CITE) for the three street locations of the second survey. Comparisons of vertical and horizontal polarization behaviour are given for each frequency. In each table, the following parameters are given: sample record length (N), polarization, number of steps (on the ACVF graph) to reach the first zero crossing (n), the corresponding spatial decorrelation interval (nT, T=sample spacing) in meters, and the spatial decorrelation interval in wavelengths.

Table (5.3.2.1). Spatial decorrelation intervals (CFQR: 92,5 MHz) on three streets. Vertical and horizontal polarization.

St. # (84/12)	Sample Size (N)	Pol.	number of steps for 1st zero	Spatial decorrel. (m)	Spatial decorrel. (wavelengths)
1	1310	V	7	9,0 m	2,78
		H	5	6,2 m	1,91
2	721	V	8-9	4,5 m	1,39
		H	14-15	8,2 m	2,53
3	283	V	7	7,2 m	2,22
		H	11-12	10,2 m	3,15

Table (5.3.2.2). Spatial decorrelation intervals (CKOI: 96,9 MHz).

St. # (84/12)	Sample Size (N)	Pol.	number of steps for 1st zero	Spatial decorrel. (m)	Spatial decorrel. (wavelengths)
1	1310	V	5-6	7,0 m	2,26
		H	4-5	6,0 m	1,94
2	721	V	25-26	13,5 m	4,36
		H	23-24	12,0 m	3,88
3	283	V	11-12	10,5 m	3,39
		H	13-14	12,2 m	3,94

Table (5.2.2.3). Spatial decorrelation intervals (CITE:107,3 MHz).

St. # (84/12)	Sample Record Length	Pol.	number of steps for 1st zero	Spatial decorrel. (Meters)	Spatial decorrel. (wavelengths)
1	N=1310	V	6-7	8,5 m	2,80
		H	9-10	12,0 m	3,88
2	N=721	V	12	6,2 m	2,00
		H	5-6	3,0 m	0,97
3	N=283	V	5	5,0 m	1,62
		H	9	15,0 m	4,85

In order to evaluate the spatial decorrelation intervals of all three stations and for both polarizations, Fig. (5.3.2.3) shows a scatter plot. For example, the scatter plot shows that the spatial decorrelation interval for station CKOI is lowest on street 1 and highest on street 2. For station CFQR, however, the decorrelation intervals are about the same on the three streets. Station CITE shows a marked difference behaviour on street 3 as compared to street 2. The reasons for such behaviour are not immediately evident. However, the observed differences in behaviour from one street to the next in the micro-environment suggest the need for further data to better understand the phenomenon.

Behavioural similarity of the vertical and horizontal polarizations is indicated by the closeness of the data points to the line $y=x$.

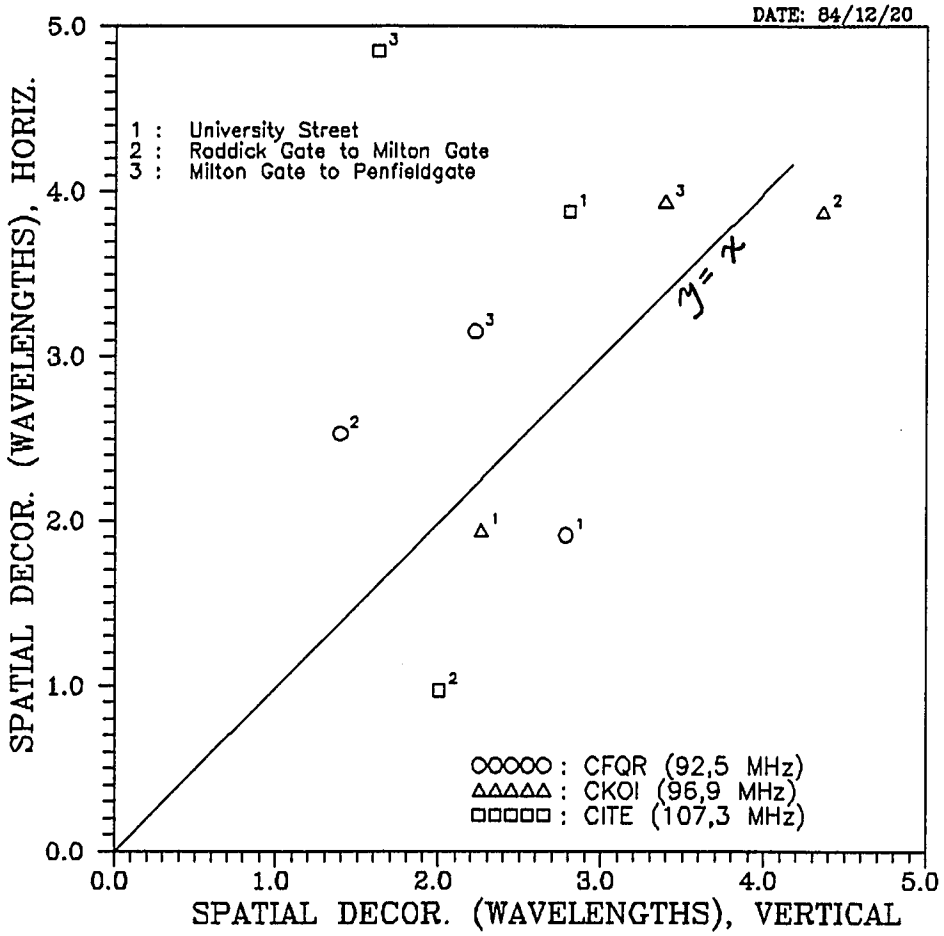

Fig. (5.3.2.3) Scatter plot comparing spatial decorrelation intervals (1st zero crossing) in wavelengths on three streets (#1,#2,#3, second survey). Stations CFQR (92,5 MHz), CKOI (96,9 MHz), CITE (107,3 MHz). Curves computed for a maximum lag of 0,1N samples. Vertical and horizontal polarization.

5.3.3 Crosscovariance Function

This section presents the experimental results of the crosscovariance function (CCVF) of the vertical and horizontal short term fading signals in a micro-environment.

The CCVF curve shows the amount of crosscorrelation on various street locations.

Figure {5.3.3.1} shows the *normalized* CCVF curves for stations CFQR (92,5 MHz) and CKOI (96,9 MHz) on Street 2 of the second outdoor survey.

In examining Fig. {5.3.3.1}, it is noted that certain features of the behaviour are evident. These are as follows:

(a) the correlation coefficient at zero shift is between 0 and 1 (unlike the ACVF curves) and changes from one station to the next,

(b) the correlation coefficient shows a peak at about 2,0 m for the three frequencies (roughly the physical separation of the vertical and horizontal dipole elements),

(c) the peak correlation is different for the three stations (e.g., for CKOI, the peak is at 0,62 but for CFQR the peak is at 0,26),

(d) beyond the peak, the correlation is generally below 0,2, thus the signals are considered uncorrelated [5.19].

Therefore, the CCVF curves can be evaluated by the following parameters:

* the value of the crosscorrelation coefficient at zero shift,
* the spatial shift at which the CCVF is maximum,
* the maximum crosscorrelation coefficient.

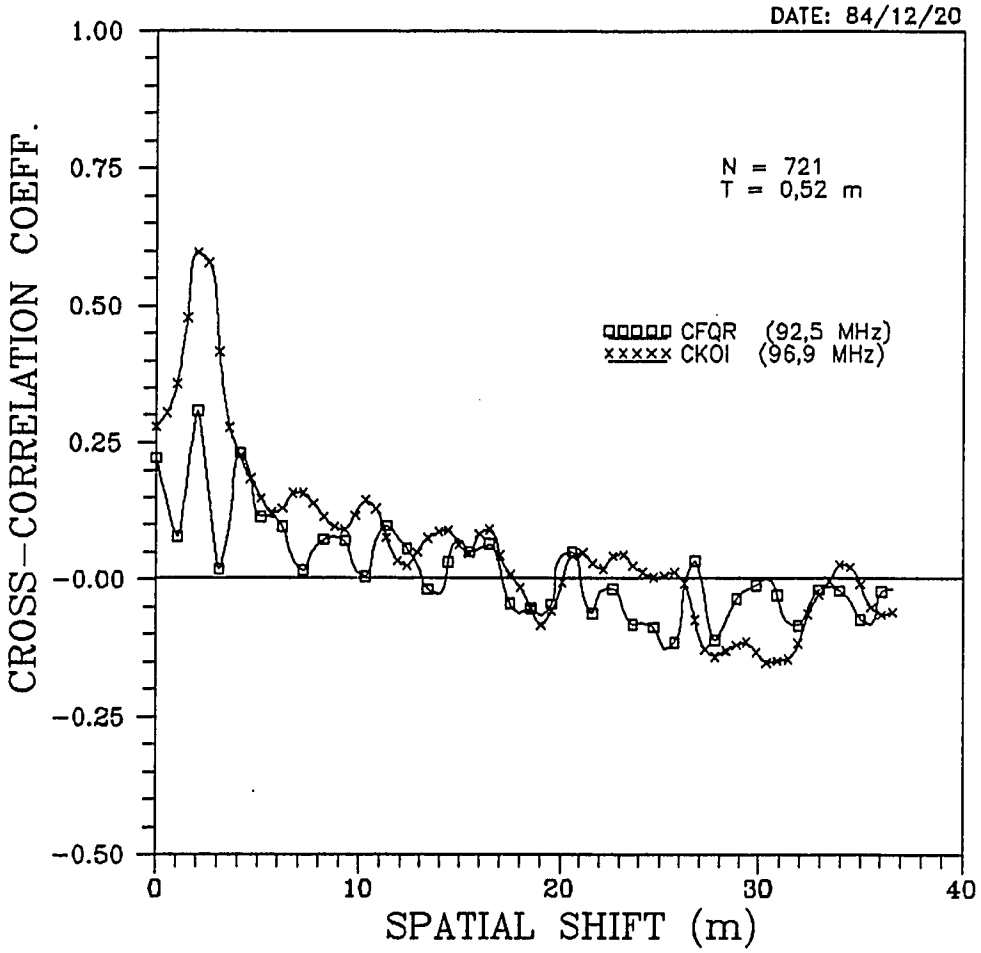

Fig. (5.3.3.1). Cross-Covariance Function (CCVF) curves of horizontal and vertical short term fading. Measured on street #2, second survey. Stations CFQR (92,5 MHz) and CKOI (96,9 MHz). Curves computed for a maximum lag of 0,1N samples. (The peak correlation corresponds roughly to the physical separation between the vertical and horizontal receiving antennas).

Table (5.3.3.1) summarizes the above CCVF parameters of three stations (CFQR,CKOI,CITE) as obtained from the measurements of the second outdoor survey. It is seen directly from the table that the spatial shift at which the maximum cross-correlation occurs is about 1,9 m in most cases, which corresponds to the physical spacing between the vertical and horizontal receiving antennas (cf. section (2.5)).

Table (5.3.3.1). Cross-Correlation coefficients between vertical and horizontal fading components. Stations CFQR (92,5 MHz), CKOI (96,9 MHz), CITE (107,3 MHz). CCVF curves computed for a maximum lag of 0,1N

Station I.D.	Street Location (84/12)	CCV Value at Zero Shift	Maximium CCV value	Spatial Separation at Max. CCV
CFQR	1	0,20	0,30	1,9 m
CKOI		0,23	0,62	1,9 m
CITE		0,13	0,17	1,9 m
CFQR	2	0,22	0,30	2,1 m
CKOI		0,27	0,32	2,1 m
CITE		0,06	0,17	2,6 m
CFQR	3	0,40	0,60	1,8 m
CKOI		0,29	0,47	1,8 m
CITE		0,24	0,28	2,7 m

Figure (5.3.3.2) shows a scatter plot of the maximum CCVF coefficients and the zero CCVF coeffcients for the three frequencies on streets 1,2,3 of the second outdoor survey. Again, a unity slope line $y=x$ is superimposed on the scatter plot. Nearness of the data points to the line indicates similarity of the ordinate (maximum crosscorrelation coeff) to the abcissa (zero crosscorrelation coeff). From the scatter

plot, it can be seen that the highest dissimilarity of the two coefficients occurs for station CKOI, street 1 and station CFQR, street 2. The scatter plot clearly shows differences in behaviour for different urban surroundings as well as for different transmitters. As with the case of the ACVF, the reasons for the observed behaviour are not evident due to a limited number of streets. However, the results demonstrate the behavioural differences from one street to the next within a micro-environment. Further investigations of this type are therefore suggested in view of the preliminary findings presented herein.

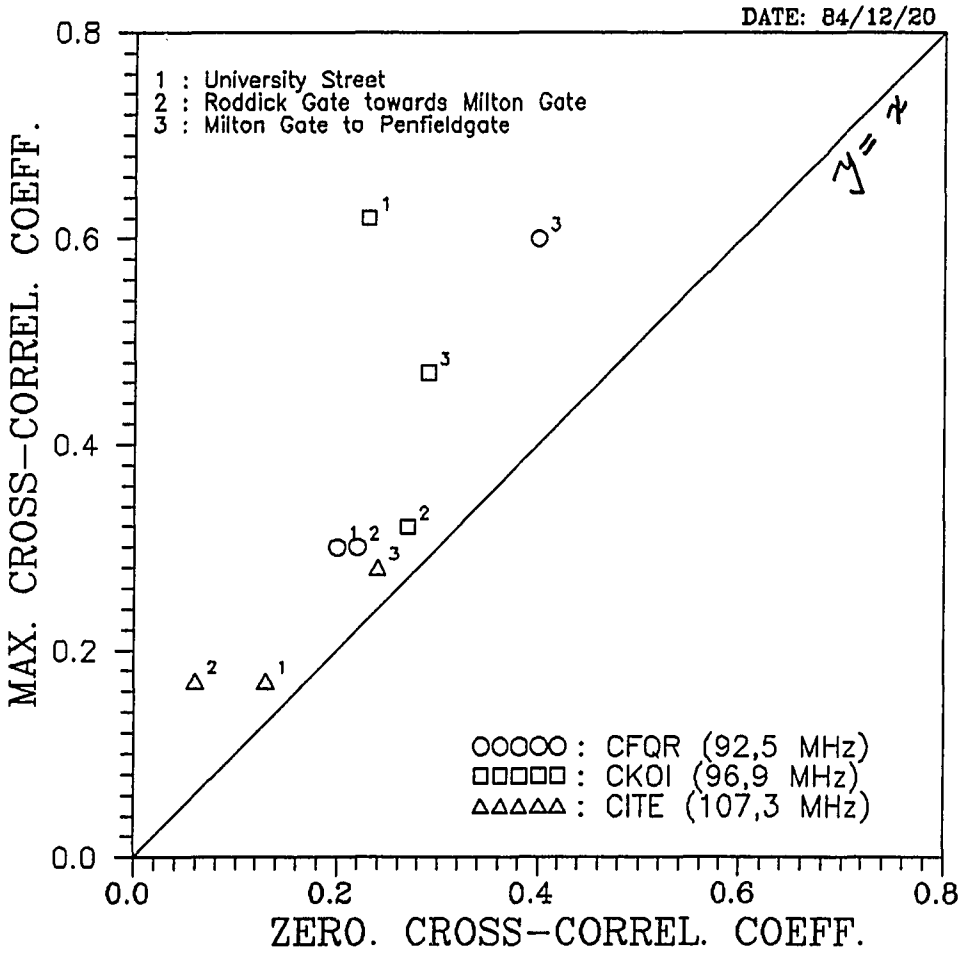

Fig. (5.3.3.2) Scatter plot comparing maximum CCVF coefficient and zero lag CCVF coefficient on three urban streets (routes #1,#2,#3, second survey). Stations CFQR (92,5 MHz), CKOI (96,9 MHz), CITE (107,3 MHz).

5.3.4 Power Spectral Density

This section presents experimental results of the (spatial) power spectral density (PSD) characterization of the short term fading in the urban micro-environment.

The PSD is a distribution of variance as a function of frequency [5.21]. The analytical expression for the continuous PSD is given by Kerr [5.22] (see Appendix D), where it is noted that the spectral density function is normalized to the total spectral power, obtained by integrating the power spectrum. This method was adopted in the course of the present work. Otnes and Enochson [5.21] suggested that the PSD be normalized by the total record length, $P=NT$, instead of by the total spectral power.

Based on the author's trial of both methods, it was decided to normalize by the total spectral power (instead of by the record length). This procedure was followed because it allows meaningful comparison between power spectra with different total spectral powers. This is is advantageous, since the emphasis is placed on the *shape* of the PSD curve (it gives very similar levels), and not on the *level* of the curve.

The PSD is estimated by computing the discrete fourier transform (DFT) of $s(x)$, denoted as $X(k)$, where k is the discrete spatial frequency index.

According to Otnes and Enochson [5.21], the discrete power spectral density estimate, $S_{xx}(k)$, is given by the following relation:

$$S_{xx}(k) = \frac{1}{P}\overline{|X(k)|^2}, \quad k = 0, 2, \ldots, N/2 \qquad (5.3.4.1)$$

In the above expression for $S_{xx}(k)$, k is the spatial frequency index, $P=NT$ is the record length in meters (N is the total spatial sample size, T is the sample spacing in meters) and bar denotes averaged spectrum (averaged over a small number of discrete spectral components). It is noted that the averaging (in this case, done by moving averages) is done after computing $|X(k)|^2$. Computational considerations of PSD estimation (e.g. choice of smoothing filter, resolution bandwidth, spectral stability) are discussed in Otnes and Enochson [5.21].

For real signals, the DFT is periodic about the Nyquist sampling frequency, *2/T*. Hence it is unecessary to compute the PSD estimate beyond the foldover frequency, *k=N/2*, since the PSD will display even symmetry about integer multiples of the foldover frequency.

As described in the Introduction, an important consideration in representing signals in the spectral domain is that the signal be sampled above the Nyquist rate [5.10]. Since the short term fading has an effective period of about $\lambda/2$ [5.2], the condition for *non-aliased* spectral domain representation is then,

$$T \leq \frac{\lambda}{4} \qquad (5.3.4.2)$$

Thus, for example, given a wavelength of 3,24 m (f=92,5 MHz), the maximum sample spacing should be 0,81 m for spectral domain representation. At the highest FM frequency, 107,3 MHz, the maximum sample spacing is 0,70 m. Referring to Table (2.7.2.1), it is evident from the point of spectral analysis, that only the data of the first two streets are valid since the sample spacings are 0,63 m and 0,52 m (i.e. less than T/4). The data of the third street should not be represented in the frequency domain since the sample spacing of T = 0,9 m is greater than $\lambda/4$ for frequencies above 83,3 MHz.

Having computed the square magnitude of the DFT for all spatial frequencies u pto the foldover frequency (*k=N/2*), the magnitudes are normalized by the total spectral power and are converted to decibels by taking the logarithm. Finally, the discrete power spectrum is smoothed out using a moving average rectangular window (MARW), identical in principle to that filtering procedure described in Chapter 4, except that the averaging length is much smaller (about 3% to 5% of the total number of samples, *k=N/2*).

Figure (5.3.4.1) shows a smoothed PSD for station CFQR, horizontal polarization, for route #2 of the second survey (Roddick Gate to Milton Gate). In this case the

sample spacing is 0,52 m, which satisfies the $\lambda/4$ sampling criterion. As shown in the graph, the average spectral density is practically the constant up to about 0,55 Lin-Hz, beyond which the average spectral power drops off quite noticeably. Details of the spectral filtering are indicated on the graph. The averaging length is chosen to be 3% of the total number of samples (N/2 = 360), or M=10 samples.

Other parameters of the PSD are the resolution bandwidth, B, which is a measure of the separation between discrete spectral components [5.21]. The resolution bandwidth is inversely proportional to the sample spacing and the number of samples of the original series, i.e., $B = 1/NT$ [5.21]. In Fig. {5.3.4.1}, the resolution bandwidth is 0,0027 Lin-Hz, corresponding to N=721 and T=0,52 m.

Figure {5.3.4.2} shows the corresponding PSD estimate for station CKOI, horizontal polarization, for route #2, as for station CFQR. The averaging length and spectral resolution are the same as for Fig.{5.3.4.1}. Note however the *shape* of the PSD in Fig. {5.3.4.2} as compared to that of station CFQR. In the PSD of Fig. {5.3.4.2}, it is observed that the average PSD values drop at a practically *linear rate* from the zero frequency, whereas, in Fig. {5.3.4.1}, a sharp decline (though not linear) occurs after 0,55 Lin-Hz. This shows a marked difference in spectral behaviour between the two stations.

Figure {5.3.4.3} is another graph of the PSD estimate for station CFQR but on University Street (route #1, second survey). It is noted that the spectral resolution is 0,0012 Lin-Hz and that the spectral smoothing window uses M=32 (5% of 1310) samples. The choice of the smoothing window size is based on considerations of spectral stability [5.21]. For a given resolution bandwidth, the greater number of samples used in the averaging, the greater the stability (or conversely, the less 'noisy' the spectral estimate) [5.21].

As can be seen in comparing Figs. {5.3.4.1} and {5.3.4.3}, the latter is more stable owing to the lower number (and size) of random peaks. The random peaks can be thought of as noise. An interesting feature of both graphs is that the basic shapes are very similar. For example, both graphs exhibit a constant behaviour up to about 0,55 Lin-Hz. Beyond 0,55 Lin-Hz, the behaviour for the two streets is also quite similar.

Figure (5.3.4.4) shows for comparison with Fig. (5.4.4.3) the corresponding graph for station CKOI on University Street (route #1, second survey). Again, it is seen that the general shape of the graph is similar to that obtained for the main campus route, showing for example, a general linear decline in average spectral power with increasing spatial frequency. Thus it is apparent that the estimate of the power spectrum in the manner described is useful in identifying differences in the short term fading behaviour.

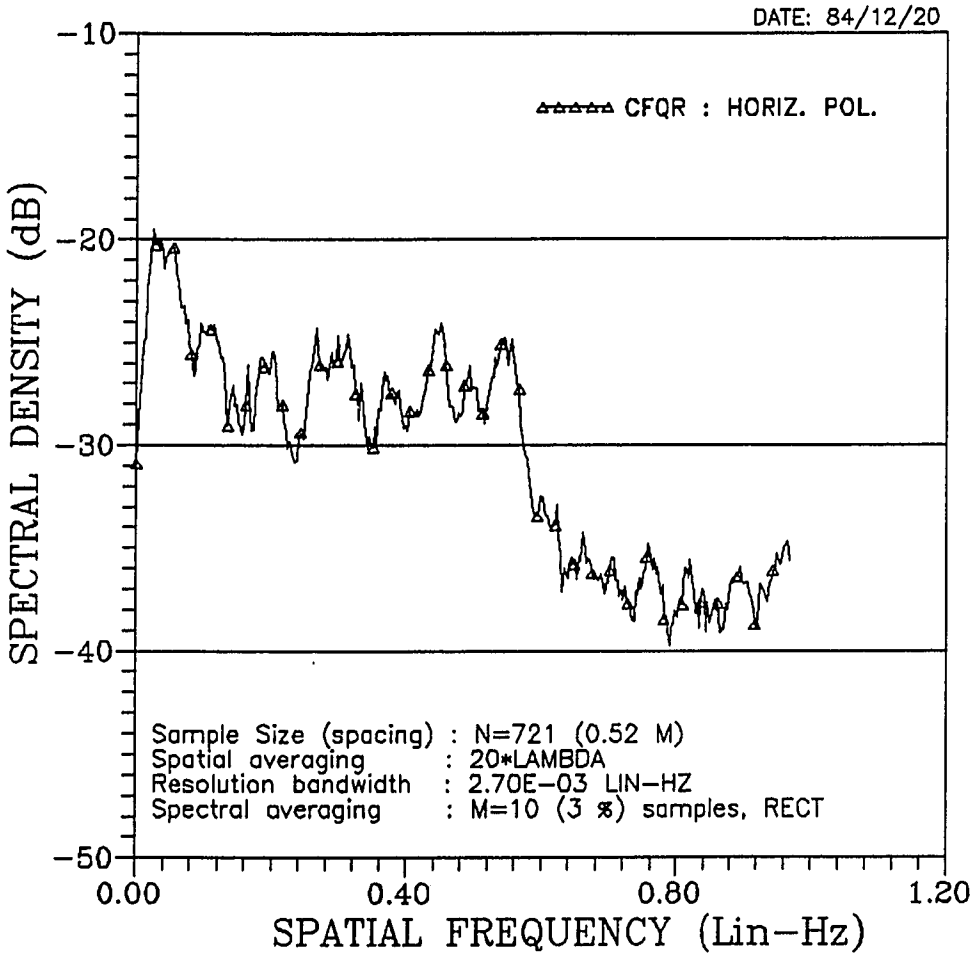

Fig. (5.3.4.1) **Power Spectral Density (PSD) function of short term fading. Station CFQR (92,5 MHz) on Roddick Gate route (#2, second survey). Horizontal polarization.**

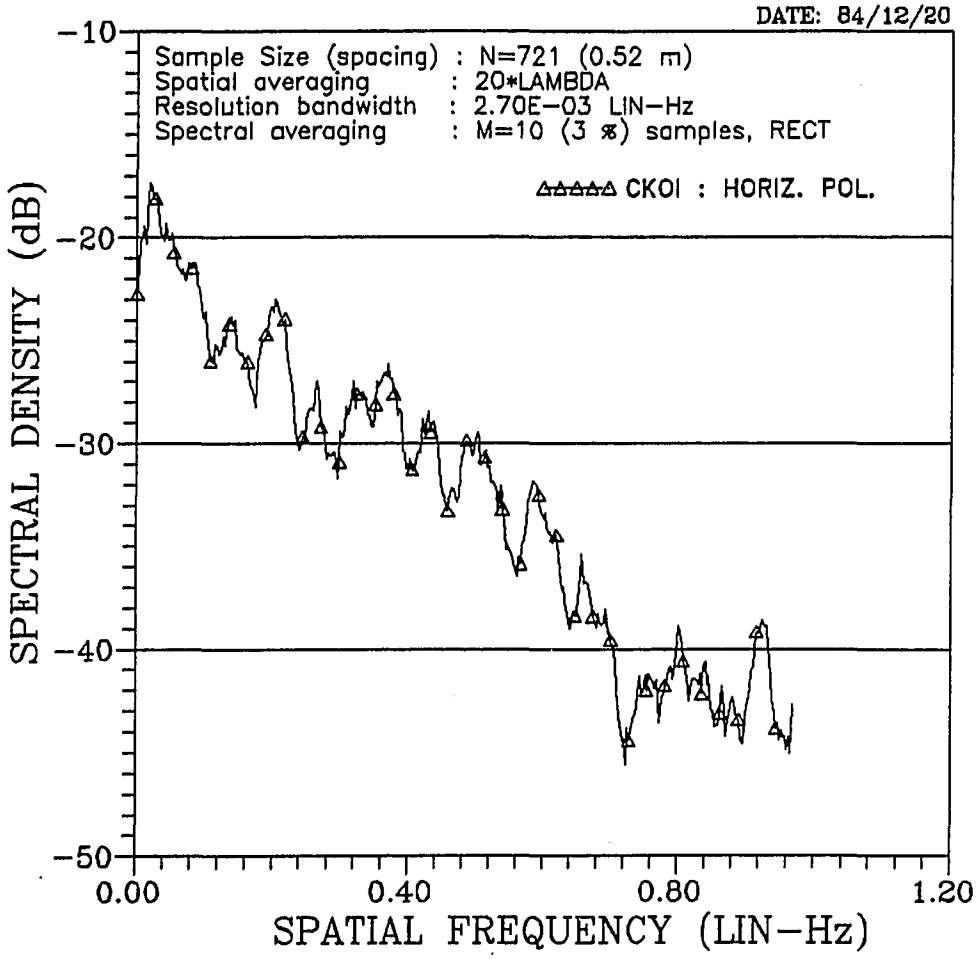

Fig. (5.3.4.2) Power Spectral Density (PSD) function of short term fading. Station CKOI (96,9 MHz) on Roddick Gate route (#2, second survey). Horizontal polarization.

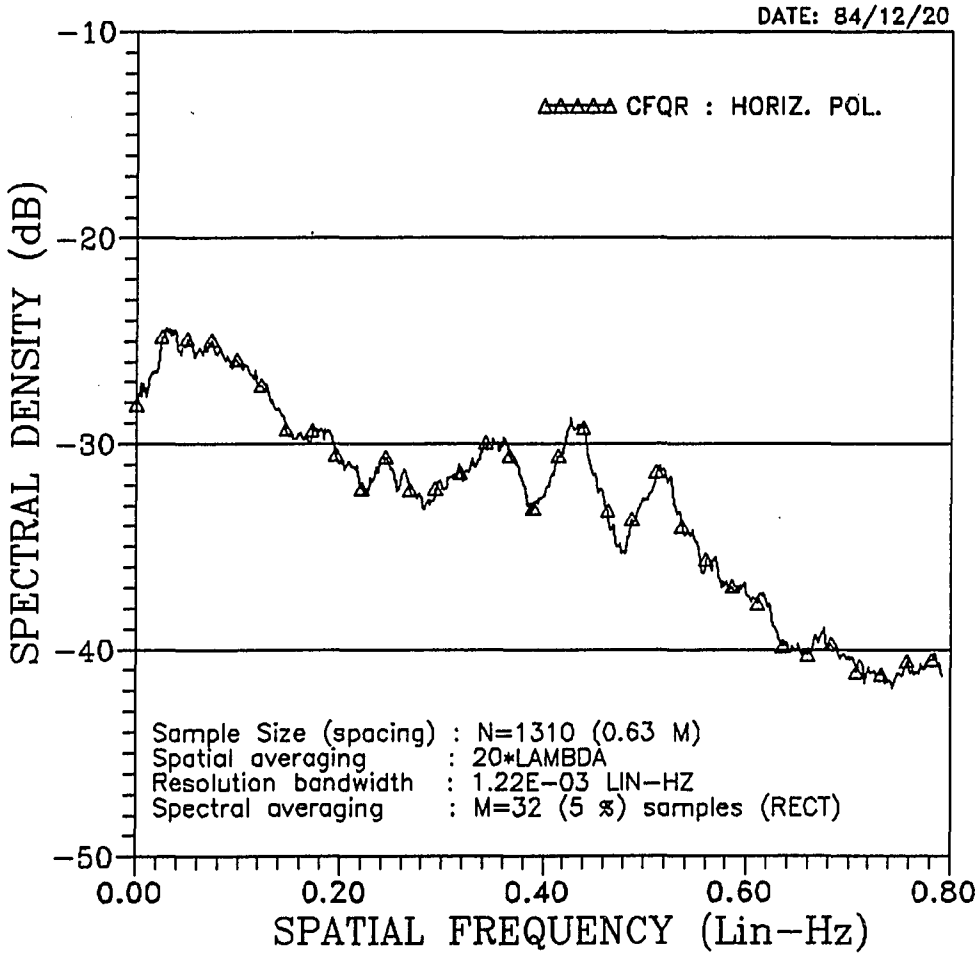

Fig. (5.3.4.3) Power Spectral Density (PSD) function of short term fading. Station CFQR (92,5 MHz) on University Street (route #1, second survey). Horizontal polarization.

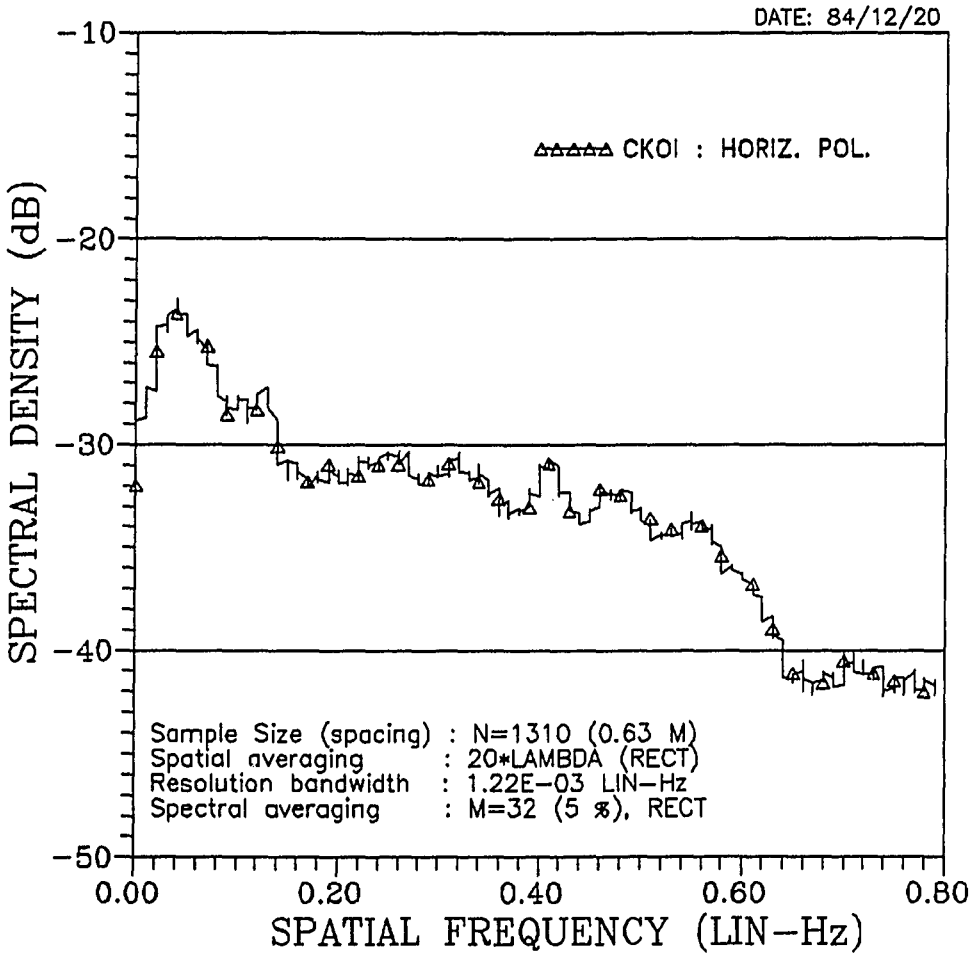

Fig. (5.3.4.4) Power Spectral Density (PSD) function of short term fading. Station CKOI (96,9 MHz) on University Street (route #2, second survey). Horizontal polarization.

5.4 Discussion of Results

5.4.1 Discussion : the PDF

It is observed that the statistical behaviour of the short term fading is well described by a logarithmic Rician PDF, giving a correlation coefficient of between 0,77 and 0,92. The lognormal model also gave a rather good fit to the experimental PDF, with correlation coefficients ranging from 0,73 to 0,92 for the three streets. However, it is observed that by combining the lognormal and log-Rician PDFs in the manner suggested in section (5.3.1), the resulting PDF gives a slightly better fit to the data than either of the individual distributions, with correlation coefficients ranging from 0,78 to 0,93. The proposed distribution, called the CLNLR, suggests the possibility of modeling a particular PDF by a combination of different theoretical distributions. The possible theoretical consequences of this concept in terms of statistical theory, however, have not been examined and are beyond the scope of the present work.

It is also found from the scatter plots of the PDF statistics that differences in behaviour (i.e., mean, standard deviation, skewness, kurtosis) are seen for different conditions of measurement such as street location, frequency, and polarization. A definitive explanation of all the phenomena as presented is not possible from a limited set of measurements (3 streets). Nevertheless, differences in behaviour between streets are evident from the PDF characteristics. Assuming that the first order PDF is statistically stationary, the moments of the PDF can be used as a basis of characterizing the statistical behaviour of short term fading in a micro-environment.

In order to develop a model based on experimental investigations of this type, it is desirable to continue such studies on a much wider scope to provide a broad base of data for comparison. Such an empirical approach, while costly to carry out in practice, may well increase the understanding of propagation in urban environments. Although no new propagation phenomena could be identified from the limited set of

measurements, the present results suggest that placing a greater importance on micro-environment field measurements may increase the basic understanding of radio wave propagation in urban areas.

5.4.2 Discussion : the ACVF

The spatial ACVF characteristics of the short term fading reveals that for certain streets the vertical polarization tends to decorrelate more rapidly than the horizontal, however, the reverse is true for other streets. Consistencies or general trends are not apparent from the limited data available (3 streets). Perhaps a better understanding of the phenomena would evolve as more comprehensive measurements in other urban micro-environments become available, and the same comment for the PDF would apply for the second order statistics, such as the covariance functions (ACVF and CCVF).

Although not examined in the present work, a suggested study would be to investigate the property of *wide sense (spatial) stationarity* (WSS) [5.23] of the short term fading. This would involve determining the spatial intervals over which the first and second order statistical behaviour remains unchanged. Such investigations have, to the best of the author's knowledge, not been reported to date. However, the concept of wide sense stationarity is well understood in the context of time domain measurements (i.e., the statistical properties are invariant under shifts of the time origin).

5.4.3 Discussion : the CCVF

The spatial CCVF characteristics of the short term fading reveal that differences in crosscorrelation behaviour do exist among different streets. As with the case of the ACVF, consistencies are not apparent from the limited data available. It is therefore suggested that further investigations in other urban micro-environments be carried out to provide further data for comparison.

As with the case of the ACVF, a suggested study would be to examine the property of *wide sense (spatial) stationarity*, that is, the investigation of the spatial

intervals over which the first and second order statistics remain unchanged. In principle, the concept of stationarity can be extended to higher orders [5.23]. Such basic studies would enhance the understanding of the stochastic nature of short term fading.

5.4.4 Discussion : the PSD

Estimation of the spatial PSD of the short term fading shows that the method can reveal differences in behaviour for different transmitters. The spectral characteristics are such that the average spectral power generally drops at higher spatial frequencies. The spatial PSD is thus proposed as a possible method for characterizing the fast fading behaviour. One should recall that for a white noise random process, the PSD characteristic should be flat [5.24]; hence departures from flat spectral behaviour indicates a departure from a purely white noise random process [5.24].

In addition, it should be remembered that increasing the rate of sampling beyond the Nyquist rate has the effect of increasing the spectral resolution in the estimate of the PSD [5.21]. Hence, for spectral domain representation of fast fading, the sampling spacing should be as small as possible, and certainly not greater than one-quarter of a wavelength.

5.5 Concluding Remarks

This chapter has shown that (spatial) short term fading can be described through the use of established time series analysis methods. Such methods include the probability density function (PDF), autocovariance function (ACVF), crosscovariance function (CCVF), and power spectral density (PSD). Using the short term fading data such methods were applied in order to compare the characteristics for different streets. Critical statistical parameters of each of the above methods were evaluated, and street level comparisons were made of the critical parameters using scatter plots. Differences between like parameters were observed for different street locations, and between the vertical and horizontal polarizations. Therefore, it is evident that short term fading

can be characterized on a *microscopic scale.*

In addition, it was observed that a new distribution, the "combination lognormal log-Rician" (CLNLR) gave a better fit to the experimental PDF than either the lognormal or the logarithmic Rician distributions. Such a *piecewise description* of statistical distributions has not, to the best of the author's knowledge, been reported in the literature. Further examination of the mathematical validity of this concept is therefore suggested.

The analysis of the the short term fading data in this chapter has illustrated the importance of urban micro-environment field measurements, and of applying statistical and time series methods to analyze the results. In order to develop further understanding of the observed phenomena, it is suggested that similar studies be continued out in other urban micro-environments, and other frequency ranges (e.g. the 800/900 MHz cellular range) to provide a broader base of data for comparison.

5.6 End Notes

[5.1] **W.C.Y. Lee**, *Mobile Communications Engineering*, New York, McGraw-Hill, 1982, p.170.

[5.2] **W.C.Y. Lee**, *Mobile Communications Engineering*, 1982, p.46.

[5.3] For a discussion of mobile radio diversity methods, see **W.C. Jakes, Jr., (Ed.)**, *Microwave Mobile Communications*, New York, Wiley, 1974.

[5.4] some early experimental studies of mobile propagation at VHF and UHF can be found in the following papers:

P.M. Trifonov, V.N. Budko, and V.S. Zotov, "Structure of USW Field-Strength Spatial Fluctuations in a City", *Telecommun. and Radio Eng.*, February 1964, pp.26-30.

D.O. Reudnik, "Properties of Mobile Radio Propagation Above 400 MHz", *IEEE Trans. Vehicular Technology*, vol. VT-23 no.4, November 1974, pp.143-159.

R.W. Young, "Comparison of Mobile Radio Transmission at 150, 450, 900 and 3700 Mc", *Bell System Technical Journal*, vol. 31, November 1952, pp.1068-1085.

[5.5] **R.H. Clarke**, "A Statistical Theory of Mobile Radio Reception", *Bell System Technical Journal*, vol. 47, July-August 1968, pp.957-1000.

[5.6] This is a consequence of the Central Limit Theorem for large N, assuming that the phases of the incoming waves are statistically independent.

[5.7] See **W.B. Davenport and W.L. Root**, *An Introduction to the Theory of Random Signals and Noise*, New York, McGraw-Hill, 1958, pp. 160-161.

[5.8] **T. Aulin**, "A Modified Model for the Fading Signal at a Mobile Radio Channel", *IEEE Trans. on Vehicular Technology*, vol. VT-28 no.3, August 1979, pp.182-203.

[5.9] **S.O. Rice**, "Mathematical Analysis of Random Noise", *Bell System Technical Journal*, vol. 24, January 1945, pp.46-156.

[5.10] See, for example, **A.V. Oppenheim and R.W Schafer**, *Digital Signal Processing*, New Jersey, Prentice-Hall, 1975, p. 29.

[5.11] **M. R. Spiegel**, *Theory and Problems of Statistics in SI Units*, Schaum's Outline Series, New York, McGraw-Hill, 1981, p.91.

[5.12] This is simply a Rician distribution plotted on a logarithmic (dB) scale. The Log-Rice distribution, $p(y)$, is obtained from the linear Rice distribution, $p(x)$, by recalling that equality of probability increments must hold for the same pdf on different scales, x and y. Thus,

$$p(x)dx = p(y)dy$$

$$p(y) = p(x)\frac{dx}{dy}$$

In the case where $y = 20 \log (x)$, $dy/dx = 20/x$, then

$$p(y) = p(x) \cdot \frac{x}{20}$$

[5.13] See **J.M. Chambers, et al.**, *Graphical Methods for Data Analysis*, Boston, Duxbury Press, 1983, pp.75-127.

[5.14] Pearson product moment correlation coefficient as given in, **M.R. Spiegel**, *Theory and Problems of Statistics in SI Units*, 1981, p.244.

[5.15] **W.C. Jakes**, *Microwave Mobile Communications*, 1974, pp.309-313.

[5.16] **W.C.Y. Lee**, "Antenna Spacing Requirement for a Mobile Radio Base-Station Diversity", *Bell System Technical Journal*, vol. 50, July-Aug. 1971, pp.1859-1974.

[5.17] **W.C.Y. Lee**, *Mobile Communications Engineering*, 1982, p.276.

[5.18] **W.C. Jakes**, *Microwave Mobile Communications*, 1974, pp.313-316.

[5.19] **B.R. Davis and R.E. Bogner**, "Propagation at 500 MHz for Mobile Radio", *Proc. IEE*, Part F, vol. 132, August 1985, p.317.

[5.20] See **R.H. Clarke**, "A Statistical Theory of Mobile Radio Reception", July-August 1968, p.965.

[5.21] See **R.K. Otnes and L. Enochson**, *Applied Time Series Analysis*, vol.1, New York, Wiley, 1978, pp.317-340.

[5.22] See **D. Kerr (Ed.)**, *Propagation of Short Radio Waves*, Dover Press, p.558.

[5.23] For an introductory discussion of stationary random processes, see, for example, **W.B. Davenport**, *Probability and Random Processes*, New York, McGraw-Hill, 1970.

[5.24] See **H.R. Raemer**, *Statistical Communication Theory and Applications*, New Jersey, Prentice-Hall, 1969, pp.60-65.

Chapter 6:

SUMMARY AND CONCLUSIONS

This chapter summarizes the present work, states the major conclusions, summarizes the contributions, and suggests a possible direction of future work.

SUMMARY

The present study has reported the measurement and characterization of spatial fading of radio signals in an urban '*micro-environment*'. Automated field strength measurements were conducted to investigate the (spatial) long term and short term fading behaviour in a small region of a large urban center (the McGill University campus in Montreal, Canada). A mobile field instumentation vehicle (MFIV) was employed to gather large amounts of data at ten FM broadcast frequencies in the micro-environment.

The data analysis involved separating the long term and short term fading components of the received signal, and analyzing the behaviour of each component separately. The methods of analysis of the long term fading included the spatial fading patterns, and the use of theoretical and empirical quantile-quantile (Q-Q) plots. The methods of analyzing the short term fading included the probability density function (PDF), the autocovariance function (ACVF), the cross-covariance function (CCVF), and the power spectral density (PSD).

A significant amount of data processing effort was required to study the data. This effort included the data reduction, preprocessing, and the development of a number of statistical analysis software packages. The analysis was transferred to a microcomputer environment to enable easier data management and lower operating cost. The software in its current form is adaptable to other field surveys of this kind.

From the analysis of the measurements, identifiable statistical characteristics of the micro-environment were observed, including the relative insensitivity to time. From

such studies, it is concluded that the micro-environment field measurements provides a basis for a statistical description of long term and short term spatial fading phenomena in urban environments.

The contributions of the thesis are therefore threefold: (i), the concept of 'micro-environment' (MCENV) field measurements, (ii), the manner of application of statistical and time series analysis methods to characterize long term and short term spatial fading phenomena, and (iii), the identification and statistical characterization of long term and short term fading phenomena of a particular micro-environment based on automated field measurements.

CONCLUSIONS

In accordance with the objectives of this work, the major conclusions of the work can be divided into three categories as follows: (1), experimental methodology, (2), application of statistical methods, and (3), statistical characterization of spatial long term and short term fading effects of an urban micro-environment based on (1) and (2).

1). Experimental Methodology

In the course of the present work, it is obvious that unless large amounts of data are collected from different base transmitters as well as on different street locations, a meaningful evaluation of signal fading effects cannot be performed. Stated below are several experimental considerations in carrying out an investigation of long term and short term fading in urban areas.

(a) *Concept of urban 'micro-environment' field surveying*; Much previous work has been reported on urban mobile propagation, however, it appears that not much attention has been devoted to local environmental effects. Such effects are inherent to urban radio propagation and need to be investigated in their own right. The study of urban propagation on a street to street level basis is referred to as a *microscopic scale*

characterization, and the importance of this approach (using test signals in the FM broadcast band) was demonstrated by the present work. The term *urban 'micro-environment'* thus refers to the study of small scale effects of the local surroundings.

The significance of *urban micro-environment* studies is that further insight of the propagation phenomena may be gained from measurements, thus leading to the development of empirical models.

(b) *Need for automated measurements*; Single point measurements at a given location are not meaningful. A statistically significant number of measurements (see (c)) is required to characterize the fading behaviour along different streets. This emphasizes the need of gathering and storing field strength data in an automated manner. It is suggested that similar data logging equipment be used in future work.

(c) *Rate of sampling*; A proper rate of sampling (at least twice the signal bandwidth) must be used to provide a unique signal representation. For long term fading, a sampling interval of about one wavelength ($T \sim \lambda$) provides uncorrelated sampling for estimating the local mean field strength. For short term fading, a sampling interval of the order of one-quarter wavelength or less ($T \leq \lambda/4$) should be used in view of $\lambda/2$ fluctuations of the envelope.

(d) *Street variety*; Single street measurements in a micro-environment field survey are not meaningful unless compared with similar measurements along other streets of different physical makeup. Ideally, a wide variety of street types should be surveyed, each with different amounts of buildup (such as shadowed, partially shadowed, and unshadowed streets). Street orientation effects should also be considered, for example, radial and circumferential streets.

2). Application of Statistical Methods

Due to the large number of measurements taken, suitable statistical methods should be employed to reduce the data to meaningful parameters. The use of statistical methods becomes necessary as the fading effects cannot be studied directly from the original data.

The statistical methods examined in the course of the present work were the following:

* *Moving Averages* - to separate the long term and short term fading components. In the present work, an averaging length of twenty wavelengths at the measured frequency was consistently used in separating the slow (long term fading) and fast (short term fading) variations of the received signal;

* *Quantile-Quantile (Q-Q) Plots* - to compare the cumulative distribution behaviour of a set of data versus a theoretical distribution (theoretical Q-Q) or another set of data (empirical Q-Q) [6.2]. In the present work, both the theoretical and empirical Q-Q plots were used to describe the cumulative distribution (CDF) of the long term fading signals of different streets;

* *Probability Density Function (PDF)* - to describe the first order statistical behaviour of the short term fading using the central moments of the PDF. In addition, an analytical description of the experimental PDF was achieved based on a *piecewise construction* of the lognormal and log-Rician PDFs. Such a procedure was observed to give a better fit to the data than either the lognormal or the log-Rician PDFs.

* *Autocovariance Function (ACVF)* - to examine the spatial correlation characteristics of the short term fading in the micro-environment. In particular, the spatial decorrelation interval was compared for different streets. Although not examined in the

present work, it is suggested that the second order statistical behaviour be investigated. The concept of *spatial wide sense stationarity* could be applied to investigate the spatial interval over which the statistics remain unchanged.

* *Crosscovariance Function (CCVF)* - to examine the cross-correlation behaviour between the vertical and horizontal short term fading signals in the micro-environment. In particular, the maximum cross-correlation coefficient and the zero shift cross-correlation coefficient were compared for different streets.

* *Power Spectral Density (PSD) Function* - to examine the spectral characteristics of the short term fading in the micro-environment.

3). Characterization of the Micro-Environment Behaviour

Based on the application of the statistical methods outlined above, a number of effects were characterized with regard to the spatial fading phenomena in the urban micro-environment. These effects are described below.

a) *Long Term Fading Effects*

Several effects were identified, listed as follows:

i) Effect of building obstruction on a given street,
ii) Effect of shadowing among parallel streets,
iii) Effect of different transmitter locations,
iv) Effect of street orientation,
v) Comparison of polarization behaviour on radial and arc streets.

In addition, the CDF behaviour of the long term fading on individual has compressed tails when compared to the lognormal behaviour. This shows agreement with similar measurements reported by Davis and Bogner [6.1].

The CDF behaviour of the long term fading (as compared with the lognormal model) can be conveniently studied by the use of theoretical *quantile-quantile plots* [6.2]. Such plots show a comparison between the experimental data versus a known theoretical distribution (e.g. Gaussian), or between two experimental distributions (empirical Q-Q plot). In view of the *behavioural information* provided by Q-Q plot techniques, a more general use of Q-Q plots is therefore suggested for the analysis of propagation data in other frequency ranges (e.g. 800/900 MHz cellular range).

b) *Short Term Fading Effects*

The following analytical methods were tried in the study of the short term fading, and the salient points of each method are summarized as follows:

(i) The probability density function (PDF) is well described by a logarithmic Rician distribution (a Rician distribution plotted on a dB scale). A new statistical description, called the '*combination lognormal log-Rician*' *(CLNLR)* evidently offers a consistently better fit to the data than either the lognormal or the log-Rician. This distribution is composed of two parts: for negative dB values, the CLNLR distribution matches the lognormal, while for positive dB values, the CLNLR matches the best fit log-Rician.

It is concluded that the experimental PDF can be studied on a street level basis by comparing the expected value (mean), the standard deviation, the coefficient of skewness, and the coefficient of kurtosis. These parameters are indicative of the shape of the PDF. From the results, it is evident that differences in behaviour occurs for changes in polarization and among different streets. The use of scatter plots is helpful in illustrating differences among like statistical parameters.

(ii) The spatial autocovariance function (ACVF) revealed behavioural differences between the vertical and horizontal polarizations and among different streets. The spatial decorrelation interval was compared for both polarizations and on different streets using scatter plots.

(iii) The spatial cross-covariance function (CCVF) revealed behavioural differences in the amount of cross-correlation between the vertical and horizontal polarizations on different streets. Two parameters of interest are the cross-correlation coefficient at zero spatial shift, and the maximum cross-correlation coefficient. The parameters can be compared for different streets through the use of scatter plots.

(iv) The power spectral density (PSD) has been considered with the objective of describing the spectral characteristics of the fast fading component. In general, it was found that the spectral behaviour decreases in magnitude at the higher spatial frequencies. However, the shape of the PSD characteristic differs from one station to another on a given street.

CONTRIBUTIONS AND SUGGESTIONS FOR FURTHER WORK

The three major contributions of the thesis were (i), the concept of 'micro-environment' field measurements, (ii), the manner in which statistical and time series analysis methods were applied, and (iii), the statistical description of long term and short term fading phenomena in a particular micro-environment based on field measurements. With the adoption of the experimental and statistical methods described, it is evident that greater understanding of fading in urban environments can be obtained from measurements.

To suggest a possible direction for future work, one could attempt to model the situations physically at smaller wavelengths [6.3]. Such methods would have to incorporate the physical details of the urban environment, including the shape, size, and

location of all buildings, and other obstacles. Precise geographical terrain data may be difficult to obtain in practice. Nevertheless, assuming that such data are available, the analytical results could be compared against experimental results (for example, the spatial long term fading patterns). Differences between theory and experiment could be examined to evaluate the validity of the model.

Based on the accuracy of the analytical model, propagation requirements of land mobile radio systems (LMRS) can be planned in a cost-effective manner. However, it is important to keep in mind that a single model may not give a good prediction of the actual behaviour in all situtations. Therefore, it is also recommended that modeling work of this kind be supplemented by ongoing experimental work.

Characterization of the urban micro-environment as applied to radio propagation is essential to the development of reliable wireless communication systems. The contributions of the present work should therefore be directed to those engaged in developing indoor or outdoor wireless radio systems. In view of recent interest in cellular radio system development, measurement and characterization of long term and short term spatial fading is suggested for other urban micro-environments and other frequency ranges, particularly the 800/900 MHz cellular band.

Finally the development of the 'combined' distribution modeling merits special comment. Such combined modeling techniques, although not properly an objective of this thesis, may bear further examination, elsewhere, of their significance. Such an examination would of course be outside the domain of radio wave propagation and would lie in the domain of mathematics.

End Notes

[6.1] **B.R. Davis and R.E. Bogner**, "Propagation at 500 MHz for Mobile Radio", *Proc. IEE*, Part F, vol. 132, August 1985, pp.307-320.

[6.2] **J.M. Chambers, W.S. Cleveland, B. Kleiner, and P.A. Tukey**, *Graphical Methods for Data Analysis*, Boston, Duxbury Press, 1983, pp. 48-57;197-227.

[6.3] **R.E. Bogner**, private communication, June 1, 1988.

APPENDIX A:

PDF AND SHORT TERM FADING

The *probability density function (PDF)* [A.1] is a useful method for describing the behaviour of random data. The PDF of the short term fading, denoted by $p(s)$, can be expressed in terms of its cumulative distribution function (CDF), $P(s)$, as follows :

$$p(s) = \frac{d}{ds} P(s) \qquad (A.1)$$

where the expression for $P(s_0)$ is given by the relative number of occurrences of s less than or equal to $s=s_0$:

$$P(s = s_0) = \frac{n(s \le s_0)}{N} \qquad (A.2)$$

In practice, $p(s)$ is computed for discrete samples by sorting the data in ascending order, dividing the data into L discrete bins (bin size is 1 dB), and obtaining the relative number of occurrences in each bin. This results in a discretized version of the continuous PDF, denoted as $p(i)$, $(i=1,L)$. The **sorted data** will be denoted by uppercase, $S(j)$, to avoid confusion with the **original data**, $s(j)$.

For example, for a signal range of 20 dB, there would be L = 20 - 1 = 19 bins of width 1 dB each. The *discrete probability density*, $p(i)$, in the *ith* to *(i+1)st.* bin inclusively, $(i=1,...L)$, is thus obtained as follows:

$$p(i) = \frac{n(i, i+1)}{N} \qquad (i = 1, \ldots, L) \qquad (A.3)$$

$$L = \frac{\{S(N) - S(1)\}}{BIN} \qquad (A.4)$$

In Eq.(A.3), *n(i,i+1)* is the number of samples lying between the *ith* and *(i+1)st* bins, *N* is the total number of samples contained in *L* bins, and *BIN* is the width of a bin (BIN = 1 unless stated otherwise). It should be noted that *n(1,L+1) = N*, the total number of samples in the record, *s(j)*. The number of bins, *L*, is the nearest integer to the range of *s(j)*.

The experimental PDF, as given by Eq. (A.3) thus completely describes the statistical behaviour of a sample record, *s(j), j=1,...,N.*

In order to compare the characteristics between different PDFs, corresponding to different sample records *s(j)*, the following descriptive statistics are helpful: mean ($\bar{s}$), standard deviation (σ), coefficient of skewness (γ), and coefficient of kurtosis (β).

Except for the mean, all the above parameters are obtained from the central moments M_j representing the *jth* central moment of *s(x)*. The statistics mentioned are computed on the basis of the discrete PDF, *p(i)*, as follows:

$$\bar{s} = E\{s(x)\} \qquad (A.5)$$

where *E(s(x))* denotes expected value of *s(x)*, defined as follows:

$$E\{s(x)\} = \int_{-\infty}^{+\infty} S \cdot p(s)ds \qquad (A.6)$$

In discrete terms, the expected value, *E (s(i))*, may be written as,

$$E\{s(i)\} = \sum_{i=1}^{i=L} S(i) \cdot p(i) = \bar{s} \qquad (A.7)$$

The *jth* central moment of *s(x)*, M_j, is given by the following expression:

$$M_j = E\left\{[S(i) - \bar{s}]^j\right\} \qquad (A.8)$$

Assuming *p(s)* is known, the central moments can be computed from the following equation:

$$M_j = \int_{-\infty}^{+\infty} p(s) \cdot [S - \bar{s}]^j ds \qquad (A.9)$$

In the discrete variable case, *S(i)* replaces *S(x)*, *p(i)* replace *p(s)*, and a summation (over L discrete bins) replaces the integration (over the range of *s*). Hence the expression for the discrete *jth* central moment becomes,

$$M_j = \sum_{i=1}^{i=L} [S(i) - \bar{s}]^j \cdot p(i) \qquad (A.10)$$

Thus the standard deviation, coefficient of skewness, and the coefficient of kurtosis [A.2], may be expressed in terms of the central moments of the discretized PDF as follows :

$$\sigma = \sqrt{M_2} \qquad (A.11)$$

$$\gamma = \frac{M_3}{\sqrt{M_2^3}} \qquad (A.12)$$

$$\beta = \frac{M_4}{M_2^2} - 3.0 \qquad (A.13)$$

End Notes

[A.1] See, for example, **A. Papoulis**, *Probability, Random Variables, and Stochastic Processes*, New York, McGraw-Hill, 1965.

[A.2] **M.R. Spiegel**, *Theory and Problems of Statistics in SI Units*, Schaum's Outline Series, New York, McGraw-Hill, 1987, p.91.

APPENDIX B:

ACVF AND SHORT TERM FADING

The *autocovariance function (ACVF)* of a continuous time (or spatial) series, $s(x)$, denoted as $R_s(x,x+\tau)$, where τ is the amount of positive (or negative) shift w.r.t. the origin ($x=0$), and T is the record length (in meters) of $s(x)$.

$$R_s(x,x+\tau) = E\{(s(x+\tau)-\bar{s})\cdot(s(x)-\bar{s})\} \qquad (B.1)$$

Assuming ergodicity of $s(x)$, ensemble averages equal time averages, Eq. (B.1) may be expressed in terms of a time (spatial) average as follows:

$$R_s(x,x+\tau) = \lim_{T\to\infty}\frac{1}{2T}\int_{-T}^{T}[s(x+\tau)-\bar{s}]\cdot[s(x)-\bar{s}]dx \qquad (B.2)$$

Since for practical series, $s(x)$, the averaging interval T is finite and the parameter x is positive, Eq. (B.2) can be written as follows:

$$\hat{R}_s(x,x+\tau) = \frac{1}{T-\tau}\int_{0}^{T-\tau}[s(x+\tau)-\bar{s}]\cdot[s(x)-\bar{s}]dx \qquad (B.3)$$

Equation (B.3) represents a biased *estimate* of the true autocovariance function, $R_s(x,x+\tau)$ because the average is taken over a finite length $(T-\tau)$ instead of an infinite interval, $T\to\infty$ [B.1].

In equation (B.3), the maximum length of the record, $s(x)$, is $x=T$, and the spatial shift parameter is τ. In practice, the autocovariance function is computed upto a maximum spatial shift of $\tau = 0,1N$ in order to keep the lag error to about 11% [B.2].

In the discrete case, equation (B.3) reduces to equation (B.4) where the continuous parameters (x,τ,T) are replaced by their discrete counterparts (i,m,N), and the integration replaced by summation :

$$\hat{R}_s(i,i+m) = \frac{1}{N-m} \sum_{i=1}^{i=N-m} [s(i+m)-\bar{s}]\cdot[s(i)-\bar{s}] \qquad (B.4)$$

$$m = 0,1,....,M \quad ; \quad M = 0,1N$$

In the present work, the autocovariance function is computed for shifts up to ten percent of the record length, that is $0 < m < 0,1N$, where N is the number of samples in the series, $s(i)$. Using larger shifts $(m > 0,1N)$ introduces a correspondingly larger *lag error* in the estimate, where the lag error is defined by K :

K = lag error in ACVF estimate

$$K = \frac{\left|\frac{1}{N} - \frac{1}{N-m}\right|}{\frac{1}{N}}$$

$$= \frac{m}{N-m} \qquad (B.5)$$

From equation (B.5), it is seen that the lag error in the estimate of R_s(i,i+m) is 11% for $m=0,1N$, while for $m=0,2N$, the bias error rises to 25%, which is rather high. Therefore, it was decided to use $m=0,1N$ in all computations of the ACVF.

At this point, we introduce the concept of (spatial) stationarity in the wide sense (WSS) in order to assess whether the statistical behaviour of $s(x)$ is independent under shifts of the independent parameter, x. This particular property has not been examined in the present work, however it is suggested to be examined in further studies. In all references to the ACVF, it is assumed that the spatial origin is at $x=0$ meters.

Recalling the definition of a wide sense (as opposed to strict sense) stationary random process, and replacing the independent parameter, time (t), by space (x), it follows that the first and second order statistics are not influenced under shifts of the spatial origin x (or time, t, hence the term stationary) [B.3]:

(1) $$E\{s_x\} = E\{s_{x_1}\} \qquad (B.6)$$

(2) $$R_s(x, x-\tau) = R_s(x_1, x_1-\tau) \qquad (B.7)$$

The first condition, Eq.(B.7), implies that the expected value of $s(x)$ is invariant under shifts of x. The second equation, Eq.(B.8), implies that $R(x, x-\tau)$ is a function of the space difference, τ, alone, and is therefore independent of the value of x. If conditions (1) & (2) are satisfied, the random process $s(x)$ is said to be stationary to the second order, or *wide sense stationary* (WSS). For a real WSS random process, the autocovariance function may be expressed in terms of τ alone, that is,

$$R_s(x, x-\tau) = R_s(\tau) \qquad (B.8)$$

In addition, if $s(x)$ is real and WSS, then it can be shown that its autocovariance function is even, that is,

$$R_s(-\tau) = R_s(\tau) \qquad (B.9)$$

The *normalized autocovariance function (NACVF),* is a convenient parameter for evaluation of many ACVF curves since the NACVF curves are normalized to a starting value of 1.0 at zero (spatial) shift. In the present work, only the normalized covariance functions are used, and any reference to ACVF must be understood to actually mean the NACVF.

Assuming that $s(x)$ is a WSS random process, the NACVF, $\rho_s(\tau)$, is obtained from the ACVF, $R_s(\tau)$, as follows:

$$\rho_s(\tau) = \frac{R_s(\tau)}{R_s(0)} \qquad (B.10)$$

End Notes

[B.1] **W.C.Y. Lee,** *Mobile Communications Engineering*, New York, McGraw-Hill, 1982, p.54.

[B.2] **R.H. Leaver and R.H. Thomas,** *Analysis and Presentation of Experimental Results*, New York, MacMillan Press, 1974.

[B.3] **W.B. Davenport,** *Probability and Random Processes*, New York, McGraw-Hill, 1970, p.325.

APPENDIX C:

CCVF AND SHORT TERM FADING

The *crosscovariance function (CCVF)* of two continuous real random processes, $a(x)$, $b(x)$, denoted as $R_{ab}(x,x+\tau)$, where τ is the spatial shift of $b(x)$ w.r.t. $a(x)$, is given by,

$$R_{ab}(x,x+\tau) = E\{(a(x)-\bar{a})\cdot(b(x+\tau)-\bar{b})\} \qquad (C.1)$$

Analogous to the ACVF, and assuming ergodicity of $a(x)$ and $b(x)$, a biased estimate of the discrete CCVF is given by Eq.(C.2) below. The lag error (K) in the estimate of the CCVF is given by Eq.(B.5) in Appendix B.

$$\hat{R}_{ab}(i,i+m) = \frac{1}{N-m}\sum_{i=1}^{i=N-m}[a(i)-\bar{a}]\cdot[b(i+m)-\bar{b}] \qquad (C.2)$$

$$m = 0,\ldots,M \quad ; \quad M = 0.1N$$

For real, WSS random processes $a(x)$, $b(x)$, the CCVF is a function of the parameter τ alone:

$$R_{ab}(x,x-\tau) = R_{ab}(\tau) \qquad (C.3)$$

The following symmetry property is true for real WSS random processes, $a(x)$ and $b(x)$ [C.1]:

$$R_{ab}(\tau) = R_{ba}(-\tau) \qquad (C.4)$$

As with the case of the ACVF, it is convenient to express the CCVF in terms of its normalized value w.r.t. its value at zero spatial shift, giving the *normalized cross-covariance function, NCCVF* [C.2]. In the present work, all references to the *CCVF* must be understood to actually refer to the *NCCVF*, expressed as follows :

$$\rho_{ab}(\tau) = \frac{R_{ab}(\tau)}{R_{ab}(0)} \qquad (C.5)$$

End Notes

[C.1] **J.J. Freeman**, *Principles of Noise*, New York, John Wiley, 1958, p.162

[C.2] **H.R. Raemer**, *Statistical Communication Theory and Applications*, Englewood Cliffs, New Jersey, Prentice-Hall, 1969, pp.65-66.

APPENDIX D:

PSD AND SHORT TERM FADING

The *power spectral density (PSD)* of a continuous stationary random process (CSRP), $s(x)$, denoted as $F_s(\omega)$, where ω is the angular spatial frequency, is given in terms of its complex (continuous) frequency spectrum, $S(\omega)$, as follows [D.1] :

$$F_s(\omega) = \frac{|S(\omega)|^2}{\int_0^{\infty} |S(\omega)|^2 \, d\omega} \qquad (D.1)$$

The continous fourier transform (CFT) of $s(x)$ is given by,

$$S(\omega) = \int_{-\infty}^{+\infty} s(x) e^{-j\omega x} dx \qquad (D.2)$$

In view of the recent availability of Fast Fourier Transform (FFT) algorithms, it is feasible to compute the Discrete Fourier Transform, $S(k)$, directly from the original sequence, s(i), without first computing the correlation function [D.2]. This gives the following expression for $S(k)$, where T is the sample spacing, k is the frequency index, and N is the number of samples [D.3] :

$$S(k) = T \sum_{i=0}^{i=N-1} s(i) \cdot \exp\left(-\frac{j2\pi ik}{N}\right) \quad k = 0, 1, 2, \ldots, N/2 \qquad (D.3)$$

The magnitude spectrum of $S(k)$ is of interest obtaining the PSD. The magnitude spectrum is given by,

$$|S(k)|^2 = [ReS(k)]^2 + [ImS(k)]^2 \qquad (D.4)$$

Thus there are half as many frequency points as time points for real sequences; computing beyond $k=N/2$ results in an even symmetry wrap of the spectrum about the Nyquist frequency.

The PSD estimate can be expressed terms of a discrete spectrum, $A(k)$, where $A(k)$ is obtained from $S(k)$ as follows:

$$A(k) = \frac{|S(k)|^2}{\sum_{k=0}^{\frac{N}{2}} |S(k)|^2} \qquad (D.5)$$

The discrete PSD estimate, $\hat{F}_s(k)$, can expressed in terms of $A(k)$ as follows, where bar denotes averaged spectral components :

$$\hat{F}_s(k) = \overline{A(k)} \qquad k = 0,\ldots,N/2 \qquad (D.6)$$

Two considerations worth mentioning in representing discrete (time) signals in the spectral domain are the resolution bandwidth, $B=1/NT$, and the spectral stability, η [D.4].

The first parameter, B, is an indicator of the spacing between adjacent frequency components. A larger sample size (N) or a smaller sampling interval (T) gives rise to a higher spectral resolution [D.4].

The second parameter, η, is an indicator of the averaging interval of $|S(k)|^2$. Generally speaking, the larger the number of samples used in the averaging, the greater the spectral stability, or conversely, the less 'noisy' the spectrum [D.4].

End Notes

[D.1] See, for example, **D.E. Kerr (Ed.)**, *Propagation of Short Radio Waves*, New York, Dover Publications, 1951, p.558.

[D.2] It is also possible to estimate the PSD by first computing the autocovariance function. For this approach the Wiener-Khintchine theorem may be used to advantage.

A brief discussion of the Wiener-Khintchine theorem is found in, **H.R. Raemer**, *Statistical Communication Theory and Applications*, Englewood Cliffs, New Jersey, 1969, pp.59-60.

[D.3] A thorough treatment of DFT computation methods is found in, **R.K. Otnes and L. Enochson**, *Applied Time Series Analysis*, New York, John Wiley, vol. 1, 1978, pp.222-224.

[D.4] Computational aspects of PSD estimation are discussed in, **R.K. Otnes and L. Enochson**, *Applied Time Series Analysis*, 1978, vol.1, pp.316-358.

APPENDIX E:

ABBREVIATIONS

ACVF	Autocovariance function
AM	Amplitude Modulation
AMPS	Advanced Mobile Phone Service
BDRS	Basic Data Retrieval Software
CCVF	Crosscovariance function
CDF	Cumulative Distribution Function
CFT	Continuous Fourier Transform
CLNLR	Combination Lognormal Log-Rician
CRC	Communications Research Centre
DFT	Discrete Fourier Transform
DOC	Department of Communications
EGA	Enhanced Graphics Adapter
ERP	Effective Radiated Power
FFT	Fast Fourier Transform
FM	Frequency Modulation
FORTRAN	Formula Translator (programming language)
IBM	International Business Machines (Corp.)
LMRS	Land Mobile Radio Systems
MCENV	Micro-Environment
LTF	Long Term Fading
MFIV	Mobile Field Instrumentation Vehicle
NACVF	Normalized Autocovariance Function

NCCVF	Normalized Crosscovariance Function
PC	Personal Computer (micrcomputer)
PDF	Probability Density Function
PSD	Power Spectral Density
Q-Q	Quantile-Quantile
RAM	Random Access Memory
RF	Radio Frequency
RMS	Root-Mean-Square
SDAS	Statistical Data Analysis Software
SLTF	Spatial Long Term Fading
STF	Short Term Fading
TV	Television
UHF	Ultra-High Frequency (300 MHz-3 GHz)
VHF	Very High Frequency (30-300 MHz)
WSS	Wide Sense Stationary

BIBLIOGRAPHY

This is a partial bibliography of conference, journal papers, and texts on various aspects of indoor, urban, and mobile radio propagation. The list is not meant to be exhaustive, however the aim is to provide related background material to the present work.

ALIMOV, V.A. et al., "Ultrashort-Wave Signal Characteristics in a Mobile Communications Channel Under Urban Conditions", *Radio Eng. Electron. Phys.*, 1985, pp.75-78.

ALLSEBROOK, K. and PARSONS, J.D.,"Mobile Radio Propagation in British Cities in the V.H.F. and U.H.F. Bands", *Proc. IEE*, vol.124 no.2, February 1977, pp.95-102.

ARNOLD, H.W., COX, D.C. and MURRAY, R.R., "Macroscopic Diversity Performance Measured in the 800-MHz Portable Radio Communications Environment", *IEEE Trans. on Antennas and Propagation*, vol.36 no.2, February 1988, pp.277-281.

AULIN, T., "A Modified Model for the Fading Signal at a Mobile Radio Channel", *IEEE Trans. on Vehicular Technology*, vol. VT-28 no.3, August 1979, pp.182-203.

BAHAR, E. and FITZWATER, M., "Shadowing by Non-Gaussian Surfaces for which Decorrelation Impiles Statistical Independence", *Radio Science*, vol. 18 no.4, July-August 1983, pp.566-572.

BANIK, T., PAVLASEK, T.J.F. and LeBEL, J., "Electric Field Strength Surveys of Broadcast Signals in an Urban Environment", *Proc. International Conference on Electromagnetic Interference and Compatibility (INCEMIC)*, Bangalore, India, September 10-11, 1987, pp. 341-344.

BANIK, T., PAVLASEK, T.J.F. and LeBEL, J., "Long Term Fading Characteristics of VHF Broadcast Signals in an Urban Environment", *Proc. 38th IEEE Conference on Vehicular Technology*, Philadelphia, Pennsylvania, U.S.A., June 15-17, 1988, pp. 205-212.

BECKMANN, P. and SPIZZICHINO, A., *The Scattering of Electromagnetic Waves from Rough Surfaces*, New York, Macmillan, 1963.

BERNHARDT, R.C., "Macroscopic Diversity in Frequency Reuse Radio Systems", *IEEE Journal on Selected Areas in Communications*, vol.SAC-5 no.5, June 1987, pp.862-870.

BLOBEL, W., "The Scale and Spatial Distribution of Random Measurements for the Determination of VHF and UHF Broadcasting Coverage Conditions", *Rundfunktech Mitt.* (German), vol. 24 no.3, June 1980, pp.117-124.

BODSON, D., McLURE, G.F. and McCONOUHGEY, S.R., (Eds.), *Land Mobile Communications Engineering*, New York, IEEE Press, 1984.

BRAYER, K., "Guest Editorial: Fading and Multipath Channel Communications - A Roadmap", *IEEE Journal on Selected Areas in Communications*, vol. SAC-5 no.2, February 1987, pp.65-67.

BIBLIOGRAPHY

BRUNEAU, M., CARON, B., GAGNON, G. and VINCENT, A., "Laboratory Evaluation of a Mobile Radio Data System", *Proc. 36th IEEE Vehicular Technology Conference*, Dallas, Texas, May 1986, pp.219-223.

BULLINGTON, K., "Radio Propagation Fundamentals", *Bell System Technical Journal*, vol.36 no.3, May 1957, pp.593-625.

BULTITUDE, R.J., "Measurement, Characterization and Modeling of Indoor 800/900 MHz Radio Channels for Digital Communications", *IEEE Communications Magazine*, vol. 25 no.6, June 1987, pp.5-12.

CHANDRA, A., "Fadings of VHF Signals at 70.3 MHz and 160.6 MHz in a Metropolitan City", *Proc. IEEE International Symposium on EMC*, San Diego, California, September 1986, pp.71-78.

CLARKE, R.H., "A Statistical Theory of Mobile Radio Reception", *Bell System Technical Journal*, vol. 47, July-August 1968, pp.957-1000.

COX, D.C., "910 MHz Urban Mobile Radio Propagation: Multipath Characteristics in New York City", *IEEE Trans. Communications*, vol.COM-21, November 1973, pp.1188-1194.

COX, D.C., ARNOLD, H.W. and PORTER, P.T., "Universal Digital Portable Communications: A System Perspective", *IEEE Journal on Selected Areas in Communications*, vol. SAC-5 no.5, June 1987, pp. 764-773.

DAVIS, B.R., "FM Noise with Fading Channels and Diversity", *IEEE Trans. Communications*, vol. COM-19, December 1971, pp.1189-1200.

DAVIS, B.R., "Random FM in Mobile Radio with Diversity", *IEEE Trans. Communications*, vol. COM-19, December 1971, pp. 1259-1267.

DAVIS, B.R. and BOGNER, R.E., "Propagation at 500 MHz for Mobile Radio", *Proc. IEE*, vol.132 Part F no.5, August 1985, pp.307-320.

EGLI, J.J., "Radio Propagation above 40 MC over Irregular Terrain", *Proc. IRE*, October 1957, pp.1383-1391.

FRAZER, E.L., "An Analysis of Propagation Measurements in the Cellular Band", *Proc. International Conference on Antennas and Propagation (ICAP 87)*, University of York, Heslington, York, U.K., Part 2, March-April 1987, pp. 2.73-2.76.

GANS, M.J., "A Power-Spectral Theory of Propagation in the Mobile Radio Environment", *IEEE Trans. Vehicular Technology*, vol.VT-21 no.1, February 1972, pp.27-38.

GILBERT, E.N., "Energy Reception for Mobile Radio", *Bell System Technical Journal*, October 1965, pp.1779-1803.

GOLOVIN, E.S., "Statistical Characteristics of Signals in a Mobile Receiver of Multipath Propagation of Radio Waves", *Telecommun. and Radio Eng.*, no.3, 1976, pp.65-69.

BIBLIOGRAPHY

GOLOVIN, E.S., "Generalized Correlation Function of a Mobile Communications Multipath Channel", *Telecommun. and Radio Eng.*, no.1, 1979, pp.103-105.

HANSEN, F. and MENO, F.I., "Mobile Fading - Rayleigh and Lognormal Superimposed", *IEEE Trans. on Vehicular Technology*, vol.VT-26 no.4, November 1977, pp.332-340.

HASHEMI, H., "Simulation of the Urban Radio Propagation Channel", *IEEE Trans. on Vehicular Technology*, vol. 28, August 1979, pp.213-225.

HORIKOSHI, J., TANAKA, K. and MORINAGA, T., "1.2 GHz Band Wave Propagation Measurements in Concrete Building for Indoor Radio Communications", *IEEE Trans. on Vehicular Technology*, vol.VT-35 no.4, November 1986, pp.146-152.

HUFF, D.L., "Advanced Mobile Phone Service : The Developmental System", *Bell System Technical Journal*, vol.58 no.1, January 1979, pp.249-269.

IBRAHIM, M.F., and PARSONS. J.D., "Signal Strength Prediction in Built-Up Areas. Part I: Median Signal Strength", *Proc. IEE*, vol.130 Pt. F no.5, August 1985, pp.377-384.

ISKAM, Y.Y., and SHAPTEV, V.A., "Properties of the Nakagami-Rice Distribution as a Model for Signal Fading", *Radio Eng. and Electron. Phys.*, 1985, pp.129-131.

JAKES, W.C. (Ed.), *Microwave Mobile Communications*, New York, John Wiley, 1974.

JAKES, W.C. and Reudnik, D.O., "Comparison of Mobile Radio Transmission at UHF and X-Bands", *IEEE Trans. on Vehicular Technology*, vol.VT-16, October 1967, pp.10-14.

JAKES, W.C., "A Comparison of Specific Space Diversity Techniques for Reduction of Fast Fading in UHF Mobile Radio Systems", *IEEE Trans. on Vehicular Technology*, vol.VT-20 no.4, November 1971, pp.81-92.

KAJI, M. and AKEYAMA, A., "UHF-Band Propagation Characteristics for Land Mobile System Using Low-Antenna Height Base Stations", *Antennas and Propagation Symposium Digest*, Vancouver, B.C., Canada, June 1985, pp.835-838.

KALININ, A.I., TROITSKIY, V.N., and SHUR, A.A., "Statistical Properties of the Signal in Long Range USW Propagation", *Telecommun. and Radio Eng.*, vol.18 Part 1, July 1964, pp. 1-12.

KERR, D.E. (Ed.), *Propagation of Short Radio Waves*, New York, Dover Publications, 1951.

KOZONO, S. and WATANABE, K., "Influence of Environmental Buildings on UHF Land Mobile Propagation", *IEEE Trans. on Communications*, vol.COM-25 no.10, October 1977, pp.1133-1143.

KOZONO, S., TSURUHARA, T. and SAKAMOTO, M., "Base Station Polarization Diversity Reception for Mobile Radio", *IEEE Trans. on Vehicular Technology*, vol.VT-33 no.4, November 1984, pp.301-304.

BIBLIOGRAPHY

KULIKOV, A.N., PONOMAREV, G.A. and SKOVRONSKIY, A.Y, "Statistical Analysis of the Multipath Field in an Urban Environment", *Radio Eng. and Electron. Phys.*, vol. 27 no. 12, December 1982, p.99.

LeBEL, J., "A Mobile Facility for Electromagnetic Environment Monitoring Applications", *Proc. IEECE Conference Digest*, Toronto, Canada, October 1981, pp.10-11.

LeBEL, J., CRAIG, G.B. and BOULIANE, P.R., "Measurement and Evaluation of Electromagnetic VHF and UHF Television Field Strength Distributions in Urban Environments", *Proc. IEEE International EMC Symposium*, Arlington, Virginia, U.S.A., August 1983, pp.147-151.

LeBEL, J., CRAIG, G.B. and BOULIANE, P.R., "Topics on the Evaluation of Electric Field Distributions in Urban Environments", *Proc. International Communications and Energy Conference*, Montreal, Canada, October 1984, pp. 305-310.

LeBEL, J., "Seasonal Mobile Radio Signal Variations in Non-Urban Environments", *Proc. IEEE MONTECH Conference*, Montreal, Canada, December 1987, pp.177-180.

LECOURS, M., CHOUINARD, J.-Y. and DESLISLE, J.R., "Statistical Modelling of a Mobile Radio Channel", *Proc. 36th IEEE Vehicular Technology Conference*, Dallas, Texas, May 1986, pp.232-238.

LEE, W.C.Y., "Antenna Spacing Requirement for a Mobile Radio Base-Station Diversity", *Bell System Technical Journal*, vol.50, July-August 1971, pp. 1859-1876.

LEE, W.C.Y., "A Study of the Antenna Array Configuration of an M-Branch Diversity Combining Mobile Radio Receiver", *IEEE Trans. on Vehicular Technology*, vol.VT-20 no.4, November 1971, pp.93-104.

LEE, W.C.Y., "Polarization Diversity System for Mobile Radio", *IEEE Trans. Commun.*, vol. COM-20 no.4, October 1971, pp.912-923.

LEE, W.C.Y., "Estimate of Local Average Power of a Mobile Radio Signal", *IEEE Trans. on Vehicular Technology*, vol.VT-34 no.1, February 1985, pp.22-27.

LEE, W.C.Y., *Mobile Communications Engineering*, New York, McGraw Hill, 1982.

LEE, W.C.Y. and YEH, Y.S., "On the Estimation of Second-Order Statistics of Log Normal Fading in a Mobile Radio Environment", *IEEE Trans. Comm.*, vol.22, June 1974, pp.869-873.

LOEW, K., "UHF Field Strength Measurements for the Determination of the Influence of Buildings and Vegetation in Land Mobile Radio Service", *Proc. 36th IEEE Vehicular Technology Conference*, Dallas, Texas, May 1986, pp.40-45.

LONGLEY, A.G., "Radio Propagation in Urban Areas", *Proc. 28th IEEE Vehicular Technology Conference*, Denver, Colorado, March 22-24, 1978, pp.503-511.

MACDONALD, V.H., "Advanced Mobile Phone Service: The Cellular Concept", *Bell System Technical Journal*, vol.58 no.1, January 1979, pp.15-41.

BIBLIOGRAPHY

MATTHEWS, P.A. and MOLDKAR, D., "Wideband Measurements of the UHF Mobile Radio Channel", *Proc. International Conference on Antennas & Propagation (ICAP 87)*, Part 2, March-April 1987, pp. 2.73-2.76.

McMAHON, J.H., "Capability of the FCC Mobile Monitoring Van", IEEE Trans. on Vehicular Technology, vol.VT-23 no.4., November 1974, pp.139-142.

MELANCON, P. and LeBEL, J., "A Characterization of the Frequency Selective Fading of the Mobile Radio Channel", *IEEE Trans. on Vehicular Technology*, vol. VT-35 no.4, November 1986, pp.153-161.

NIELSON, D.N., "Microwave Propagation Measurements for Mobile Digital Radio Application", *IEEE Trans. on Vehicular Technology*, vol.VT-27, August 1978, pp.117-131.

NAKAGAMI, M., "The m-Distribution - A General Formula of Intensity Distribution of Rapid Fading", in: *Statistical Methods in Radio Propagation*, W.C. Hoffman, Ed., Pergamon Press, 1960.

OLIVIER, P. and TIFFON, J., "Transfer Function Measurement as a Characterization of the Urban Mobile Channel", *Proc. International Conference on Antennas & Propagation (ICAP 87)*, Part 2, March-April 1987, pp. 2.95-2.98.

OKUMURA, Y., OHMORI, E., KAWANO, T. and FUKUDA, K., "Field Strength and Its Variability in VHF and UHF Land-Mobile Radio Service", *Rev. Electrical Communication Laboratories*, vol.16, September-October 1968, pp.825-873.

OSSANA, J.F., Jr., "A Model for Mobile Radio Fading Due to Building Reflections: Theoretical and Experimental Fading Waveform Power Spectra", *Bell System Technical Journal*, vol.43, November 1964, pp.2935-2971.

PARSONS, J.D. and IBRAHIM, M.F., "Signal Strength Prediction in Built-Up Areas Part 2: Signal Variability", *Proc. IEE*, vol.130 Pt. F no.5, August 1985, pp.385-391.

PERITSKY, M.M., "Statistical Estimation of Mean Signal Strength in a Rayleigh Fading Environment", *IEEE Trans. on Vehicular Technology*, vol. VT-22 no.4, November 1973, pp.123-129.

PONOMAREV, G.A., TEL 'PUKHOVSKIY, Y.D. and KUILKOV, A.N., "Spatial Correlation of an Ultrashort Wave Field Under Urban Conditions", *Radio Eng. and Electron. Phys.*, no.11, 1984, pp.95-99.

REUDNIK, D.O., "Properties of Mobile Radio Propagation Above 400 MHz", *IEEE Trans. Vehicular Technology*", vol. VT-23 no.4, November 1974, pp.143-159.

RICE, S.O., "Mathematical Analysis of Random Noise", *Bell Syst. Tech. J.*, vol. 23, July 1944, pp.282-332; vol.24, January 1945, pp.46-156; "Statistical Properties of a Sine Wave Plus Random Noise", *Bell Syst. Tech. J.*, vol. 27, January 1948, pp.109-157.

RUBINSTEIN, T., "The Standard Deviations of the Local Means of Mobile Radio Signals in Flat, Suburban Terrain", *Proc. 36th IEEE Vehicular Technology Conference*, Dallas, Texas, May 1986, pp.52-56.

BIBLIOGRAPHY

SALEH, A.A.M. and VALENZUELA, R.A., "A Statistical Model for Indoor Multipath Propagation", *IEEE Journal on Selected Areas in Communications*, vol. SAC-5 no.2, February 1987, pp.128-137.

SAMUEL, R.J., PARSONS, J.D. and IBRAHIM, M.F., "Mobile Radio Propagation in Inner London", *Second International Conference on Antennas and Propagation*, Heslington, York, England, Part 2, April 1981, pp.143-147.

SHEPHERD, N.H., "Radio Wave Loss Deviation and Shadow Loss at 900 MHz", *IEEE Trans. on Vehicular Technology*, vol. VT-26, November 1977, pp.309-313.

SKOMAL, E. and SMITH, A.A., *Measuring the Radio Frequency Environment*, New York, Van Nostrand Reinhold, 1985.

STEIN, S., "Fading Channel Issues in System Engineering", *IEEE Journal on Selected Areas in Communications*, vol. SAC-5, no.2, February 1987, pp.68-89.

SUZUKI, H., "A Statistical Model for Urban Radio Propagation", *IEEE Trans. Commun.*, vol. COM-25 no.7, July 1977, pp.673-680.

TRIFONOV, P.M., BUDKO, V.N. and ZOTOV, V.S., "Structure of USW Field-Strength Spatial Fluctuations in a City", *Telecommun. and Radio Eng.*, February 1964, pp.26-30.

TURIN, G.L., CLAPP, F.D., JOHNSTON, T.L., FINE, S.B., and LAVRY, D., "A Statistical Model of Urban Multipath Propagation", *IEEE Trans. on Vehicular Technology*, vol.21 no.1, Feb. 1972, pp.1-9.

VAN REES, J., "Measurements of the Wide-Band Radio Channel Characteristics for Rural, Residential, and Suburban Areas", *IEEE Trans. on Vehicular Technology*, vol. VT-36 no.1, February 1987, pp.2-6.

VAUGHAN, R.G., "Signals in Mobile Communications: A Review", *IEEE Trans. on Vehicular Technology*, vol. VT-35 no.4, November 1986, pp.133-147.

VINOGRADOV, A.G. and TEOKHAROV, A.N., "Correlation Properties of Field Propagation in a Medium with Multiscale Inhomogeneities", *Radiophys. Quantum Electron.*, vol.23 no.10, October 1980, pp.780-785.

YOUNG, B.R., "Advanced Mobile Phone Service: Introduction, Background, and Objectives", *Bell System Technical Journal*, no.1, January 1979, pp.1-14.

YOUNG, R.W., "Comparison of Mobile Radio Transmission at 150, 450, 900 and 3700 Mc", *Bell System Technical Journal*, vol.31, November 1952, pp.1068-1085.

ZANDER, J., "Stochastical Model of the UHF Radio Channel", *IEEE Trans. Vehicular Technology*, vol.VT-30 no.4, November 1971, pp.145-155.